US Army Corps of Engineers

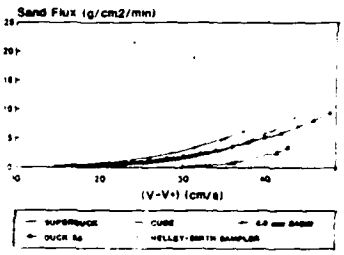

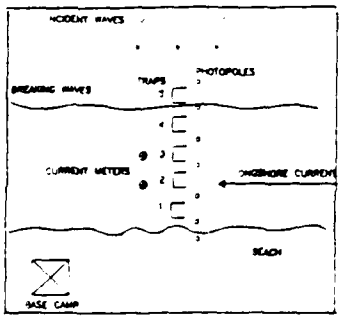

COASTAL ENGINEERING RESEARCH CENTER

TECHNICAL REPORT CERC-89-11

(2)

DEVELOPMENT OF A PORTABLE SAND TRAP FOR USE IN THE NEARSHORE

by

Julie Dean Rosati, Nicholas C. Kraus

Coastal Engineering Research Center

DEPARTMENT OF THE ARMY
Waterways Experiment Station, Corps of Engineers
3909 Halls Ferry Road, Vicksburg, Mississippi 39180-6199

US ARMY ENGINEER WATERWAYS EXPERIMENT STATION

September 1989
Final Report

Approved For Public Release; Distribution Unlimited

Prepared for DEPARTMENT OF THE ARMY
US Army Corps of Engineers
Washington, DC 20314-1000
Under Surf Zone Sediment Transport Processes
Work Unit 34321

Destroy this report when no longer needed. Do not return it to the originator.

The findings in this report are not to be construed as an official Department of the Army position unless so designated by other authorized documents.

The contents of this report are not to be used for advertising, publication, or promotional purposes. Citation of trade names does not constitute an official endorsement or approval of the use of such commercial products.

Unclassified
SECURITY CLASSIFICATION OF THIS PAGE

REPORT DOCUMENTATION PAGE

Form Approved
OMB No. 0704-0188

1a REPORT SECURITY CLASSIFICATION Unclassified	1b RESTRICTIVE MARKINGS
2a SECURITY CLASSIFICATION AUTHORITY	3 DISTRIBUTION/AVAILABILITY OF REPORT Approved for public release; distribution unlimited.
2b DECLASSIFICATION/DOWNGRADING SCHEDULE	
4 PERFORMING ORGANIZATION REPORT NUMBER(S) Technical Report CERC-89-11	5 MONITORING ORGANIZATION REPORT NUMBER(S)
6a NAME OF PERFORMING ORGANIZATION USAEWES, Coastal Engineering Research Center 6b OFFICE SYMBOL (If applicable)	7a NAME OF MONITORING ORGANIZATION
6c ADDRESS (City, State, and ZIP Code) 3909 Halls Ferry Road Vicksburg, MS 39180-6199	7b ADDRESS (City, State, and ZIP Code)
8a NAME OF FUNDING/SPONSORING ORGANIZATION US Army Corps of Engineers 8b OFFICE SYMBOL (If applicable)	9 PROCUREMENT INSTRUMENT IDENTIFICATION NUMBER
8c ADDRESS (City, State, and ZIP Code) Washington, DC 20314-1000	10 SOURCE OF FUNDING NUMBERS PROGRAM ELEMENT NO. / PROJECT NO / TASK NO / WORK UNIT ACCESSION NO 34321

11 TITLE (Include Security Classification)
Development of a Portable Sand Trap for Use in the Nearshore

12 PERSONAL AUTHOR(S)
Rosati, Julie Dean; Kraus, Nicholas C.

13a TYPE OF REPORT	13b TIME COVERED	14 DATE OF REPORT (Year, Month, Day)	15 PAGE COUNT
Final report	FROM _____ TO _____	September 1989	181

16 SUPPLEMENTARY NOTATION
Available from National Technical Information Service, 5285 Port Royal Road, Springfield, VA 22161.

17 COSATI CODES			18 SUBJECT TERMS (Continue on reverse if necessary and identify by block number)
FIELD	GROUP	SUB-GROUP	See reverse.

19 ABSTRACT (Continue on reverse if necessary and identify by block number)

This study presents an evaluation of and improvement upon the hydraulic and sand-trapping characteristics of the streamer trap, a sand trap developed for use in the nearshore zone. Twenty-three streamer trap nozzles were evaluated in laboratory hydraulic efficiency tests; three nozzles with near-optimum hydraulic behavior were further evaluated in laboratory sand-trapping efficiency tests. A comparison of measurements made with two closely spaced traps in the field was conducted as an indication of consistency. The Helley-Smith sampler, a popular riverine sediment trap reported in the literature, was also tested in the laboratory for comparison.

Laboratory testing indicated that the nozzle previously used in the DUCK85 field data collection project performed well at an off-bed elevation; however, sand-trapping efficiency at the bed was low, with significant scour developing during a 5-min testing
(Continued)

20 DISTRIBUTION/AVAILABILITY OF ABSTRACT	21 ABSTRACT SECURITY CLASSIFICATION
☒ UNCLASSIFIED/UNLIMITED ☐ SAME AS RPT ☐ DTIC USERS	Unclassified
22a NAME OF RESPONSIBLE INDIVIDUAL	22b TELEPHONE (Include Area Code) / 22c OFFICE SYMBOL

18. SUBJECT TERMS (Continued).

Apparatus
Helley-Smith sampler
Laboratory experiment
Longshore transport
Riverine transport
Sand trap
Sediment trap
Sediment transport
Transport rate

19. ABSTRACT (Continued).

period. The SUPERDUCK nozzle, previously used in the SUPERDUCK field data collection project, performed near optimally at an off-bed elevation in the laboratory. When the nozzle was positioned at the bed, scour occurred at the base over approximately half the testing period. A new cube-shaped nozzle design performed near optimally at both off- and on-bed elevations in the laboratory. Hydraulic efficiencies measured in the laboratory for the Helley-Smith sampler were comparable to those reported in the literature; however, transport processes with the sampler located on the bed were distorted and deviated greatly from the normal patterns of sand movement in the tank tests. Field testing of the DUCK85 and SUPERDUCK nozzles indicated that both nozzle types were reasonably consistent, assuming that the transport rate was uniform over the region occupied by the traps. On the basis of this testing program, portable traps are recommended as a reliable and accurate method of measuring sand transport under low to moderate wave energy contitions.

PREFACE

The work described herein was authorized as a part of the Civil Works Research and Development Program by the US Army Corps of Engineers (USACE). Work was performed under the Surf Zone Sediment Transport Processes Work Unit 34321 which is part of the Shore Protection and Restoration Program at the Coastal Engineering Research Center (CERC) at the US Army Engineer Waterways Experiment Station (WES). Messrs. John H. Lockhart, Jr., James E. Crews, Charles W. Hummer, and John G. Housley are USACE Technical Monitors. Dr. Charles L. Vincent is Program Manager for the Shore Protection and Restoration Program at CERC.

This study was performed and the report prepared over the period 1 January 1986 through 30 November 1988 by Ms. Julie Dean Rosati, Hydraulic Engineer, Coastal Structures and Evaluation Branch (CD-S), Engineering Development Division (CD), CERC, and Dr. Nicholas C. Kraus, Senior Scientist, Research Division (CR), CERC. The content of this report is substantially the same as the thesis submitted to Mississippi State University by Ms. Rosati in partial fulfillment of the requirements for an M.S. degree in civil engineering. Dr. Kraus was the WES thesis advisor.

This study was under general administrative supervision of Dr. James R. Houston and Mr. Charles C. Calhoun, Jr., Chief and Assistant Chief, CERC, respectively; and under direct supervision of Mr. Thomas A. Richardson, Chief, CD, Mr. H. Lee Butler, Chief, CR, and Ms. Joan Pope, Chief, CD-S, CERC.

Dr. Kraus was Principal Investigator of Work Unit 34321 during the major portion of the study. Ms. Kathryn J. Gingerich, Coastal Processes Branch (CR-P), CR, was Principal Investigator during publication of this report and provided review and technical editing. Ms. Carolyn J. Dickson (CR-P) assisted in formatting and production of the final manuscript. Mr. Bruce A. Ebersole was Chief, CR-P. This report was edited by Ms. Shirley A. J. Hanshaw, Information Products Division, Information Technology Laboratory, WES.

Commander and Director of WES during report publication was COL Larry B. Fulton, EN. Dr. Robert W. Whalin was Technical Director.

CONTENTS

CONTENTS (continued)

LIST OF TABLES

LIST OF FIGURES

LIST OF FIGURES (continued)

DEVELOPMENT OF A PORTABLE SAND TRAP FOR USE IN THE NEARSHORE

PART I: INTRODUCTION

Background

Characteristics of sediment transport

1. Sediment transport by water is a complex phenomenon that is little understood despite more than 200 years of intense study by engineers and scientists. Riverine sediment transport occurs in predominantly unidirectional and slowly varying flows, with the transport rate dependent primarily on flow speed, water depth, turbulence, sediment grain size, and channel morphology. Although riverine sediment transport may appear to be a relatively simple problem because the flow is unidirectional, a universally valid predictive formula for sediment transport in rivers does not exist. Instead, specific formulae have been developed for particular rivers. Sediment transport in the nearshore -- the narrow zone of the coast in which waves shoal, break, and run up on the beach -- is even more complex because of the presence of wave-induced oscillatory flow that acts simultaneously with the unidirectional and quasi-steady current moving along the shore (the longshore current).

2. In general terms, sediment transport occurs as bed load and suspended load. Bed load is defined as those particles which are supported by the bed and move in continuous or near-continuous contact with the bed by rolling, skipping, or sliding along the bottom. Suspended sediment is that part of the transported material which is supported by the surrounding fluid during its motion (Shen 1971). Many measurements of bed-load and suspended load transport rates have been made in the unidirectional flow regime of rivers and laboratory tank facilities. In contrast, few corresponding measurements have been made in the nearshore.

3. This report is concerned with sediment transport along the coast. Of particular interest is longshore transport in the nearshore zone, since permanent beach change c natural and engineered beaches is primarily controlled by the movement of sediment alongshore under prebreaking and breaking

waves. However, techniques to measure longshore transport described below and further developed herein are equally applicable to riverine transport. A review of riverine methods and apparatus for measuring sediment transport is presented in Appendix A together with methods for measuring transport in the nearshore.

Methods of estimating transport

4. Sediment transport rates have traditionally been determined using one of four methods: measurement of topographic change occurring as a result of the transport, such as erosion or deposition at a coastal structure; measurement of fluorescent-dyed or radioactive sand tracer movement; use of an analytic or empirical relationship with measured or calculated waves and/or currents to infer a rate; and measurement of the transport through time using some type of apparatus or instrument. Each of these methods has particular advantages and disadvantages.

5. The topographic change method (e.g., Caldwell 1956; Bruno, Dean, and Gable 1981) results in an estimate of relatively long-term sediment transport (on the order of weeks to months) and has the advantage of being capable of encompassing high-energy events. However, the relationship between wave and current conditions during the averaging period and the resulting transport cannot be sharply defined, as the processes are smoothed through time. In addition, it is difficult to distinguish between changes caused by cross-shore and longshore components of transport.

6. The use of a tracer consisting of dyed ambient sand (Komar and Inman 1970, Inman et al. 1980, Kraus et al. 1982) can provide an estimate of transport on the order of hours to days in a relatively low-energy wave environment; however, this method is extremely labor-intensive, and consistent results are difficult to obtain (Kraus et al. 1982).

7. Empirical relationships relating sand transport to measured forcing quantities (wave characteristics, water velocity, etc.) can be used to estimate transport over any time interval, depending on the type of input data. However, the correlation between longshore transport rates measured in the field and rates predicted using an empirical or analytical relationship is relatively weak and may be questioned (Greer and Madsen 1978).

8. Various instruments and apparatus have been developed to allow measurement of transport rates over intervals on the order of seconds, minutes, and hours. It is relatively easy to measure wave and current conditions occurring during such an interval, as opposed to long-term, spatially integrated deployments. Apparatus that have been developed for use in the nearshore zone include those that collect an instantaneous bulk water-sediment sample (e.g., Kana 1976, 1977; Zampol and Waldorf in press; Inman 1978); time-integrating samplers that pump or siphon sediment-laden water (e.g., Watts 1953, Thornton 1972, Fairchild 1972, Thornton and Morris 1977); pit samplers that collect material moving into an excavated region of the bed (e.g., Inman and Bowen 1963, Anderson 1987); and direct-measuring traps that retain sediment moving into some collection area (e.g., Inman 1949, James and Brenninkmeyer 1971, Lee 1975, Pickrill 1986, Kraus 1987). Indirect-measurement instruments measure some phenomena occurring over a fixed distance as a result of sediment transport, such as the attenuation of light (Hom-ma, Horikawa, and Kashima 1965; Thornton and Morris 1977; Brenninkmeyer 1973, 1974), intensity of backscattered light (Jaffe, Sternberg, and Sallenger 1984, Hanes and Huntley 1986, Downing 1984, Beach and Sternberg 1987), absorption of nuclear radiation (Basinski and Lewandowski 1974), or absorption or backscatter of sound (Tamura and Hanes 1986, Hanes and Vincent 1987).

9. An apparatus such as a direct-measurement trap allows a representative sample of the moving sediment to be collected and retained for further analysis. Traps are also economical to construct and maintain, and the data analysis procedure requires no specialized software or electronic expertise. On the other hand, such an apparatus does have disadvantages. Sediment traps present an obstruction to the wave and current fields; therefore, transport may be significantly altered in the vicinity of the device. Traps can cause scour near the bed, thereby creating an artificial transport rate. However, if these limitations can be overcome, traps are well-suited for obtaining short-term measurements of sand transport as a function of the existing environmental conditions. Very few apparatus or instruments have been developed to measure sand transport both at the bed and throughout the water column. Data collected with sand traps can be used to supplement, verify, and improve other, perhaps longer-term, measurement methods discussed above.

10. Trap development and applications for use in the nearshore have not been extensively investigated, as opposed to other apparatus and instrumentation. Therefore, it is worthwhile to investigate this technique because it appears to hold promise as a method of obtaining accurate estimates of sediment transport under a certain range of environmental conditions. In the nearshore, sediment consists primarily of sand-sized quartz particles (grain diameters in the range of 0.074 to 1.0 mm); therefore, discussions to follow will focus on particles in the sand range. However, the basic principle of trapping is applicable, with certain modifications and restrictions, to almost any size sediment particles.

Sand traps

11. The use of traps to estimate sand transport rates and collect a representative sample of moving material has been limited in coastal engineering. However, the study and use of traps in the riverine environment has been documented since 1808 (see Appendix A). In the United States, the most comprehensively studied riverine trap is the Helley-Smith (H-S) sampler (Helley and Smith 1971) (Figure 1). The H-S sampler is a direct-measurement trap designed to rest on the river bed and sample bed load. The sampler consists of an expanding metal nozzle connected to an inflexible mesh cloth bag which retains the collected material. Designed to eliminate a possible decrease in water speed at the sampler entrance, the expanding nozzle creates a pressure difference between the entrance and exit regions of the trap. Thus, the intake rate is controlled by the nozzle geometry and is effectively constant, independent of the amount of sediment in the collection bag.

12. The streamer trap is a sand trap recently developed for use in the coastal zone (Katori 1982, 1983). Similar to the H-S sampler, the streamer trap uses a mesh cloth bag attached to a metal nozzle to collect sand. However, the streamers are light and can be mounted vertically on a metal frame (Kraus 1987) so that sand moving in suspension can be collected at any point in the water column (Figure 2). Streamer traps have recently been used in major field data collection projects in the surf zone to estimate longshore sand transport rates (Kraus 1987; Kraus and Dean 1987; Kraus, Gingerich, and Rosati 1989; Kraus, Gingerich, and Rosati in preparation). Placement of several streamer traps across the surf zone results in a measurement of the

Figure 1. The H-S sampler (after Helley and Smith 1971)

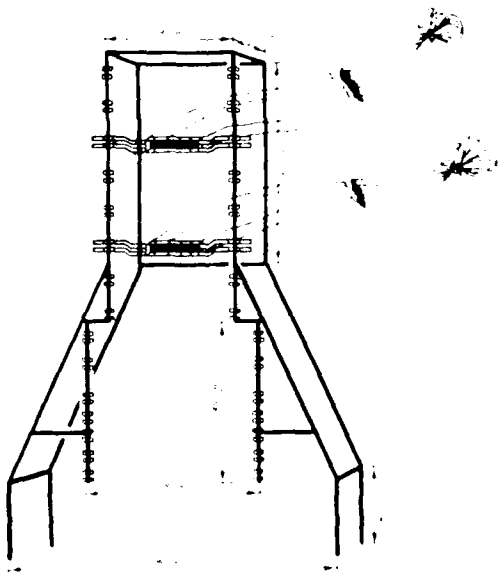

Figure 2. The streamer trap

cross-shore distribution of longshore sand transport which can be integrated to obtain the total longshore transport rate.

Problem Statement

13. Estimation of longshore sand transport rates is essential for the design of coastal and riverine structures and construction and maintenance of navigable waterways. Design of structures penetrating the surf zone, such as groins and jetties, and the resultant erosional or depositional features they are expected to produce requires estimation of the cross-shore distribution of longshore transport. Low-crested structures such as reef breakwaters and weir jetty sections can be optimally designed with information about relative magnitudes of bed load and suspended load or, ideally, a prediction of the vertical distribution of transport.

14. The streamer trap shows much promise for use in the nearshore, yet the hydraulic and sand-trapping properties of the streamer trap were not investigated by its developer (Katori 1982, 1983). Therefore, in the present study, extensive laboratory investigations augmented by limited field investigations were conducted to determine these properties. Two unidirectional flow experiments were performed in the laboratory to replicate the longshore current occurring in the field. The first experiment determined the hydraulic characteristics of 23 streamer trap nozzles and identified several nozzles with near-optimum hydraulic efficiencies. The second experiment, qualitatively and quantitatively, evaluated the sand-trapping efficiency of those nozzles determined to have near-optimum hydraulic efficiencies. Characteristics of the H-S sampler were also investigated for comparison with results previously reported in the literature.

Report Organization

15. Uses of the streamer trap are described in Part II. Part III presents results of the hydraulic tests. Part IV discusses hydrodynamic elements of the coastal zone and unidirectional flow regime and presents results of the sand-trapping efficiency tests. Field experiment results are

discussed in light of the laboratory experiments in Part V, and recommendations are made for further use of the streamer trap in Part VI. A review of other types of transport rate measurement apparatus is presented in Appendix A. Hydraulic data from the laboratory experiments are presented in Appendices B and C, and sand-trapping data are given in Appendix D. Notation used in the report is listed in Appendix E.

PART II: STREAMER TRAP

16. The basic sand collection element of the streamer trap was developed in Japan to measure longshore sand transport rates in the surf zone (Katori 1982). The name of the apparatus derives from the mesh collection bags which stream out with the current during operation. The device has been used in the United States to measure cross-shore distributions of the longshore sand transport rate (Kraus 198/; Kraus and Dean 1987; Kraus, Gingerich, and Rosati 1988, 1989), variations in longshore sand transport at a point (Kraus, Gingerich, and Rosati 1989: Kraus, Gingerich, and Rosati in preparation), sand transport rates in the offshore*; sand transport in a rip current (Kraus and Nakashima 1987); and deposition of sand into a submarine canyon.** In Japan, modified versions of the streamer trap have been used to measure cross-shore sand transport rates (Katori 1983) and the rate of wind-blown sand transport in a large wind tunnel (Hotta 1988). In general, the streamer trap can be used to measure sand-sized sediment transport in almost any quasi-steady and unidirectional flow.

Description of the Streamer Trap

17. The streamer trap consists of rectangular sand collection bags vertically mounted on a rack (Figure 2). The collection bags (streamers) are sewn of technical grade monofilament sieve cloth, and each streamer is attached to a nozzle which functions to facilitate the flow of sand-laden water into the streamer (Figure 3). Sand of nominal diameter greater than the mesh is collected in the streamer while water flows through the bag. Streamers are made approximately 1.5 m long to ensure that long-period deployment and/or deployment in high-transport regimes will not cause the streamer to fill and thereby reduce its sand-trapping efficiency. A long streamer also prevents loss of collected material if the flow momentarily

---

* Personal Communication, 1986, Jim Clausner, Hydraulic Engineer, US Army Engineer Waterways Experiment Station, Vicksburg, Mississippi.

** Personal Communication, 1987, Craig Everts, Moffatt and Nichol, Engineers, Long Beach, California.

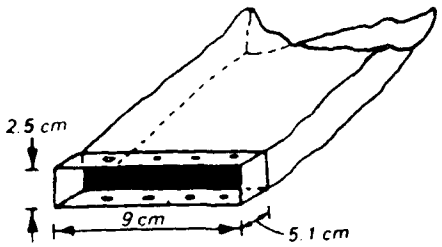

Figure 3. Streamer nozzle

reverses. The stainless steel rack holds each nozzle and streamer securely at a particular elevation in the flow. The 40-cm-long rack legs are embedded in the sand bed during use for stabilization of the trap. The streamers have an end which can be untied and opened to remove collected sand; during operation, the streamer is closed by folding the end of the cloth over on itself then looping an attached nylon string around the gathered end and tying it securely (Figure 4).

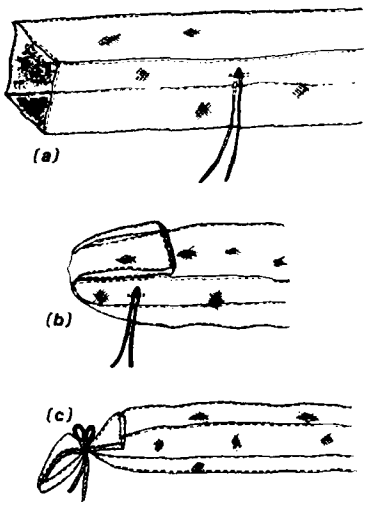

Figure 4. Method of closing streamer

Trap Operation

Longshore sand transport sampling

18. The streamer trap has been used in the surf zone under significant breaking wave heights exceeding 1 m and average longshore currents up to 0.60 m/sec. The trap can be used in these conditions because scour around the rack legs and bottom nozzle is usually relatively minor for short sampling intervals, and the trap and its operator can remain stable and in the same location during sampling.

19. Prior to deployment of the streamer trap, streamers are secured on the rack at selected elevations. For operation in average water depths on the order of 1 m, typically five streamers have been used per trap. The nylon string fastening the end of each streamer is checked to ensure that it is tight and secure. Each trap is carried by one or two operators to a specified position in the surf zone. Vertical poles previously placed across the surf zone assist trap operators in accurate positioning (Figure 5). The traps are held out of the water until sampling begins.

20. At the start of the collection period, the traps are simultaneously thrust into the sea bottom, and the operators secure the traps by rocking the rack and pushing the rack legs into the bed by standing on the horizontal bars located at the bottom. When the bars reach the seabed, preventing further penetration, the bottom edge of the lowest nozzle should lie on the bed. Trap operators sometimes use dive masks to ensure that the bottom edge of the lowest nozzle is flush with the bed and to monitor development of scour. During the collection period of typically 5 to 10 min, the trap operator stands near the trap on the down-current side, thereby avoiding any collection of operator-induced suspended sand. A 5- to 10-min collection interval is recommended to avoid excessive filling of the streamer and scour at the bed. Trap operators are instructed to note excessive scour and report this condition after the collection period as an indication of data quality. High waves passing through the surf zone may tip the trap. If tipping occurs, the trap operator immediately stands on the rack bars, righting the rack and again aligning the bottommost nozzle with the bed. The streamer trap is usually more stable in the surf zone environment than a human. In weak longshore

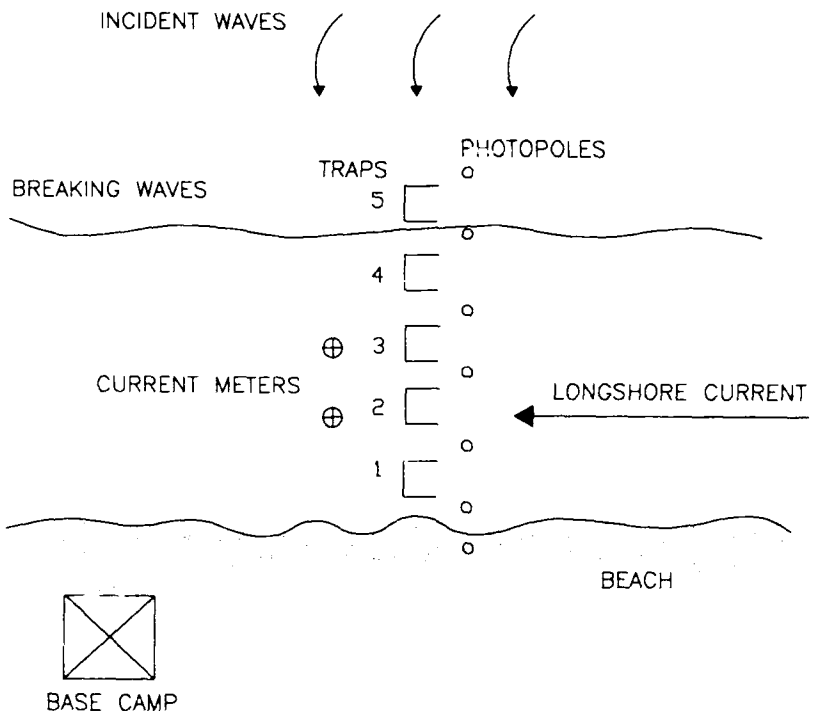

Figure 5. Typical arrangement for field experiment

currents, streamers tend to wrap around the rack, reducing the effective length to approximately 38 cm (the width of the rack). The trap operators then unwrap and, as necessary, untwist the streamers to allow them to extend freely in the flow.

21. At the end of the sampling period, the operators lift the traps out of the water and carry them to shore. Most of the collected sand is located at the end of the streamers, although some particles may cling to the sides. The streamers are removed from the rack, and sand clinging on the sides of the cloth is washed to the end by holding the nozzle upright and dipping the tied streamer into a large (for example, 110-liter) barrel filled with seawater. The streamer end can then be untied and the collected sand washed into a patch of sieve cloth which had previously been weighed when wet. Alternatively, the sample can be washed into a collection bag and taken to the laboratory for weighing and analysis.

22. The collected sand can be weighed and its dry weight estimated on the beach using a linear relationship between drip-free wet weight and dry weight of cohesionless sand found by Kraus and Nakashima (1986):

$$DW = C\ WW \tag{1}$$

where

DW = dry weight of sand

WW = wet weight of sand

C = empirical coefficient, typically ranging from 0.77 to 0.83

It is recommended that some samples from each test be retained for laboratory calibration of C , because its value depends on the weighing procedure (the balance operator's judgement of the drip-free condition) and the nature of the sand. The clean streamers can then be secured onto the rack and the traps prepared for another sampling sequence. Use of a vertical array of streamers results in a sand flux and grain size distribution at each elevation.

23. In field data collection projects conducted at Duck, North Carolina (Kraus and Dean 1987; Kraus, Gingerich, and Rosati 1988, 1989), two to four complete longshore testing sequences were conducted per day. Kraus (1987) also describes the streamer trap and its use in the surf zone.

Other field data collection

24. Use of the streamer trap is not limited to longshore sand transport collection experiments. Other types of surf zone sand transport experiments in which streamer traps have been used include measurement of sand transport rates in two longshore current feeders and the throat of a rip current (Kraus and Nakashima 1987), comparison of sand collected with two closely spaced traps (consistency tests) (Kraus 1987) (detailed in Part V), measurement of cross-shore sand transport rates (Katori 1983), and point-measurements of sand transport through time (Kraus, Gingerich, and Rosati 1988, 1989).

Calculation of Sand Transport Rate

25. Figure 6 defines the variables used in the sand transport rate calculation. The weight of sand collected in streamer k is S(k). The

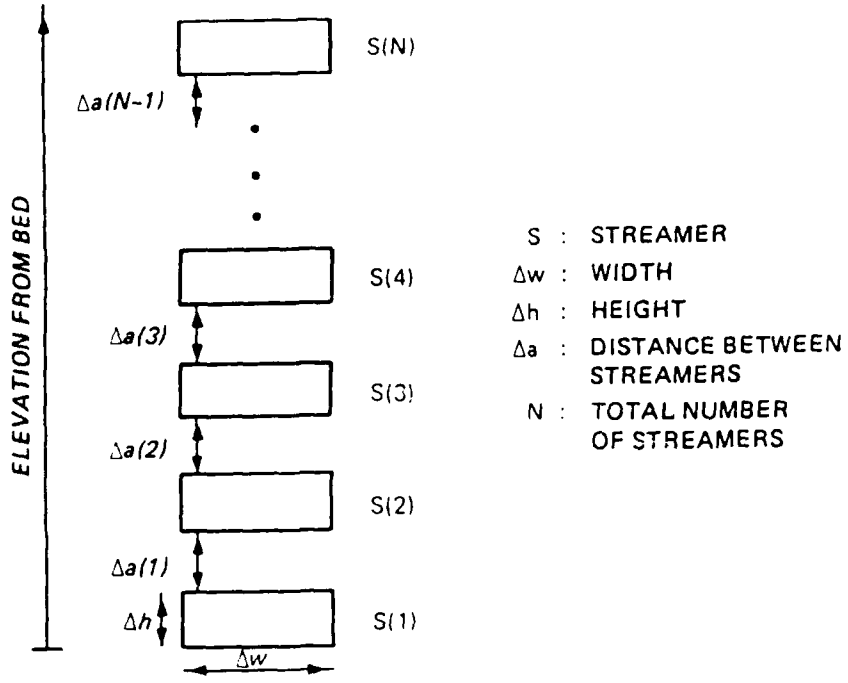

Figure 6. Variables used in transport calculations

index k increases from k=1 at the bottom to k=N , where N is the total number of streamers in a particular trap. Streamer width is Δw , streamer height is Δh , and the sampling interval is Δt. If these quantities are used, the flux of sand at streamer k , F(k) (units of weight per unit area and unit time), can be calculated using Equation 2:

$$F(k) = \frac{S(k)}{\Delta h \, \Delta w \, \Delta t} \tag{2}$$

26. The flux between neighboring streamers FE(k) can be estimated by linear interpolation between adjacent measured fluxes:

$$FE(k) = 0.5 \, [F(k) + F(k+1)] \tag{3}$$

27. The transport rate density for a trap i (units of sand weight per unit width of surf zone per unit time) can be calculated using previously

defined quantities and the distance between nozzles $\Delta a(k)$ (units of length) as follows:

$$i = \Delta h \sum_{k=1}^{N} F(k) + \sum_{k=1}^{N-1} \Delta a(k)\ FE(k) \qquad (4)$$

28. If traps are positioned across the surf zone, the total longshore sand transport rate through the surf zone can be estimated using the distances between traps, the transport rate density i at each trap, and the trapezoidal rule applied over the distance between the shoreline and the average wave breaker line.

PART III: HYDRAULIC EFFICIENCY TESTS

29. Experiments were conducted in a unidirectional flow tank to evaluate the hydraulic and sand-trapping efficiencies of streamer trap sand collection elements of various nozzle types, streamer length, and cloth mesh size. For comparison, hydraulic and sand-trapping efficiencies were also evaluated for the H-S sampler, a popular pressure-difference bed-load trap developed for use in the riverine environment (Helley and Smith 1971, Druffel et al. 1976, Emmett 1980, Hubbell et al. 1985, 1987) (see Appendix A). A unidirectional flow tank was used to simulate the quasi-steady state longshore current that drives longshore sand transport in the surf zone. It would be most realistic to conduct the tests in a cross-flow facility to simulate wave action or oscillatory motion orthogonal to the unidirectional flow. However, facilities of the scale required to test a prototype streamer trap do not exist.

30. Twenty-three streamer trap nozzle variations were tested to determine nozzle parameters defining optimal hydraulic and sand-trapping efficiencies. This chapter describes the facility used for the experiments, the streamer elements tested, and results from hydraulic efficiency experiments. Results of similar sand-trapping tests are given in Part IV.

Description of Facility and Equipment

Tank

31. Both the hydraulic and sand-trapping tests were conducted in an 18.3-m-long unidirectional flow tank with a cross-sectional area of 0.76 m by 0.76 m and a maximum water discharge of 0.2 m^3/sec. The tank sides are made of iron panels bolted together, except for a plexiglass viewing section approximately 4.6 m in length located in the middle of the tank (Figure 7). Prior to the experiment, joints between adjoining panels were filled with caulk and smoothed to minimize turbulence and flow separation at these indentations in the tank walls. Nevertheless, small-amplitude ripples did form at the seams (Figure 8). Water used in the testing was supplied by a circulating system, and discharges in the model were measured with venturi

Figure 7. Tank used for hydraulic and sand-trapping tests

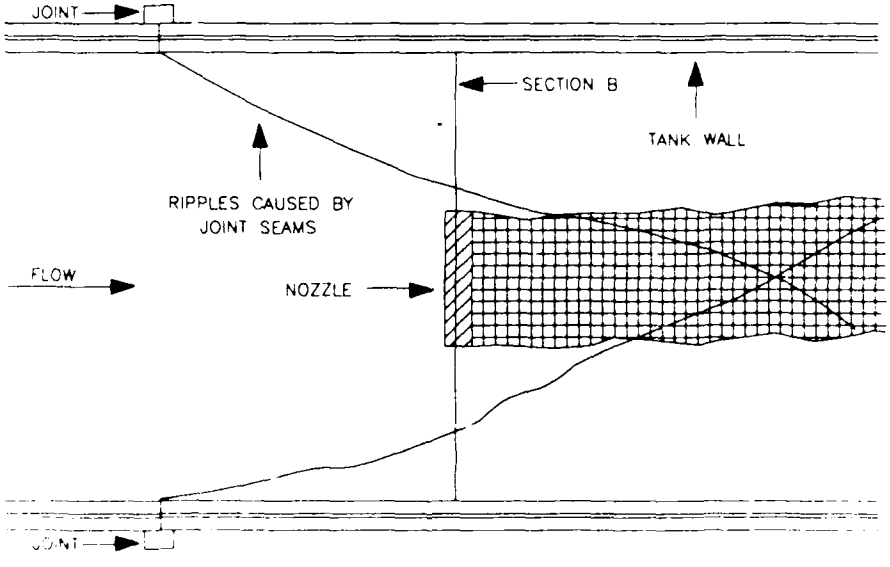

Figure 8. Location of nozzle during testing

meters installed in the inflow lines. Baffles and a fiber mat floating on the water surface at the tank entrance were used to smooth and steady the flow.

32. For the hydraulic efficiency tests, a 10-m length of plastic grass mat carpet approximately 1.3 cm in height was glued to the floor of the tank to create a uniform roughness. The plastic grass mat carpet was emplaced to extend beyond both sides of the center portion of the flume with plexiglass walls which served as the testing area. Section A (Figure 9), located at the upflow side of the plexiglass panel approximately 7.6 m from the water inflow, was used as a control area for measuring vertical profiles of flow speed. Section B, located near the end of the plexiglass panel and 12.2 m from the water inflow, was used as the test section. Section B was chosen such that flow at the trap nozzles would not be influenced by the ripples from panel seams during testing.

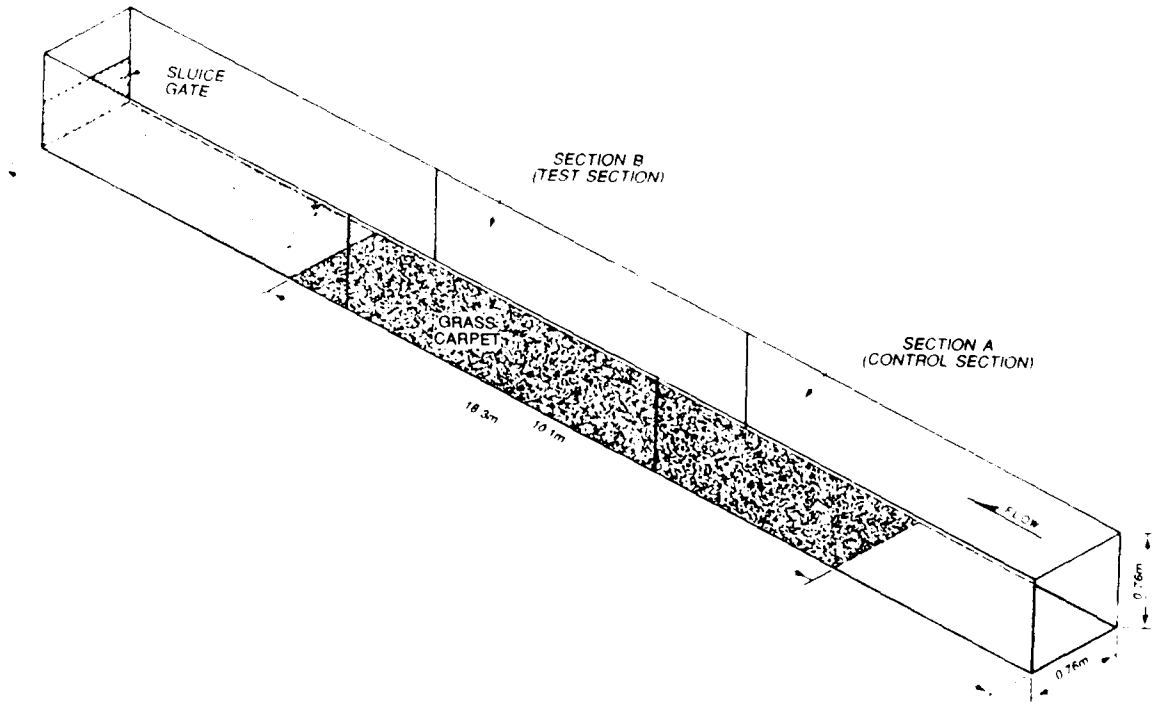

Figure 9. Locations of testing and control sections for hydraulic test

33. Water speed was measured with a Nixon velocity meter, a miniature propeller flow meter approximately 1 cm in diameter. Data were recorded in units of Hertz from a digital readout display; the 1-sec flow meter readings were internally averaged over a 10-sec interval. A linear calibration curve supplied by the manufacturer was used to convert propeller cycles to flow speed. The usable range of the flow meter is from 2.5 to 150 cm/sec with an accuracy of +/- 1 percent, according to the manufacturer. Vertical positioning of the flow meter was accomplished with a point gage; both the point gage and flow meter were mounted on a movable carriage riding on rails above the tank which controlled stationing of the device along the width and length of the tank (Figure 10).

Flow characteristics

34. Two characteristics of the tank flow, its steadiness through time and cross-sectional asymmetry in speed at the test section (Section B), were examined prior to actual testing. Figure 11 presents the temporal variation in flow speed about the respective mean at a Section B midflow elevation for four flow conditions (average midflow speeds equal to 32.3, 44.0, 49.5, and 51.9 cm/sec). Standard deviations in flow speed over a 3.8-min time period ranged from approximately 0.6 to 1.5 cm/sec if individual points were weighted equally (relative deviation between 1.1 and 4.2 percent of mean flow speed). As expected, averaging three consecutive speeds reduced the standard deviation to approximately 0.2 to 0.7 cm/sec (relative variation between 0.4 and 1.5 percent of mean flow speed). Therefore, three consecutive flow speed measurements were averaged for each data point in all calculations.

35. Flow speed characteristics were measured along the width of Section B for various depths (Figure 12). Flow speeds on the tank side opposite the viewing window (left side in Figure 12) were consistently lower than those on the near side. Slightly misaligned steel plate baffles (flow straighteners) at the inflow end of the tank were found to be the cause of the asymmetry. During testing, care was taken to place the nozzles at the center of the tank where the flow speed at all depths was most symmetric. Figure 12 also illustrates the decrease in flow speed in the upper layer of flow ($z = 26.4$ cm) caused by resistance from the fiber mat baffle at the tank entrance and the air-water interface.

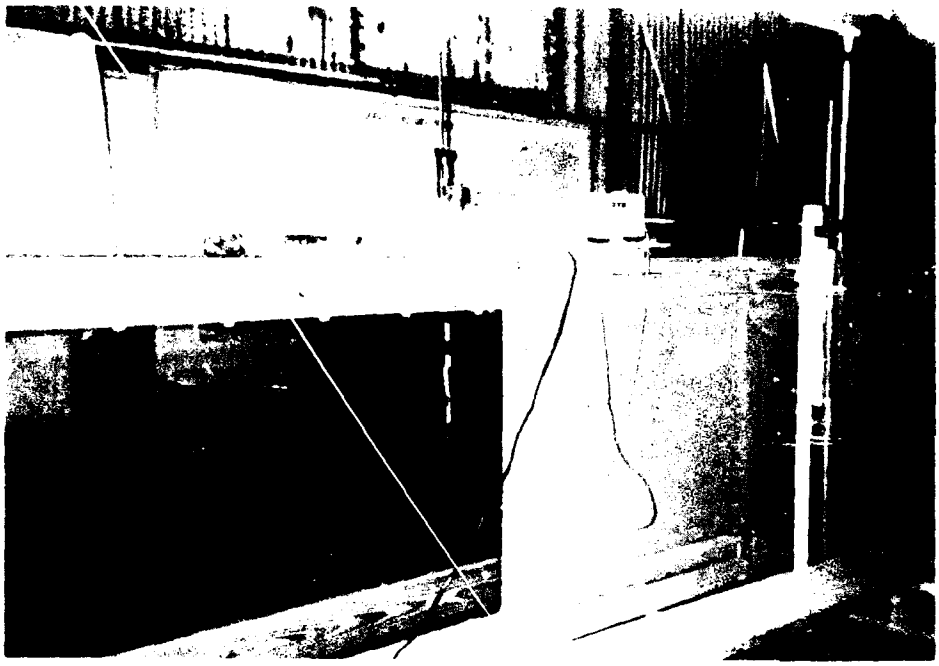

Figure 10. Photograph of point gage and flow meter setup

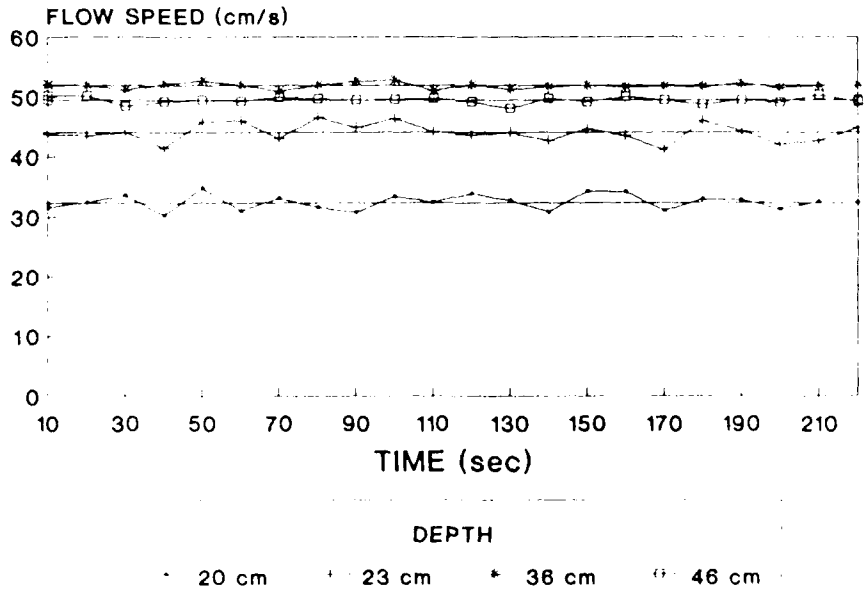

Figure 11. Flow speed at test section B

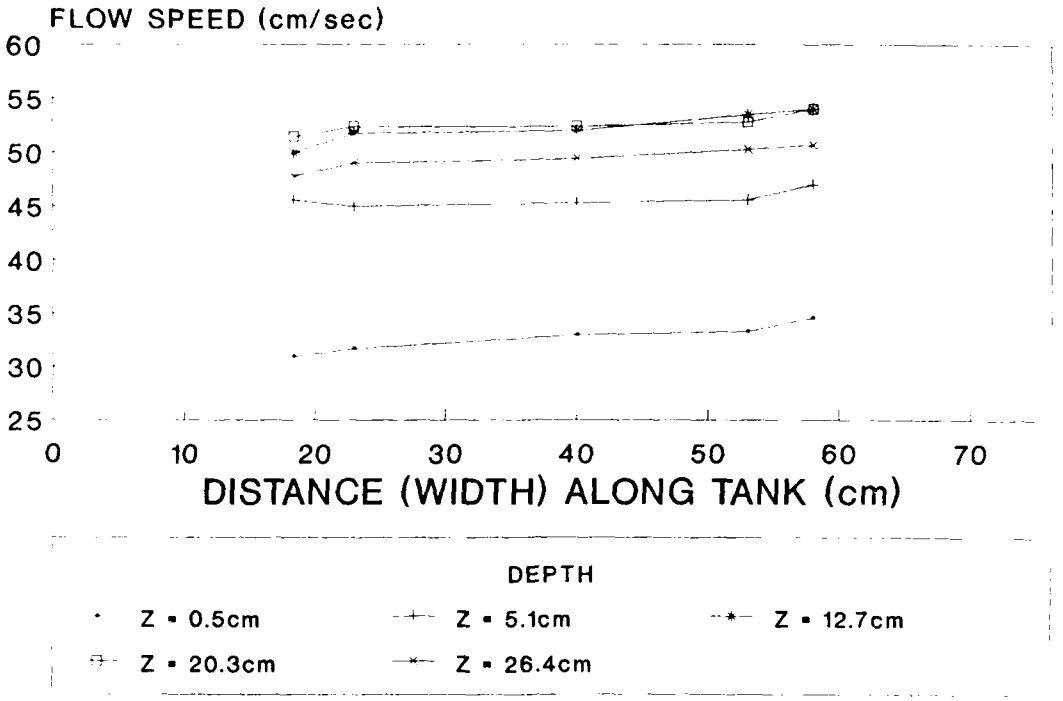

Figure 12. Variation of flow speed with depth at test section B

Streamer nozzles

36. Streamer trap nozzle parameters investigated in the hydraulic tests are illustrated in Figure 13: nozzle height and width (varied between 2.5 by 15 cm and 25 by 20 cm); presence or absence of a hood (extending from 2.5 to 5.1 cm forward of the element); presence or absence of a bottom lip (curved or straight); and streamer length (varied between 0.36 and 2.0 m). Dimensions of the streamer trap nozzles were chosen to be large enough to collect a significant (field measurable) quantity of sand during the testing period, yet small enough such that a rack with a vertical array of streamers would be of a size and weight that could be deployed during testing by one person. (See Part II for a general description of the streamer trap.) Bottom lips were tested on the lowermost streamers with the intention to streamline flow into the streamer and decrease scour (tested during the sand-trapping phase). Other components such as streamer mesh size (0.074, 0.105, and 0.149 mm) and a plexiglass door designed to shut during reversals in flow (as occurs in on-offshore sediment transport under oscillatory waves) were also evaluated.

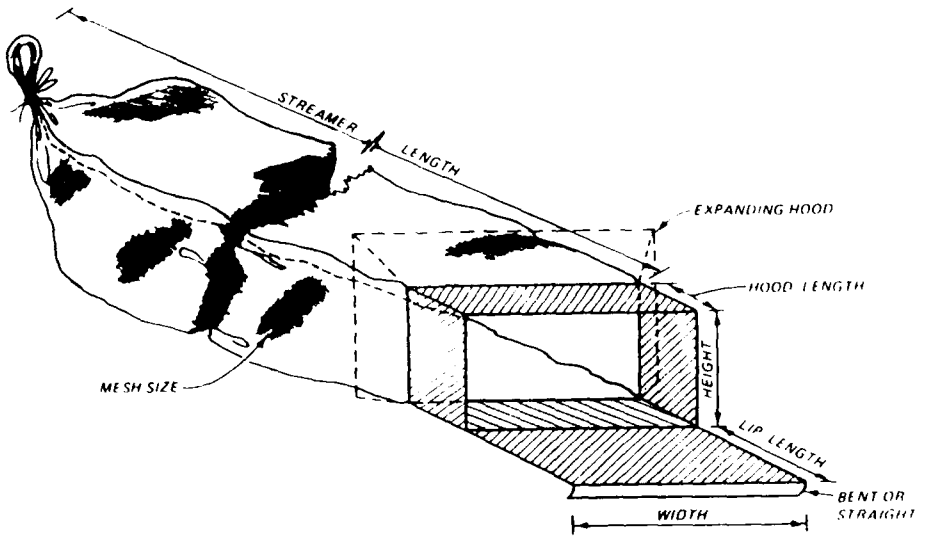

Figure 13. Nozzle parameters varied in hydraulic test (after Rosati and Kraus 1988)

By means of either the nozzle design or by bending the bars used to mount the nozzle to the rack, the entrance to each nozzle was positioned upstream from the rack to minimize flow disturbance caused by the mounts and rack. A prototype streamer trap rack as used in the field was employed to position nozzles at a particular elevation for hydraulic testing; the 0.4-m-long rack legs were removed because they served no purpose on the metal floor of the tank. Tape was used to attach nozzles to the rack.

Test Conditions

Definition of terms

37. Hydraulic efficiency E_h is defined as the ratio of the average flow speed directly in front of the sampler nozzle V_t (units of distance per time) to the average speed for the same ambient flow condition at the same

vertical and horizontal location without the sampler present V_o (in units of distance per time). The hydraulic efficiency is commonly expressed as a percentage:

$$E_h = \frac{V_t}{V_o} 100 \quad (\%) \tag{5}$$

38. Hydraulic efficiencies for all nozzles were first measured for two flow conditions (midflow speeds V_{mid} equal to 43 and 74 cm/sec); nozzles found to have hydraulic efficiencies near unity were then tested in an additional two flow conditions (V_{mid} equal to 22 and 59 cm/sec). Water depth during all tests was approximately 30 cm (see step c below). The minimum test flow speed was chosen to be on the order of the threshold velocity for 0.25-mm sand movement as estimated from the Shield's diagram (Vanoni 1977, p. 96). The maximum test flow was chosen as representing an upper longshore current speed in the field in which traps and their operators could be expected to function.

Vertical profiles of flow speed

39. Representative vertical distributions of flow speed for the four flow conditions are presented in Figure 14. Because of the size of the flow propeller (1 cm in diameter), the first flow speed measurement from the bed was located at z = 0.5 cm, where z is the elevation measured from the bed. Values for the shear flow speed U_* and the representative bed roughness z_o were calculated using the logarithmic law as follows:

$$u(z) = \frac{U_*}{k} \ln\left[\frac{z}{z_o}\right] + c \tag{6}$$

where

u(z) = flow speed at elevation z

k = Von Karman constant, taken to be 0.4

c = constant, taken to be zero

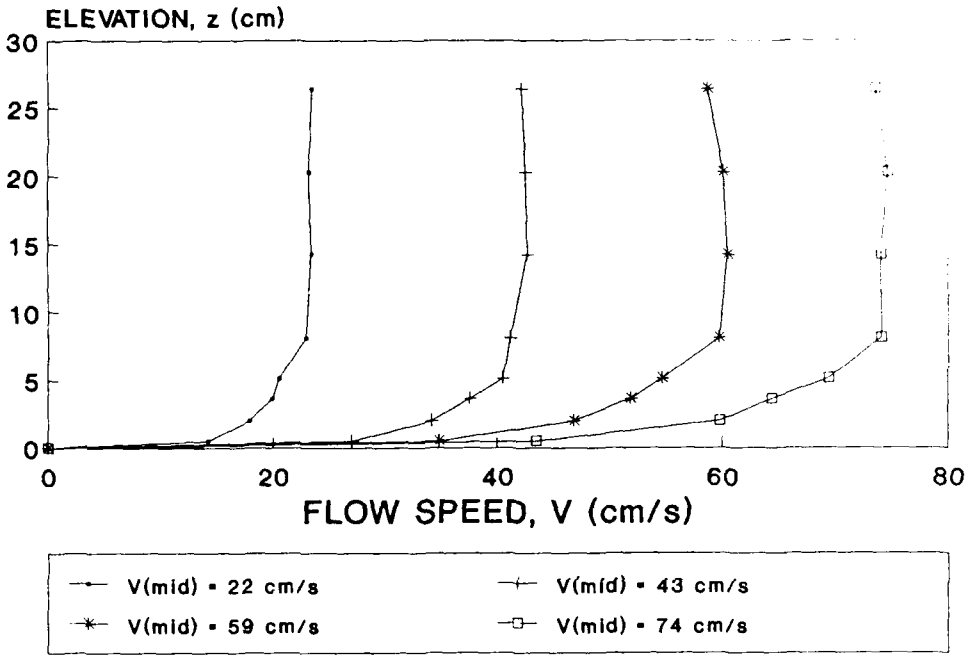

Figure 14. Vertical distributions of flow speed

If vertical profiles of flow speed are plotted on semilog paper, those following the logarithmic law will appear as straight lines, with the slope of the line equal to U_* and the y-axis intercept equal to z_o. Table 1 presents U_* (cm/sec), z_o (cm), and squared correlation coefficient r^2 calculated for the profile data using the logarithmic law as a function of midflow speed V_{mid}. The flow speed profiles followed a logarithmic profile well, with squared correlation coefficients ranging from 0.96 to 0.98.

Testing procedure

40. Most nozzles were tested both at middepth, for which the flow speed was determined to be fairly uniform over the region occupied by the nozzle, and on the tank bottom (resting on the carpet) where the flow increased from the bed in a logarithmic manner. Three consecutive readings from the flow meter were taken at each point to ensure that flow conditions in the tank were stationary and then averaged.

Table 1

Values of U_* , z_o , and r^2 for Vertical Flow Speed Data

V_{mid} cm/sec	Number of Profiles	U_* cm/sec	z_o cm	r^2
22	5	1.13	0.0036	0.98
43	47	2.26	0.0046	0.97
59	4	3.36	0.0090	0.97
74	48	3.68	0.0036	0.96

41. The following procedure was used in the testing of each nozzle:

a. The equilibrium design flow condition was established and defined by achieving consistent vertical profiles of flow speed taken along the center line of the test section (Sections A and B). If the vertical profiles at Sections A and B differed significantly (more than 5 percent) from the design flow, the discharge was either increased or decreased until the desired speed profiles were obtained. Typically, the profile was measured at eight points.

b. Vertical profiles of flow speed, consisting of eight points with increasing spacing from the bottom, were measured at the control location (Section A). This profile defined the reference flow profile without the trap in the tank.

c. The rack with the nozzle to be tested was placed at the test section (Section B), and the vertical profile of flow speed was measured at Section A. If the speed at any location differed by more than 5 percent from that of the reference profile measured in step b, the water level was lowered (to increase the discharge and compensate for the flow resistance caused by the trap) until all measurements fell within this tolerance. The water level was never lowered more than 1.3 cm. Because flow speeds were measured below the elevation $z = 26.4$ cm in obtaining vertical profiles, lowering of the water level did not require modification of the usual measurement point elevations.

d. The flow speed at points distributed uniformly across the area of the streamer nozzle was measured (3, 4, or 9 points, depending on nozzle size and geometry). These point measurements defined the flow field directly in front of the nozzle.

e. The rack and nozzle were removed, and the reference profile was reestablished at Section A.

f. Ambient flow speeds were measured at the same locations as in step d. These point measurements defined the flow field without the nozzle.

42. Figure 15 presents a comparison of typical profiles measured in Step b (without trap) and Step c (with trap) for the highest flow condition (V_{mid} equal to 74 cm/sec). In all cases, the difference between two speed measurements at the same elevation was no more than 5 percent, and values of the majority of point measurements with the trap in place were slightly smaller than those taken without the trap in the tank.

Calculation of hydraulic efficiency

43. Hydraulic efficiencies were calculated from the flow speed data using the point measurements and the area each measurement represented. An example nozzle cross section with measurement locations is presented in Figure 16. Data corresponding to the point measurements are presented in Appendix B. The hydraulic efficiency is calculated from these data as

$$E_h = \frac{\sum V_{tjk} \Delta y_j \Delta z_k}{\sum V_{ojk} \Delta y_j \Delta z_k} \quad (7)$$

where

V_{tjk} = flow speed directly in front of trap nozzle

Δy_j = representative horizontal distance

Δz_k = representative vertical distance

V_{ojk} = flow speed at same location without the trap

Hydraulic Test Results

Overview

44. One hundred and seventeen combinations of nozzle type, elevation of nozzle in the water column, and flow condition were tested. Computed hydraulic efficiencies for each test and average hydraulic efficiencies for each nozzle are presented in Table 2. Tests were conducted with nozzles positioned on the bed (BOT), at midflow (MID), and at both positions using two

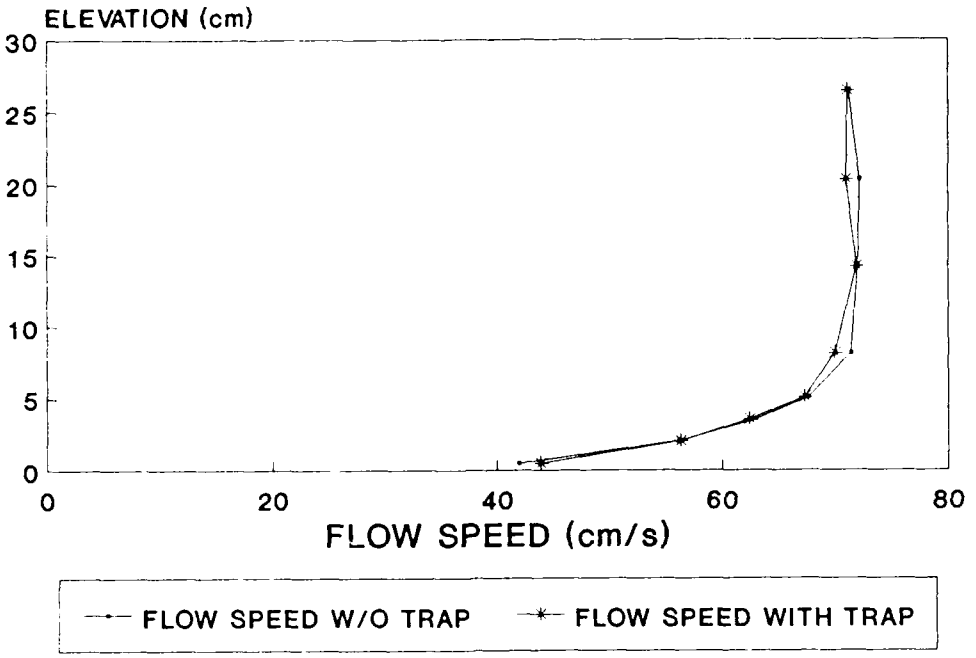

Figure 15. Typical flow speed profiles

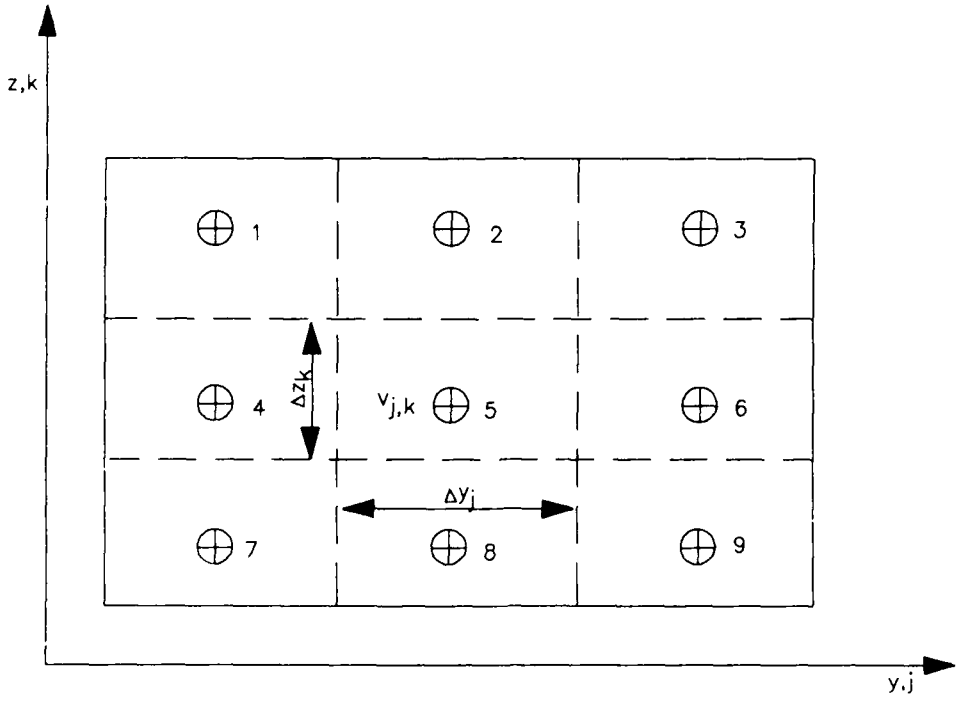

Figure 16. Example nozzle cross section

streamers (2ST). The nozzle description presented in Table 2 includes the height and width of the nozzle, indicates whether the nozzle had a curved lip (CL), hood (H), straight lip (SL), or door, and describes any special testing conditions (type of streamer cloth, orientation of nozzle relative to flow direction, etc.). Photographs of the nozzles tested, referenced in Table 2, are shown in Appendix C (Figures C1 through C8).

45. Hydraulic testing was conducted by initially evaluating each nozzle for midrange and high-range flow conditions (V_{mid} = 43 and 74 cm/sec). Hydraulic efficiencies for these two flow conditions ranged from 0.75 for the 2.5- by 15-cm streamer nozzle, to 1.30 for the H-S sampler. The average hydraulic efficiency for the "standard" 9- by 15-cm nozzle previously used in the DUCK85 field data collection project (hereafter referred to as the DUCK85 nozzle) was close to optimum for these two flow conditions (E_h = 0.94). Tests conducted with the DUCK85 nozzle turned at 10- and 30-deg angles to the flow (as might occur in the field), reducing the hydraulic efficiency slightly; but values for the two initial flow speeds used in these variations were still above 0.90. Comparison of three streamer mesh sizes indicated that the 0.105-mm mesh diameter cloth (56.9 mesh/cm) previously used in the DUCK85 experiment had a hydraulic efficiency closest to optimum. Because the 0.105-mm diameter cloth was the most economical mesh size, all but two streamers used in the hydraulic efficiency tests were constructed of this material. Shortening streamer lengths to 36 cm resulted in only a 2 percent reduction in hydraulic efficiency.

46. From the initial evaluation using two flow conditions, four nozzles were identified for further testing over additional flow speeds (V_{mid} = 22 and 74 cm/sec): two streamer trap nozzles with hydraulic efficiencies close to optimum (2.5- by 15-cm nozzle with 5.1-cm hood (hereafter referred to as the SUPERDUCK nozzle); and the 5.1- by 5.1-cm nozzle with 5.1-cm hood, hereafter referred to as the Cube (C) nozzle); the H-S sampler for comparison; and the DUCK85 nozzle.

47. The hydraulic efficiency of the H-S sampler over the range of flow conditions (E_h = 1.30) confirms the study by Druffel et al. (1976) who calculated an average hydraulic efficiency for the sampler equal to 1.54 for

Table 2
Hydraulic Efficiency for Each Nozzle, Testing Condition, and Midflow Speed

Figure	Nozzle	Test Cond	V_{mid}, cm/sec 22	43	59	74	E_h	Mean E_h
C1a	2.5cm x 15cm	BOT		0.70		0.87		
						0.84	0.78	
		MID		0.68		0.80		
						0.76	0.73	
		2ST		0.66		0.81		
							0.74	
								0.75
C1b	2.5cm x 15cm, CL	BOT		0.78		0.84	0.81	
								0.81
C1c	2.5cm x 15cm, 2.5cm H	MID		0.93		0.97	0.95	
		2ST		0.95		0.98	0.96	
								0.96
C1d	2.5cm x 15cm, 5.1 cm H (SUPERDUCK)	BOT	0.50	0.75	0.95	1.03	0.81	
		MID	0.96	1.02	1.06	1.04	1.02	
		2ST	0.59	0.96	0.90	0.99	0.86	
								0.90
C1e	2.5cm x 15cm, 5.1cm H, CL	BOT		0.96		1.03	0.99	
								0.99
C2a	5.1cm x 15cm	BOT		0.86		0.92	0.89	
		MID		0.92		0.97	0.95	
		2ST		0.88		0.97	0.93	
								0.92
C2b	5.1cm x 15cm, CL	BOT		0.78		0.87	0.83	
								0.83
C2c	5.1cm x 15cm, 2.5cm H, CL	BOT		0.90		0.95	0.93	
								0.93
C2d	5.1cm x 15cm, 5.1cm H	BOT		0.97		0.89	0.93	
		MID		0.94		0.92	0.93	
								0.93
C2e	5.1cm x 15cm, 5.1cm H, CL	BOT		0.97		1.02	1.00	
								1.00

(continued)

Table 2 (Continued)

Figure	Nozzle	Test Cond	V_{mid}, cm/sec 22	43	59	74	E_h	Mean E_h
C3	5.1cm x 15cm, 5.1cm H (C)	BOT	0.90	0.89	1.03	1.00	0.96	
		MID	0.77	0.97	0.97	1.00	0.93	
		2ST	0.83	0.96	0.98	1.01	0.95	0.94
C4a	9cm x 15cm 0.105-mm diam Cloth V (DUCK85)	BOT	0.61	0.93	0.93	0.97	0.86	
				0.91				
		MID	0.80	1.00	0.95	0.91	0.91	
				0.97				
		2ST	0.73	0.92	0.91	0.94	0.88	
				0.94				0.88
C4b	9cm x 15cm, SL	BOT		0.78		0.88	0.83	0.83
C4c	9cm x 15cm, CL	BOT		0.81		0.99	0.91	
				0.87				0.91
C4a	9cm x 15cm, 36 cm str	MID		0.92		0.93	0.92	0.92
C4a	9cm x 15cm, 0.149-mm diam Cloth T	MID		0.77		0.91	0.85	
				0.80				0.85
C4a	9cm x 15cm, 0.074-mm diam Cloth X	MID		0.89		0.96	0.93	
				0.92				0.93
C4a	9cm x 15cm, Open str	MID		0.95		1.00	0.97	0.97
C4d	9cm x 15cm, Door	MID		0.98		0.95	0.96	0.96
C4e	9cm x 15cm, Door, CL	BOT		0.99		0.97	0.98	0.98
C4f	9cm x 15cm, Door, SL	BOT		1.01		1.03	1.02	1.02

(Continued)

Table 2 (Concluded)

Figure	Nozzle	Test Cond	V_{mid}, cm/sec 22	43	59	74	E_h	Mean E_h
C4a	9cm x 15cm, with person	2ST		0.95		1.02	0.99	0.99
C4a	9cm x 15cm, 10 deg angle	MID		0.95		0.96	0.96	0.96
C4a	9cm x 15cm, 30 deg angle	MID		0.89		0.93	0.91	0.91
C4g	9cm x 15cm, 5.1 cm H	MID		0.93		0.93	0.93	0.93
C4h	9cm x 15cm, 5.1cm H, SL	BOT		0.88 0.93		0.95	0.93	0.93
C4i	9cm x 15cm, 5.1cm H, 5.1cm SL	BOT		0.89		0.93	0.91	0.91
C4j	9cm x 15cm, 30 cm H, CL	BOT		0.92 0.93		0.96 0.98	0.95	0.95
C5a	7.6cm x 7.6cm	MID		0.78		0.91	0.84	0.84
C5b	7.6cm x 7.6cm, H, CL	BOT MID		0.89 0.94		0.93 0.96 1.02	 0.92 0.98	0.95
C6	7.6cm x 7.6cm (H-S)	BOT MID	1.32 1.23	1.30 1.24	1.48 1.20	1.44 1.35 1.26	 1.37 1.23	1.30
C7	20cm x 24.4cm,	BOT	1.14	1.10		1.19	1.14	1.14
C8	24.4cm x 20cm,	BOT		1.05		1.15	1.10	1.10

(Sheet 3 of 3)

flow speeds ranging from 94 to 133 cm/sec. The streamer trap nozzle with a hydraulic efficiency closest to optimum (E_h = 0.94) was the C nozzle. Both the DUCK85 and SUPERDUCK nozzles had hydraulic efficiencies near optimum over the full range of flow conditions (E_h = 0.88 and 0.90, respectively).

Flow visualization tests

48. String and dye were used as qualitative indicators of flow patterns around selected nozzle types. Several pieces of string approximately 30 cm in length were tied to two steel reinforcement bars which were placed upright in front of nozzles, as indicated in Figures 17a and b. The string became aligned with the flow, giving qualitative indications of flow patterns in the vicinity of the nozzle. The only nozzle with a noticeable effect on the string patterns was the H-S trap, which tended to suck the string into the nozzle. Dye released from a plastic tube immersed in the flow gave similar qualitative information about flow characteristics in the vicinity of the nozzle, with the H-S trap exhibiting a similar suction effect.

Summary of Hydraulic Test Results

49. From the hydraulic tests, four nozzles were identified for further analysis: the SUPERDUCK and C nozzles, because of their near-optimum hydraulic efficiencies; the DUCK85 nozzle, because it had been used in the DUCK85 field project, is easy to manufacture, and proved to have a hydraulic efficiency close to unity; and the H-S nozzle for comparison.

50. Figures 18 and 19 present the uniform flow (midflow) and bottom flow hydraulic efficiencies and standard deviations for the four nozzles at the four flow conditions (V_{mid} equal to 22, 43, 59, and 74 cm/sec). Values of hydraulic efficiency at each measurement point (Figure 16) in the nozzle were used to calculate the standard deviation. The hydraulic efficiency at each point in the nozzle was calculated by dividing the flow speed at a point with the trap in place by the ambient flow speed at that same point. Lengths of vertical lines at each point represent one standard deviation about the mean. Standard deviations therefore give an indication of the spatial variability of flow speed at the nozzle. Figure 20 presents the variation in hydraulic efficiency with flow speed for the two-streamer (2ST) tests. The SUPERDUCK

(a) Streamer trap

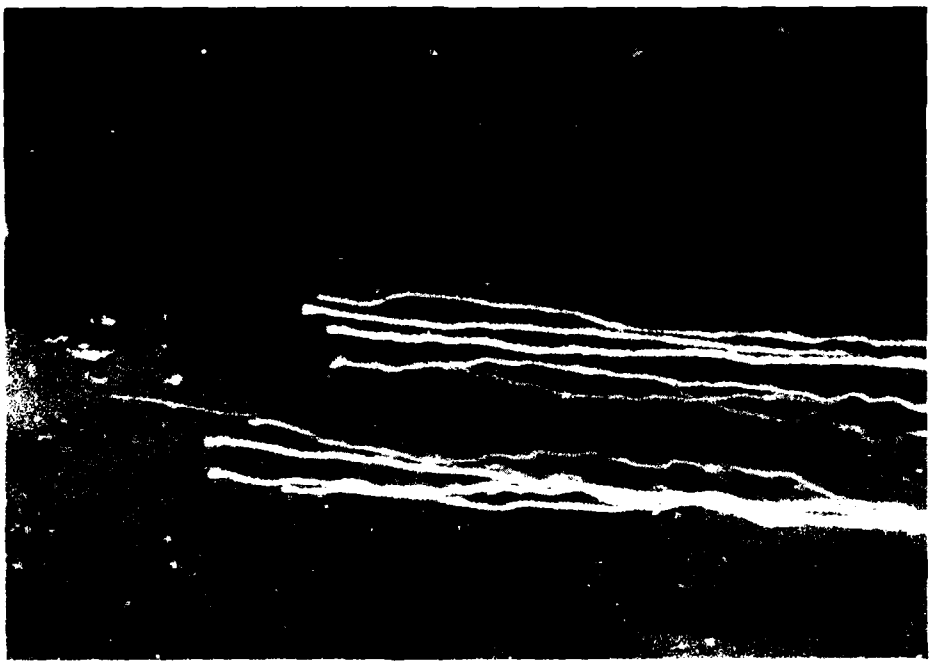

(b) Helley-Smith sampler

Figure 17. Flow visualization around nozzles using string

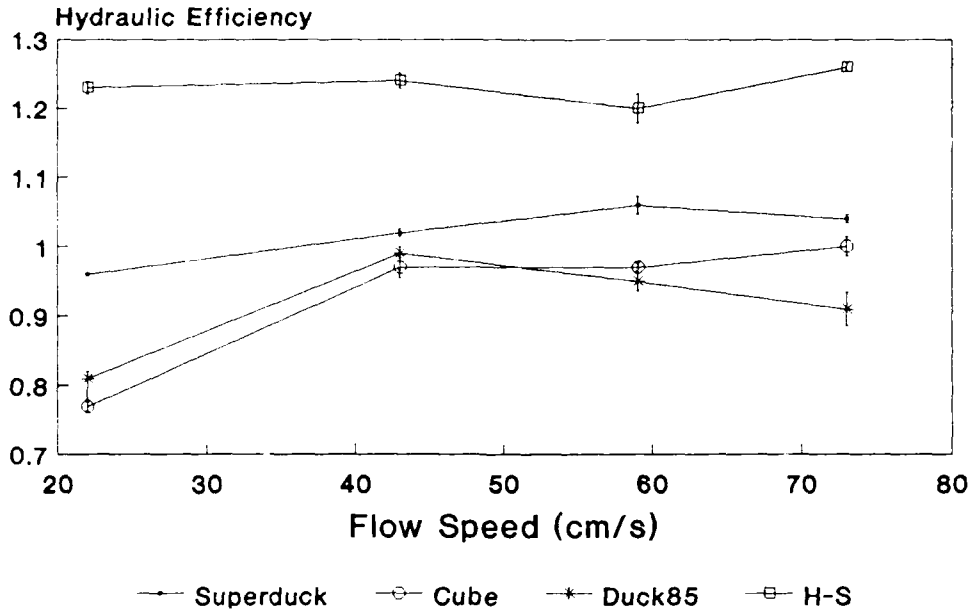

Figure 18. Midflow hydraulic efficiency

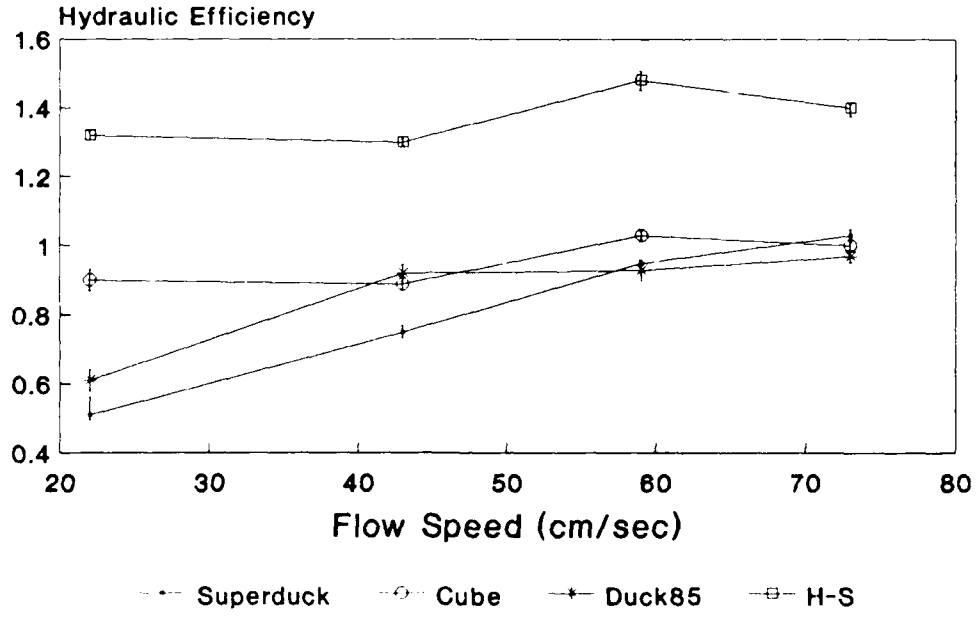

Figure 19. Bottom flow hydraulic efficiency

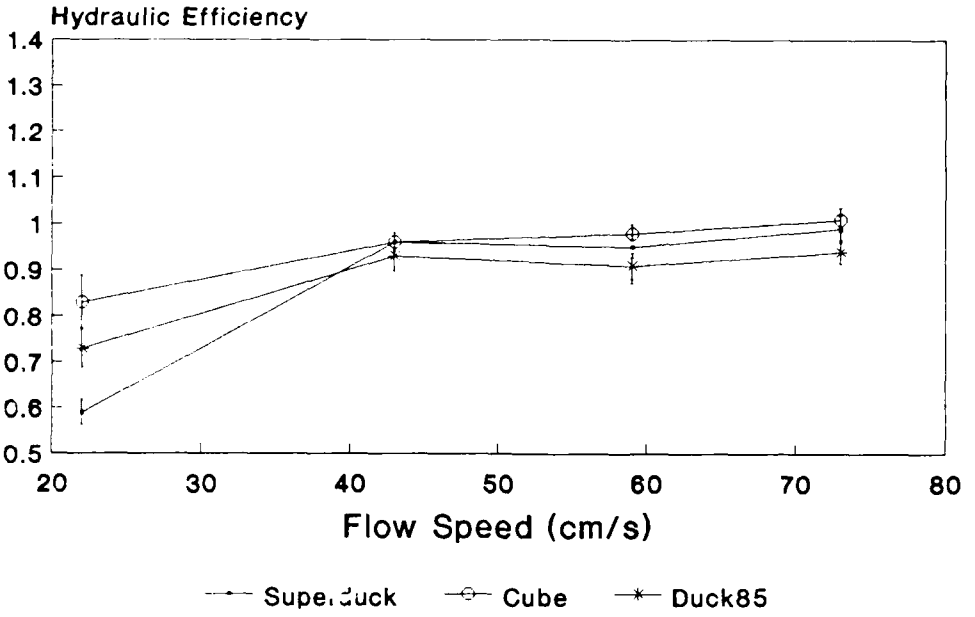

Figure 20. Hydraulic efficiency with midflow speed

nozzle had hydraulic efficiencies closest to unity for the uniform flow case; however, the C nozzle performed best for the bottom flow condition. Both the DUCK85 and SUPERDUCK nozzles had low hydraulic efficiencies for the lower flow speeds in Figure 19 (bottom flow condition).

51. The H-S sampler consistently had hydraulic efficiencies greater than unity, with significant variations in flow speed at the nozzle at higher flow rates. The C nozzle had the highest average efficiency for the two-streamer tests, with the SUPERDUCK and DUCK85 nozzles having similar efficiencies (Figure 20).

52. Table 3 presents a summary of the average hydraulic efficiency for each nozzle for each testing condition (on bed, off bed, and two streamers). The maximum standard deviation for a nozzle for a flow speed during a particular testing condition was chosen as a conservative representative value. These four nozzles, as well as selected other nozzles of special interest, were further examined in the sand-trapping test (Part IV).

Table 3

Average Hydraulic Efficiency and Standard Deviation for Each Nozzle Tested

Testing Condition	DUCK85	SUPERDUCK	CUBE	H-S
BOT (on bed)	0.86+/-0.031	0.81+/-0.033	0.96+/-0.031	1.38+/-0.029
MID (off bed)	0.92+/-0.024	1.02+/-0.013	0.93+/-0.015	1.23+/-0.021
2ST	0.88+/-0.043	0.87+/-0.029	0.95+/-0.059	----

PART IV: SAND-TRAPPING EFFICIENCY TESTS

53. The hydraulic efficiency tests described in Part III were designed to quantitatively determine the degree to which nozzles and streamers disturbed the fluid flow. However, sand particles moving on or off the bed may behave differently than fluid particles, possibly moving at lower speeds and having different paths of movement. For example, the velocity of a sand particle has a constant vertical component (fall speed). A moveable bed has a different roughness than the grass mat used in the hydraulic tests, resulting in a different time-varying vertical profile of flow speed as the bed surface changes. In addition, an apparatus installed on the bed to collect bed load may cause scour, thereby artificially increasing or decreasing the local transport rate. Therefore, an experiment was conducted to measure the sand-trapping efficiency of nozzles placed on the bed or completely in the flow off the bed to provide an indication of how well the nozzles predict ambient sand transport.

54. Sand-trapping characteristics of selected streamer trap nozzles were evaluated in the unidirectional flow tank described in Part III. Nozzles found to have near-optimal hydraulic efficiencies, as well as nozzles with characteristics designed to decrease scour at the bed (straight and curved bottom lips), were examined in the sand-trapping efficiency tests. The H-S sampler, a riverine sampler discussed in Part III and Appendix A, was also evaluated for comparison.

55. The purpose of these tests was to quantify the sand-trapping efficiency of nozzles with previously determined near-optimal hydraulic efficiencies over a range of flow speeds and bedforms representative of the surf zone. Sand-trapping efficiency E_s is defined as the ratio of a trap-predicted sand transport rate q_t (weight per unit width per unit time) to the ambient sand transport rate q_o (weight per unit width per unit time) that occurs for the same flow condition without the trap:

$$E_s = \frac{q_t}{q_o} \tag{8}$$

Qualitative characteristics of bottom nozzle behavior in the sand environment, particularly the potential for scour, were also observed. Part IV describes the trapping efficiency tests and presents sand-trapping rates and efficiencies for each nozzle tested.

Experiment Design

Measurement of ambient sand transport rates

56. An evaluation of nozzle sand-trapping efficiency requires either a measurement or reliable prediction of the ambient sand transport rate occurring over the range of flow conditions tested. Methods considered to measure this rate include: a streamer large enough to fit at the rear of the tank to collect all moving sand; a syphon concentration sampler to sample suspended sand at various elevations; dyed sand to serve as a tracer for sand movement; and a pit sampler. Appendix A gives a description of the latter three methods.

57. A streamer of cross section 0.76 by 0.76 m constructed to fit tightly inside the rear of the tank and collect moving sand was tested and rejected as a method to measure the total ambient sand transport rate. This giant streamer presented a large obstruction to the flow and significantly altered flow conditions as compared to the situation with only a single streamer trap in the tank. It would have been extremely difficult to achieve the same with- and without-large streamer flow conditions, and there was concern about maintaining structural integrity of the giant streamer throughout the tests. The giant streamer concept was therefore abandoned.

58. Collection of a representative sand concentration with a syphon concentration sampler involves positioning the intake tube exactly in the direction of the flow and withdrawing the sample at the flow speed. This type of sampler was not chosen because it would have been beyond the time and cost limitations of this experiment to develop, test, and use, including preparation of a sand sample collection facility. Also, concentration methods do not provide a direct measurement of the transport rate; rather the rate must be calculated as the product of concentration and flow speed. Finally, bed-load sand transport rates, expected to be the dominant mode in the unidirectional flow tank, could not be measured by using this method.

59. The use of sand tracer to predict sand transport rates is a labor-intensive process. This method of measuring ambient sand transport rates was rejected because of tedious data reduction, time constraints, and the expected variability in repetitive tests.

60. A pit sampler consists of an open area at the bed into which moving sand falls either as contiguous bed load or descending suspended particles. After some experimentation, three basins located adjacent to each other in the direction of flow were implemented as a means of measuring the ambient sand transport rate. The pit sampler, or catch basin, was constructed as a series of three sections aligned in the direction of flow so that suspended load would settle in the downflow basins and give an indication of the efficiency of the pit sampler itself by the relative amounts of sand trapped in successive sections. An efficient sampler would presumably show a small amount of material in the farthest downflow basin. The pit sampler method was chosen for its simplicity and inherent nonintrusiveness to the flow.

Test section

61. The unidirectional flow tank used for the hydraulic tests described in Part III was modified for the sand-trapping tests. A 15.2-m-long test section consisting of a 3.0-m-long ramp, a 6.1-m-long sand transport testing area that was 15.2 cm deep, and a 6.1-m-long pit (divided into three catch basins) was installed in the tank (Figure 21). The test section was made of 2- by 6-in. (5.1- by 15.2-cm) wooden boards at the sides and cut plywood for the ramps. The entire apparatus was tightly wedged into the tank and caulked along the sides. The sand transport testing area served to contain the sand used in the experiment and provided a reference volume to be filled with sand and leveled prior to each run. Quartz sand with a median grain size of 0.23 mm was used.

62. Large sheets of monofilament sieve cloth identical to the streamer cloth were secured to the bottom of individual catch basins using tacks. Sand transport rates without the trap for a range of flow conditions were determined by the quantity of sand collected in the cloths placed as linings in these basins over the sampling interval.

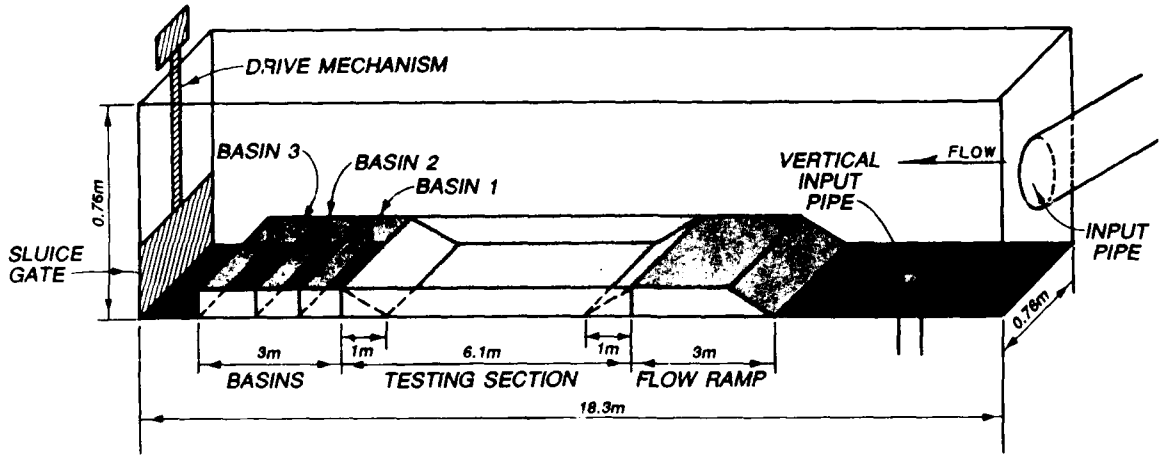

Figure 21. Test section used in sand trapping tests

Flow and Transport Conditions

Comparison with other measurements

63. During the transport rate tests, the condition of the bed surface was recorded. The type of sand motion and the configuration of the bed surface were characterized by the Reynolds and Shields numbers, as will be discussed in this section with reference to Figure 22.

64. Figure 22 may be compared to a three-dimensional diagram proposed by Southard (1971) to characterize bed configurations in uniform open-channel flow. He used the variables of depth, mean flow speed, and sediment grain size. Southard's diagram was presented as a series of depth-flow speed sections (graphs) for various sediment grain sizes. Therefore, the bed configuration and transport rate in uniform flow are functions of water depth, indicating that Figure 22 is not universal but pertains to the 20-cm depth used in the experiment. Simons, Richardson, and Nordin (1965) discuss bedforms generated under uniform flow in a large tank.

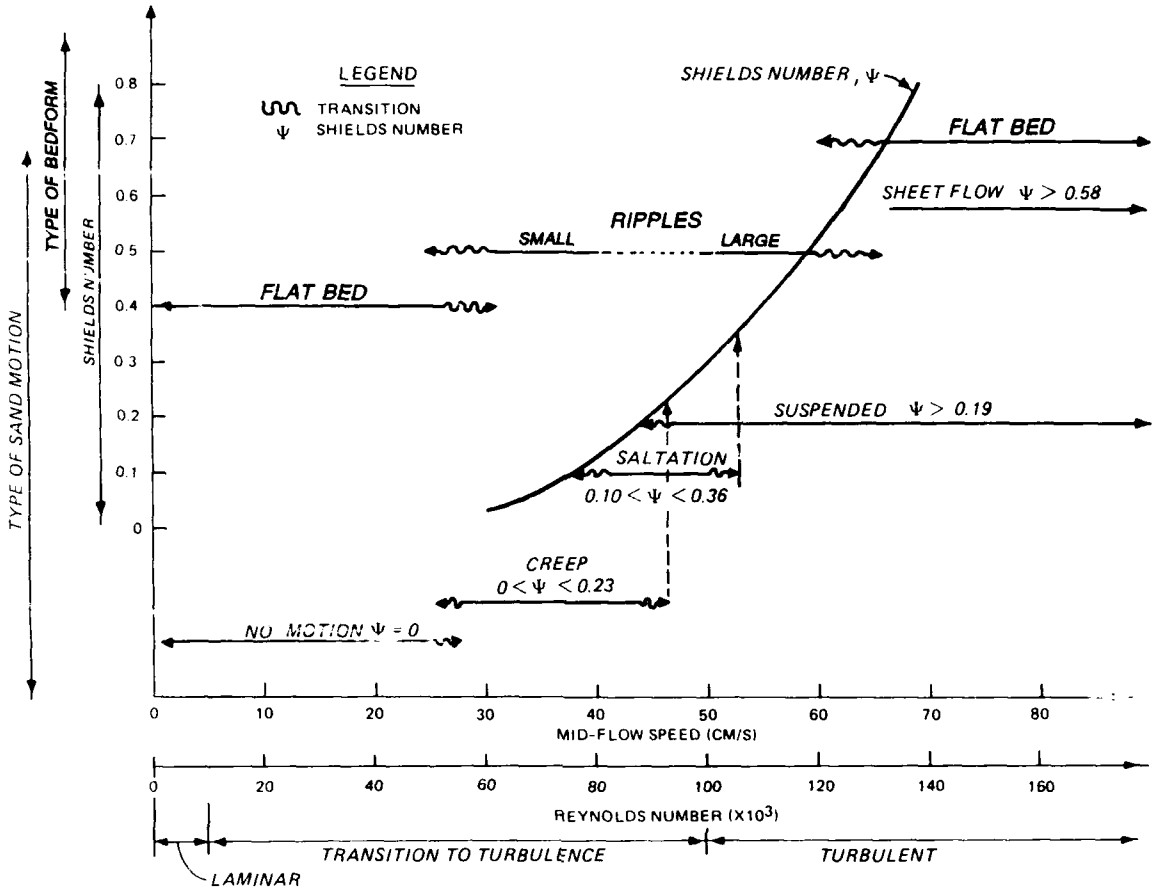

Figure 22. Bed configuration and sand movement as a function of midflow speed, Reynolds number, and Shields number

65. Water depth and flow speed were controlled by raising and lowering a sluice gate at the end of the tank and by opening or closing the flow input pipe (Figure 21). Water depth for all sand transport tests was fixed at 20 cm. This water depth allowed two to three nozzles (depending on nozzle design) to be fully immersed in the flow and produced a flat-bed (sheet-flow) transport condition as normally exists in the surf zone (absence or near absence of bedforms) at higher flow speeds. Water temperature over the course of the 1.5-month-long experiment was approximately 20° C.

66. The threshold flow speed for sand movement in the 20-cm-deep water was found to be 28 cm/sec in the middle of the water column and 18 cm/sec approximately 0.5 cm (half probe diameter) from the bed. Significant sand movement occurred at flow speeds greater than 42 cm/sec. At the 42-cm/sec

midflow speed, material rolled and saltated along the bed. The use of high flow speeds was found to be limited by the depletion of sand in the test section because of the resultant high transport rate. The practical upper limit on flow speed was found to be 72 cm/sec, and the mode of sand movement at this high flow condition was full sheet flow

67. The Reynolds number is the dimensionless ratio of the inertia force to friction force; two flows are dynamically similar if the Reynolds number is equal for both. Use of the Reynolds number to model flow conditions presumes that gravitational force is neglected, implying that the free surface boundary is not of significance and that buoyancy balances the force of gravity in the interior of the fluid. Reynolds numbers Re were calculated and compared for both laboratory and typical field conditions to verify that the field flow regimes were replicated in the tank as follows:

$$Re = \frac{VD}{\nu} \tag{9}$$

where

V = midflow speed (laboratory) or longshore current speed (field)

D = characteristic depth, taken as the water depth in the tank (laboratory) or average water depth in the surf zone (field)

ν = kinematic viscosity of water at 20° C, equal to 0.0100 cm^2/sec (fresh water) or 0.0105 cm^2/sec (salt water)

68. Reynolds numbers determined for the tank tests for the 42 and 72 cm/sec midflow speeds ranged from approximately 80,000 "transition to turbulence," to 140,000 "turbulent," according to White (1979). Mean longshore current speeds measured during trap deployments at the DUCK85 field data collection project varied from 11 to 31 cm/sec (Kraus and Dean 1987), with a representative surf zone depth equal to 1.0 m, resulting in field Reynolds numbers ranging from 105,000 to 295,000 "turbulent" (White 1979). Therefore, typical nonstorm field conditions can evidently produce turbulent flow even if the dissipation of wave energy due to breaking in the surf zone is not taken into account. Comparison of the Reynolds numbers indicates that the laboratory conditions were comparable to those in the surf zone. However, it is

noted that additional turbulence is injected into the water column by wave breaking in the surf zone.

69. The Shields number is used as an indicator of incipient motion and type of bedform development both in unidirectional flow (Shen 1971, Vanoni 1977) and the surf zone (Madsen and Grant 1976, Nielsen 1979, Watanabe 1988). Shields numbers were calculated for the range of midflow speeds used in the laboratory (Figure 22) and compared with Shields numbers for the surf zone to indicate how well the laboratory transport condition replicated field conditions. The Shields number Ψ is defined as

$$\Psi = \frac{\rho U_*^2}{(\rho_s - \rho) g d_s} \tag{10}$$

where

ρ = density of water, taken as 1 g/cm^3

U_* = shear speed, obtained empirically as a function of midflow speed from Figure 23 (cm/sec)

ρ_s = density of sand, taken as 2.6 g/cm^3 for quartz

g = acceleration due to gravity, 980 cm/sec^2

d_s = mean diameter of sand, 0.023 cm

70. The shear speed U_* was obtained empirically from a series of vertical flow speed profiles measured in the laboratory. By using the logarithmic law (see Part III), values of U_* and the representative roughness length z_o were calculated (Table 4). The profiles of flow speed over the movable bottom followed the logarithmic law well, as is evidenced by the high squared correlation coefficients r^2, ranging from 0.91 to 0.99. The large value of bed roughness z_o corresponding to a midflow speed equal to 45.7 cm/sec occurred with large bedforms that moved as sand was transported either as saltating or bed-load material. The empirical relationship of shear speed U_* as a function of midflow speed is presented in Figure 23.

71. As shown in Figure 22, the value of the Shields number at the observed inception of sheet flow in the laboratory was approximately 0.58. Values of Shields numbers for inception of sheet flow in an oscillatory flow tank have been found to be in the range of Ψ = 0.5 to 0.6, and other

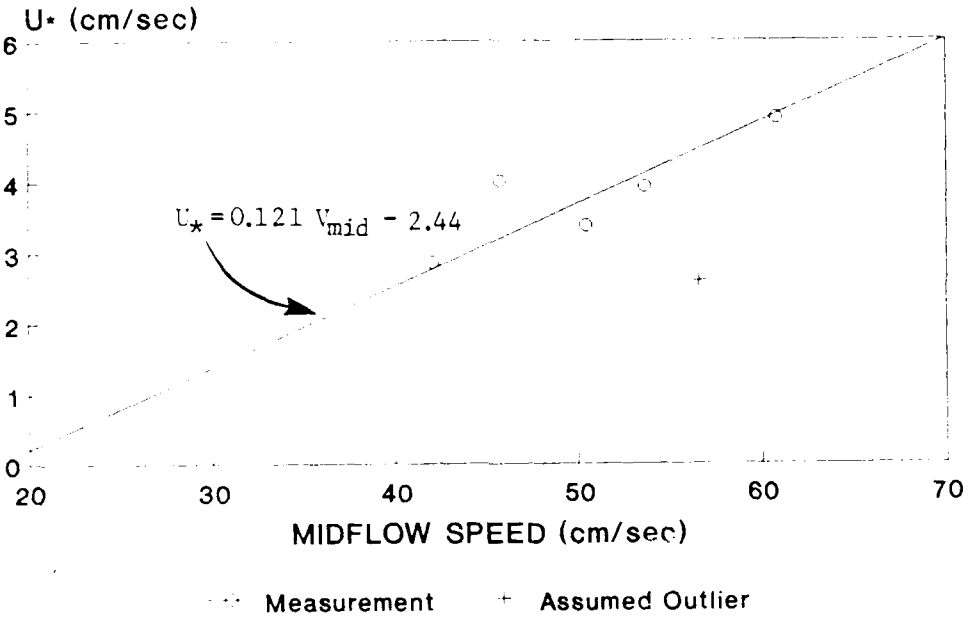

Figure 23. Relationship between shear flow and midflow speed

Table 4

Values of U_*, z_o, and r^2 as a Function of Midflow Speed V_{mid}

Midflow Speed V_{mid} cm/sec	Shear Speed U_* cm/sec	Representative Bed Roughness z_o cm	r^2
31.1	1.21	0.0003	0.97
42.0	2.86	0.035	0.91
45.7	4.00	0.13	0.99
50.4	3.38	0.038	0.97
53.6	3.92	0.049	0.97
56.6*	2.60	0.002	0.93
60.8	4.89	0.088	0.99

* Assumed outlier.

researchers have found values of the Shields parameter equal to 1.5 for inception of sheet flow in a large wave tank (Watanabe 1988). Therefore, the laboratory tests indeed replicated field sheet flow conditions.

Development of testing procedure

72. The development of a sand transport testing procedure that would simulate longshore transport in the surf zone (although with the absence of wave motion) and accurately test nozzle designs was more difficult than anticipated. The first procedure attempted for both the trap-predicted sand transport tests (nozzle tests) and the ambient sand transport tests (basin tests) began by establishing an equilibrium flow condition with equilibrated bedforms. The flow was then stopped and either the cloths tacked into the basins or the trap placed at the test section. The flow was reestablished and a test conducted for a specific time period. Finally, either the trap or the basin cloths were removed from the tank and the collected sand weighed.

73. However, a problem was encountered with this procedure. Sand transport rates measured with the traps and basins were found to depend on the relative location of the measurement device to transverse bedforms that migrated along the test section. When a trap nozzle was placed just downflow of a large sand ripple, the determined transport rate was much larger than when the nozzle was placed at the crest of a ripple. At lower flow speeds, ripples 10 cm in length migrated with a speed of approximately 0.6 cm/min; therefore, a 17-min-long testing period would be required to measure sand moving along a full ripple length. To observe the time variation of scour near the bed-load nozzle, it was desirable to have a 5- to 10-min testing interval on the order of the field tests. In addition, such bedforms moving in the direction of flow are not characteristic of surf zone conditions. The initial testing procedure did not result in reproducible measurements of both trap-predicted and basin sand transport rates within the 5- to 10-min time interval.

74. A transport regime similar to the surf zone (flat-bed transport) was found to occur for short time periods (5 min) if testing was begun from a smooth, flat-bed condition. A second testing procedure was therefore

developed in which the flow was started from a smooth-bed condition with either the basin cloths or trap in place, and sand was collected for approximately 5 minutes. However, significant scour occurred at the bottom nozzle over the time interval during which the flow speed increased from zero to the final testing flow speed. In contrast, it was found that scour at the bottom nozzle did not occur to such a degree when the trap was placed in a previously established flow. Two slightly different testing procedures for the basin and nozzle tests, outlined below, eliminated both the ripple formation and initial nozzle-scour problems described previously.

Testing procedure

a. Basin tests

(1) A test flow condition was established and setup parameters (aperture diameter of input pipe and height of sluice gate) were recorded.

(2) The surface of the sand test section was smoothed to a uniform thickness along the length of the section.

(3) The tank was filled from a vertical flow pipe (located at the far upstream end of the tank) until the sluice gate was overflowed. Slow filling of the tank prevented disturbance of the smoothed sand bed.

(4) Large sheets of streamer cloth were secured in the basins with tacks at the end of the test section.

(5) The vertical flow pipe was shut off, and a 2.5-min-long test was run to establish a 'startup' sand transport rate for the test flow condition. Midflow speeds at point A (Figure 21) approximately 6.1 m upstream from the basin were recorded during the test.

(6) After completion of a run, sand collected in the basins was weighed in a drip-free wet condition, which has been shown to be linearly correlated with the dry weight for sand-sized material (Kraus and Nakashima 1986). Selected sand samples were retained for laboratory analysis.

b. Nozzle tests

(1) The test flow condition was established and tank setup parameters (height of sluice gate, number of seconds input pipe opened) were determined with the trap frame and nozzles to be tested in place.

(2) Identical to basin test step (2).

(3) Identical to basin test step (3).

(4) The test flow condition was initiated and allowed to establish for 2.5 min.

(5) The trap was placed in the tank after an elapsed time of 2.5 min, and sand was collected for 5.0 min. Midflow and bottom flow speeds at Point A (Figure 21) were recorded during the test. The bottom nozzle's streamer bag was "swished" slightly back and forth in the flow during the testing period to eliminate settling of large slugs of sand which tended to settle near the nozzle entrance and reduce the area of the nozzle opening. Clogging of the streamer bags was an artifact of the laboratory flow environment. In the surf zone wave action clears streamer bags during typical field conditions.

(6) After a test was completed, collected sand was removed from the streamers, weighed in a drip-free state, and recorded. Selected samples were retained for laboratory analysis and comparison with the remaining bed material and the sand collected in the basin.

75. Steps a(1) through a(6) were then repeated for a 7.5-min test for the same flow condition, except that the longer testing period enabled both midflow and bottom flow speeds to be recorded in step a(5). The quantity of material collected during the 2.5-min run was subtracted from that collected during a 7.5-min run, with the same midflow speed, and divided by the elapsed time (5.0 min) and test section width (of the sand-filled area) to obtain an "equilibrium flow" basin transport rate for the 5-min run.

Sand-Trapping Efficiency Tests

76. One hundred and one nozzle and basin sand-trapping efficiency tests were conducted over a period of 40 lab days. Quantities of material collected in the basins and by each type of nozzle at each elevation in the flow are tabulated in Appendix D. Qualitative observations of nozzle performance during testing were conducted. The DUCK85 bottom nozzle began scouring around its outer edges immediately after testing began, and the scour increased

during the test until sand began passing under the nozzle near the end of the test. The SUPERDUCK bottom nozzle occasionally scoured around its outer edges, and sand would either pass around or under the outer edges. Sometimes scour would occur at the SUPERDUCK nozzle during the entire 5-min test; at other times it would be intermittent and disappear after a few seconds. The H-S sampler effectively behaved as a vacuum cleaner, creating turbulence and large-scale longitudinal eddies such that even sand to the rear of the sampler moved upstream and into the nozzle at the higher flow speeds. The H-S sampler thus dug into the bed and buried itself. Qualitatively, the C nozzle appeared to function optimally ("perfectly"). The moving sheet of sand and occasional small bedforms were observed to continuously enter unhindered into the nozzle. Nozzles with both long and short, straight and curved, bottom lips tended to enhance scour rather than reduce it.

Basin efficiency

77. The efficiency of the catch basins was qualitatively evaluated relative to characteristics of an ideal pit sampler. An ideally functioning pit sampler comprised of a large number of independent basins aligned in the direction of flow is expected to function as follows:

a. The quantity of sand collected in each basin would decrease in the downflow direction such that the farthest downflow basin would not collect any sand.

b. The quantity of sand collected in the downflow basins would increase as the midflow speed increased.

c. The sizes of grains collected in the downflow basins would increase as midflow speed increased, as the flow could entrain and transport larger-sized sediment.

78. In the experiment, the average percentages of sand collected in Basins 1 (upflow), 2 (middle), and 3 (downflow) were 97.7, 1.7, and 0.6 percent, respectively. The quantity of sand in each basin thus decreased significantly in the downflow direction. Figure 24 presents the percent of the total amount of sand collected in the second and third basins as a function of midflow speed. There is much scatter in the data; however, a trend for an increase in the quantity of sand collected in Basins 2 and 3 can be observed

if the data are averaged below and above a midflow speed equal to 60 cm/sec (approximate starting flow speed for sheet flow). The quantity of sand collected in the second basin increases from 1.3 percent for midflow speeds below 60 cm/sec to 2.0 percent for flows greater than 60 cm/sec. Similarly, the quantity of sand collected in the third basin also increases from 0.6 to 0.7 percent as the data are averaged below and above 60 cm/sec, respectively.

79. The expected tendency for grain size to decrease in the downflow basin was observed in the analyzed basin sand samples. For samples taken after a test with midflow speed equal to 68.7 cm/sec, median grain size decreased from 0.32 mm in Basin 1 to 0.22 and 0.21 mm in Basins 2 and 3, respectively. Since the basins used in this experiment program closely replicate all characteristics of an ideal basin, it is concluded that the basins were efficient.

Method of data analysis

80. The method for obtaining the sand transport rate for a particular trap deployed in the surf zone is to integrate the nozzle predicted fluxes (weight per unit area per unit time) through the sampling depth. The flux between nozzles is estimated by linearly interpolating from adjacent nozzle fluxes (see Part II). Because of the existence of eddies in the surf zone caused by injection of turbulence from the water surface, suspended sediment is typically more homogeneous through the water column than was observed in the laboratory. Linear interpolation of fluxes between nozzles does not appear reasonable for the laboratory measurements, since sand fluxes for adjacent streamers varied by more than an order of magnitude. The total sand flux at an elevation above approximately 5 cm from the bed in the laboratory tests was, at the most, an average of 4.3 percent of the sand flux at the bottom nozzle (Table 5). Therefore, linear interpolation for fluxes between streamers would introduce significant error into the calculations.

81. The 4.3 percent of sand flux occurring above 5 cm is probably lower in value, based on qualitative observations of nozzle performance. The percentage was calculated by totaling the upper nozzle sand flux, dividing that quantity by the bottom nozzle flux, and multiplying by 100 to obtain a percentage. Because of scour that occurred at the bottom edge of SUPERDUCK bottom nozzles during some flow conditions, the bottom nozzle flux may be too

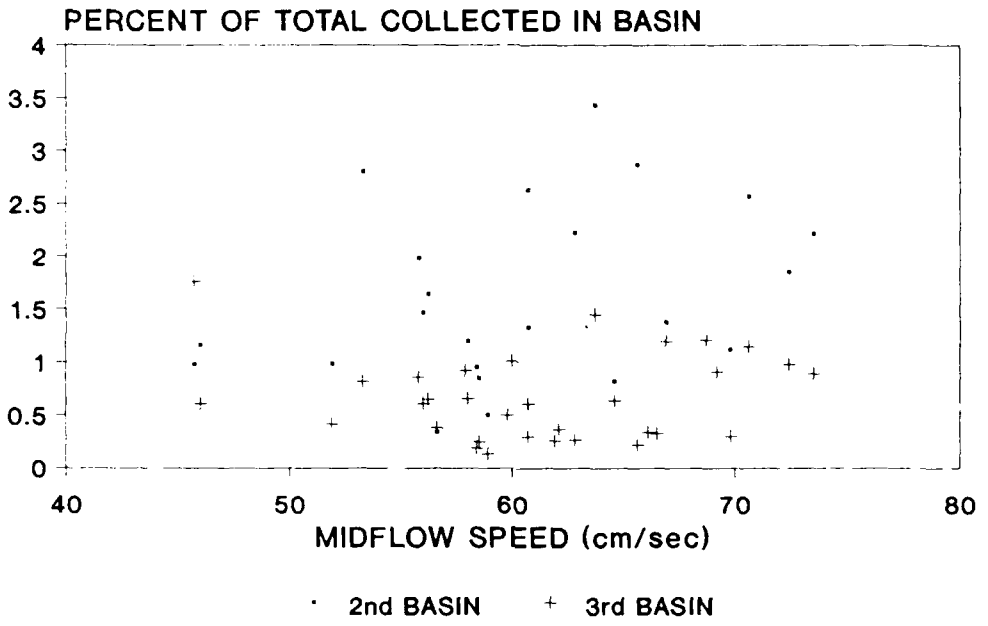

Figure 24. Percent of total sand collected in second and third basins

Table 5

Percent Sand Flux Measured above a Specified Elevation

Nozzle Type	Elevation cm	Number of Data Points	Percent Sand above Elevation	Standard Deviation percent
DUCK85	9.0	6	1.8	2.7
SUPERDUCK	4.5	20*	4.3	2.7
	4.8	2	2.8	3.0
	6.5	4	3.5	4.3
CUBE	8.3	9	1.0	1.6

* Omit outlier (Run 4, 4-6-88, 25.4 percent collected above 4.5 cm with mid-flow speed equal to 43.8 cm/sec).

small, thereby tending to increase the relative percentage of sand flux in the upper nozzles.

82. Either an exponential or a power law fit to the vertical distribution of sand flux could be used to mathematically interpolate for fluxes between adjacent nozzles. However, because only three vertical point measurements were available to fit the curves, this procedure was found to either over- or under-predict point measurements of sand flux by as much as 100 percent.

83. Because methods of integrating the vertical distribution of sand flux through the water column introduced unacceptable error into the data analysis, another approach was used to calculate sand-trapping efficiencies for the nozzles. It was assumed that nozzles collecting only suspended material (all those except the bottom nozzle) had a sand-trapping efficiency equal to their hydraulic efficiency. This procedure is considered reasonable for a quasi-steady unidirectional flow condition, implying that suspended sand behaves in the same manner as the fluid particles. This assumption should be acceptable for the grain sizes and flow conditions found on typical sandy beaches. However, bed load and saltating material near the bed were observed to move at lower speeds than the fluid flow. This characteristic of sand movement near the bed as well as the potential for scour near the lower edge of the bottom nozzle prohibited assigning a hydraulic efficiency equal to the sand-trapping efficiency to these lowest nozzles. Fluxes for the bottom nozzles and basin were calculated and compared using 5 cm as the maximum vertical elevation from the bed for significant (at least 96 percent of the total) sand transport. Sand fluxes for the bottom nozzles were then compared directly to the basin sand-trapping fluxes. It is noted that the 5-cm elevation delineating significant sand transport pertains to the present laboratory conditions and is not considered to be a general result.

Results

84. All nozzle and basin tests indicated increasing sand flux as midflow and bottom flow speeds increased. Four types of equations were fit to the transport rate data sets using the midflow and bottom flow speeds as the independent variable: linear, exponential, power, and a power fit incorporating the threshold midflow or bottom flow speed. Because of the short time

period of the 2.5-min basin tests, only the midflow speed could be measured and subsequently used as the independent variable. The different types of equations are as indicated below:

$$\text{Linear:} \quad F = aV + b \tag{11}$$

$$\text{Exponential:} \quad F = ae^{bV} \tag{12}$$

$$\text{Power:} \quad F = aV^{b} \tag{13}$$

$$\text{Power Threshold:} \quad F = a(V - V_*)^{b} \tag{14}$$

where

F = sand flux, in $g/cm^2/min$

a = empirically determined coefficient, with dimensions consistent with variables in equation

V = either midflow (V_{mid}) or bottom flow (V_{bot}) speed in cm/sec

b = empirically determined coefficient, with dimensions consistent with variables in equation

V_* = threshold midflow (28 cm/sec) or bottom (18 cm/sec) flow speed for sand movement, determined experimentally, in cm/sec

85. Table 6 presents the empirically determined coefficients and squared correlation coefficients resulting from regression analyses for each type of fit for each type of nozzle and basin test. Both the power fit and threshold power fit with the midflow speed had identical average squared correlation coefficients ($r^2 = 0.94$). Because most modern sediment transport formulae incorporate a threshold flow speed or shear velocity, the threshold power fit was chosen to represent the data and for use in further analysis. The term "threshold flow speed" V_* used in this analysis refers to the measured flow speed either in the middle or bottom (approximately 0.5 cm above the bed) of the flow corresponding to incipient motion. The threshold flow speed is related, but not equal, to the critical shear velocity U_{*c}, the shear velocity (discussed previously in the section entitled "Flow conditions") at incipient motion. Midflow as well as bottom and threshold flow speeds were used in this analysis rather than corresponding values of shear

Table 6

Constants and Squared Correlation Coefficients r^2 for Equation Fits to Basin and Nozzle Fluxes

Type of Test	Flow Speed	Coefficients*	Type of Equation: Linear	Exponential	Power	Power-Threshold
2.5 to 8-min basin test	V_{mid}	r^2	0.86	0.93	0.93	0.92
		a	0.239	$4.10(10^{-4})$	$9.05(10^{-15})$	$1.21(10^{-6})$
		b	-12.2	0.135	7.98	4.05
7.5-min basin test	V_{mid}	r^2	0.89	0.95	0.95	0.95
		a	0.251	$1.61(10^{-3})$	$8.79(10^{-13})$	$1.04(10^{-5})$
		b	-12.4	0.118	6.95	3.52
	V_{bot}	r^2	0.86	0.95	0.96	0.95
		a	0.299	$2.18(10^{-3})$	$1.82(10^{-11})$	$3.55(10^{-6})$
		b	-11.5	0.143	6.59	3.93
DUCK85	V_{mid}	r^2	0.85	0.97	0.97	0.98
		a	0.253	$2.79(10^{-7})$	$8.83(10^{-28})$	$6.86(10^{-14})$
		b	-14.9	0.231	14.9	8.40
	V_{bot}	r^2	0.82	0.96	0.97	0.97
		a	0.284	$1.08(10^{-7})$	$6.88(10^{-24})$	$4.79(10^{-14})$
		b	-13.2	0.264	13.5	8.71
SUPER-DUCK	V_{mid}	r^2	0.78	0.87	0.89	0.90
		a	0.309	$1.49(10^{-4})$	$8.50(10^{-17})$	$2.29(10^{-7})$
		b	-15.7	0.157	9.20	4.62
	V_{bot}	r^2	0.76	0.84	0.86	0.88
		a	0.344	$5.48(10^{-4})$	$7.21(10^{-14})$	$1.89(10^{-7})$
		b	-13.3	0.173	8.04	4.18
Cube	V_{mid}	r^2	0.83	0.99	0.99	0.98
		a	0.294	$6.54(10^{-4})$	$8.09(10^{-14})$	$1.78(10^{-5})$
		b	-13.5	0.143	7.67	3.53
	V_{bot}	r^2	0.85	0.98	0.98	0.98
		a	0.373	$8.43(10^{-4})$	$1.21(10^{-12})$	$3.11(10^{-6})$
		b	-13.2	0.178	7.47	4.16

* Dimensions of coefficients a and b are consistent with variables in the equation.

velocities because the former quantities were directly measured, whereas the shear velocity must be inferred from a flow speed profile.

86. Figures 25 and 26 present the 2.5- and 7.5-min basin-determined fluxes with the power threshold fit equations. A relationship for basin flux F with a 5.0-min testing period was obtained by subtracting values obtained with the 2.5-min equation from values obtained using the 7.5-min threshold power equation:

$$F = 2.06\ (10^{-5})\ (V_{mid} - 28)^{3.37} \tag{15}$$

87. Figures 27 through 29 present threshold power equations and data for the DUCK85, SUPERDUCK, and C nozzles, respectively. An equation was not fit to the H-S data; evaluation of this nozzle was terminated after two tests because of its unrealistic sand-trapping characteristics.

88. Sand flux data and power threshold predictive equations for the bottom nozzles and basin are summarized in Figure 30. The DUCK85 nozzle collected the least amount of sand over the flow conditions tested. Fluxes obtained with the SUPERDUCK nozzle fall quite close to the basin transport fluxes for most flow conditions. The SUPERDUCK fluxes with midflow minus threshold flow speeds ($V_{mid} - V_*$) from approximately 28 to 32 cm/sec show considerable scatter. Occasionally developed bedforms in this flow range were observed to occur as migrating ripples, and the SUPERDUCK nozzle occasionally scoured at the bottom lip in this flow range. Results for the H-S sampler lie far above values in the plot for the two flow conditions tested; indeed, the greater-than-unity hydraulic efficiency of the H-S sampler caused it to become buried in the test section almost to the top of the sampler.

Comparison of transport formulae

89. A comparison of the form of various transport formulae compiled from Sleath (1984) and Horikawa (1988) for both unidirectional and oscillatory flow was conducted to evaluate how well the laboratory tests agreed with theoretical and empirical relationships. Table 6 indicates that all of the threshold power formulae, with the exception of the DUCK85 equation, relate sand flux to a form of flow speed raised to a power ranging from 3.5 to 4.6.

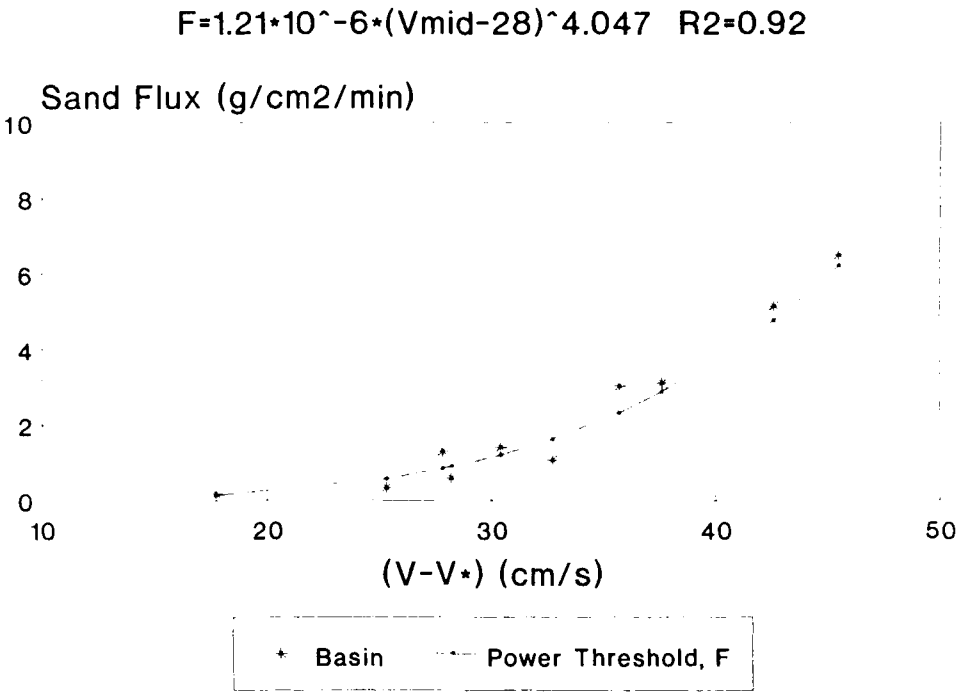

Figure 25. Basin flux for 7.5-min test

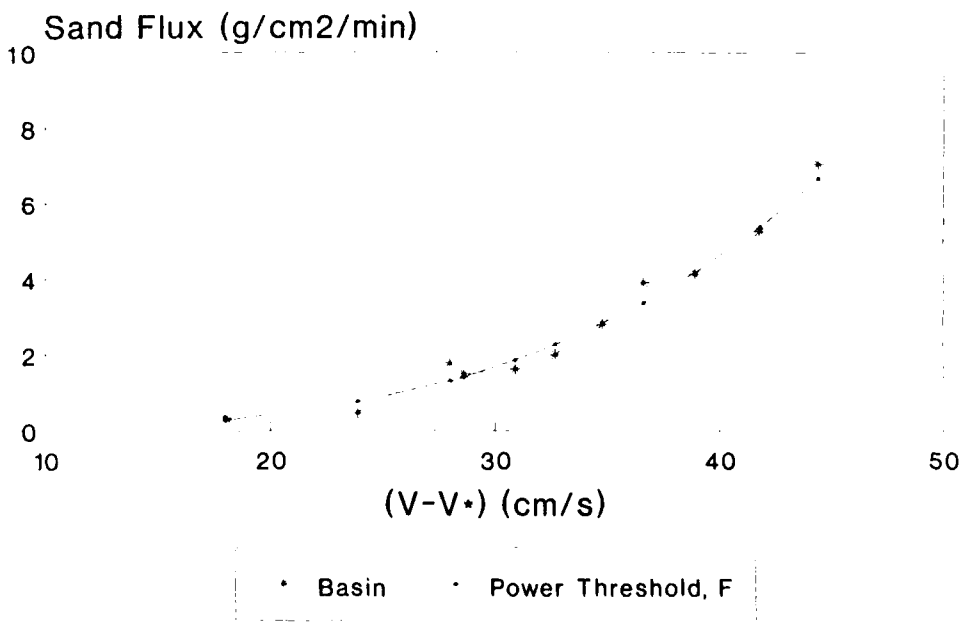

Figure 26. Basin flux for 2.5-min test

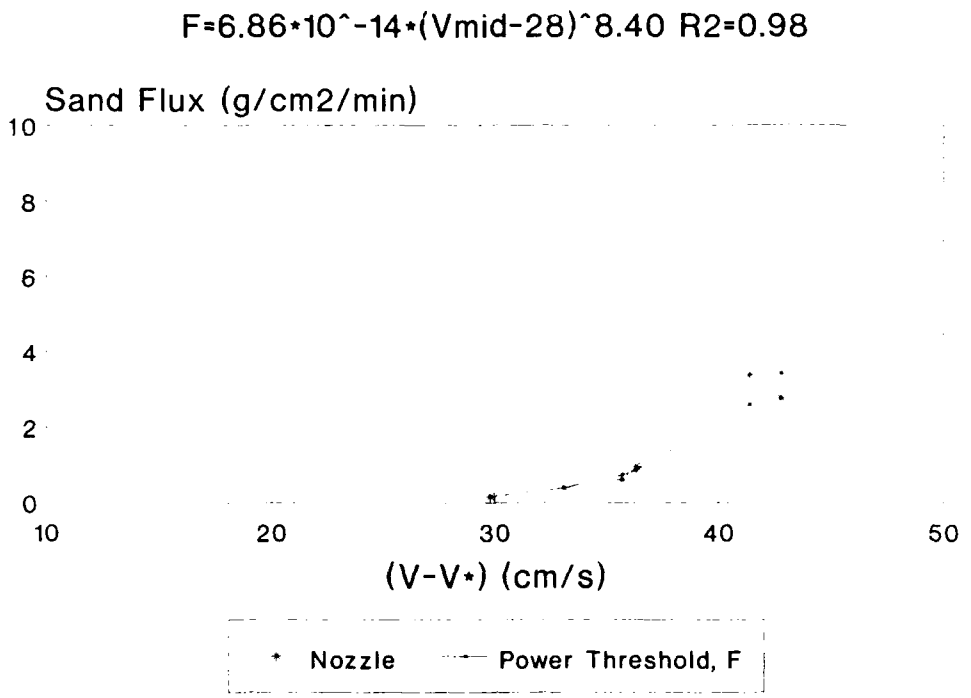

Figure 27. Flux measured with DUCK85 nozzle

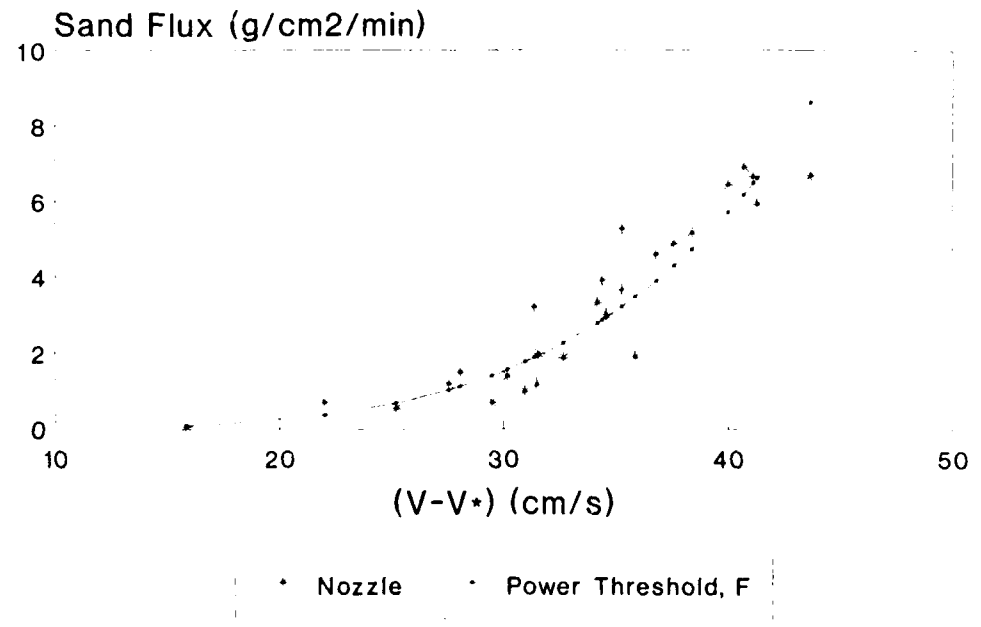

Figure 28. Flux measured with SUPERDUCK nozzle

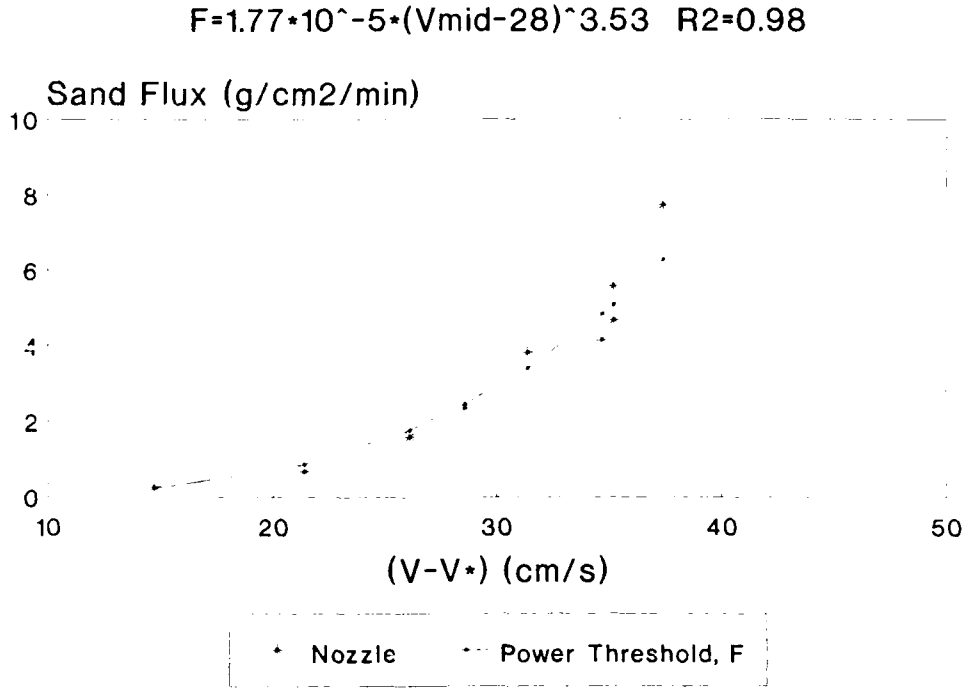

Figure 29. Flux measured with C nozzle

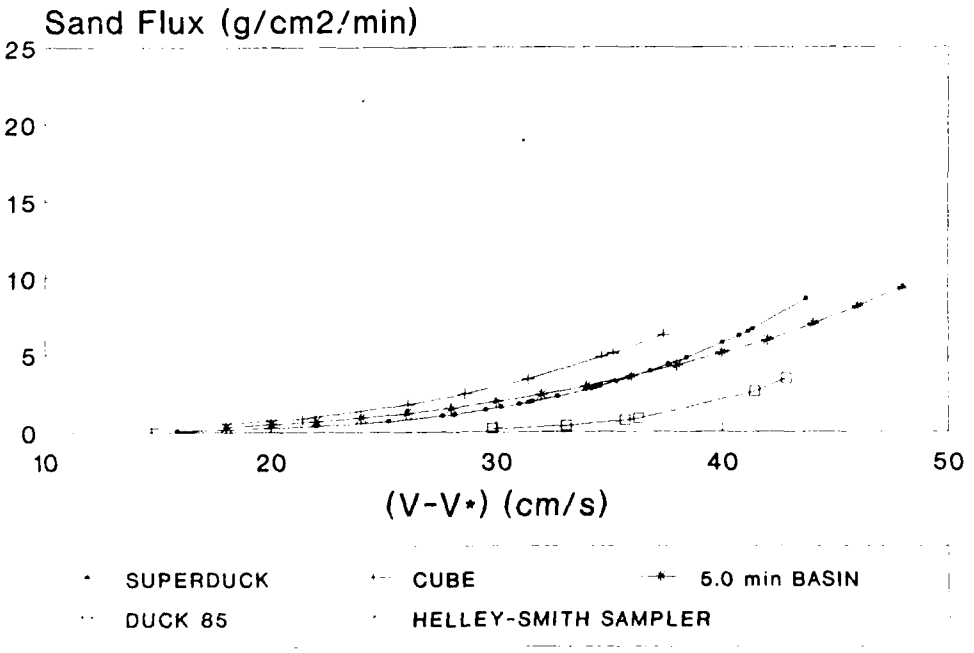

Figure 30. Summary of power threshold fits

Table 7 presents the relationship between bed-load transport Q_s and flow speed V for many transport formulae. The variables in Table 7 are defined as follows:

Q_s = volumetric bed-load transport

A, m, n = empirical coefficients

τ_o = shear stress at the bed ($\tau_o = \rho\ U_*^2$)

τ_c = critical shear stress at the bed ($\tau_c = \rho\ U_{*c}^2$)

U_{*c} = critical threshold shear speed

S = energy grade line

U_* = average shear speed

D = grain diameter

f = friction factor

u_m = maximum horizontal orbital speed

90. There obviously is a wide range in the power to which speed is raised in the sand transport relationships. The 3.5 to 4.6 range determined in the laboratory is reasonable if compared to the transport formulae presented in Table 7. Sawamoto and Yamashita (1986) related bed-load transport to the cube of the speed for a sheet flow condition, which agrees well with the powers of flow speed determined in the present experiment program. Kraus, Gingerich, and Rosati (1988) compared results from the SUPERDUCK field data collection project to the expression for sand transport given by Katori et al. (1984) and found that the field data agree well with Katori et al.'s transport formula expressed in terms of the flow speed cubed. Kraus, Gingerich, and Rosati (1988) developed an equation relating the total immersed weight longshore sand transport rate to a discharge parameter $R = H_b^2\ V$, where H_b is the breaking wave height if the surf zone bed is approximated as a plane sloping surface. The breaking wave height, however, is directly proportional to the maximum wave orbital velocity u_m. Therefore, the equation given by Kraus, Gingerich, and Rosati (1988) expresses the sand transport rate in the surf zone as $u_m^2\ V$ presented in Table 7. It is concluded that data from the present study are consistent with laboratory and field experiments relating sediment transport to flow speed raised to the 3rd or 4th power.

Table 7
Forms of Various Bed-Load Transport Formulae

Author/Date	Formula	Dependence of Q_s on V
DuBoys (1879)	$Q_s = A \tau_o (\tau_o - \tau_c)$	V^4
Waterways Experiment Station (1935)	$Q_s = \frac{A}{n} (\tau_o - \tau_c)^m$	V^m
Shields (1936)	$Q_s = A Q S \frac{(\tau_o - \tau_c)}{(\rho_s - \rho) g D}$	V^2
Kalinske (1942)	$Q_s = \bar{U}_* D f \frac{(\tau_o)}{(\tau_c)}$	V
Meyer-Peter-Muller (1948)	$Q_s = A \frac{(\tau_o - \tau_c)^{1.5}}{(\rho_s - \rho) g D}$	V^3
Brown (1950)	$Q_s = A D^{1.5} \Psi^3$	V^6
Madsen and Grant (1976)	Oscillatory flow	u_m^6
Hallermeier (1982)	Oscillatory flow	u_m^3
Sawamoto and Yamashita (1986)	Sheet flow	V^3
Katori et al. (1984)	Oscillatory tank with unidirectional current	V^3
Kraus, Gingerich, and Rosati (1988)	Field longshore sand transport	$u_m^2 V$

Experiment variability

91. The standard error of estimate (Miller and Freund 1985), an indication of the deviation of measured from predicted flux, was calculated for each type of nozzle and basin test using N-2 degrees of freedom as follows:

$$S_y = \left[\frac{\sum (f_m - f_p)^2}{N-2} \right] \quad (16)$$

where

S_y = standard error of estimate ($g/cm^2/min$)

f_m = measured flux ($g/cm^2/min$)

f_p = predicted flux ($g/cm^2/min$), calculated using the threshold power fit equations and midflow speeds

N = number of data points

92. The results of this analysis are presented in Table 8. Values of S_y are considered reasonable, with the SUPERDUCK nozzle and 2.5-min basin data having the highest error of estimate, followed by the 7.5-min basin data, and the DUCK85 and C nozzle results, respectively. If values of predicted flux f_p are taken to represent the true flux, then the error of estimate gives a measure of nozzle reliability. If transport processes in the vicinity of a particular nozzle occurred similarly for all flow conditions, then the nozzle would be easily modeled with a single equation, and the standard error of estimate would be lower in value. Transport processes with the SUPERDUCK nozzle were variable, with scour occurring approximately half the testing period. Scour consistently occurred at the DUCK85 nozzle; hence the lower error of estimate value. The low value of S_y calculated for the C nozzle reinforces the observed consistency in transport processes in the vicinity of the nozzle.

Table 8

Experiment Variability for Nozzle and Basin Data

Type of Test	Standard Error of Estimate $g/cm^2/min$	$t_{0.025}$ Statistic	Number of Data Points
2.5-min Basin	0.35	2.306	10
7.5-min Basin	0.22	2.262	11
DUCK85	0.20	2.776	6
SUPERDUCK	0.35	2.064	26
CUBE	0.17	2.365	9

93. Assuming that the measured fluxes are normally distributed about their respective mean values, the appropriate t-statistic can be utilized with the standard error of estimate to obtain confidence limits for the linearized empirical relationships, as follows:

$$\ln y = [\ln(a) + b \ln(x)] \pm t_{\alpha/2} \; S_y \sqrt{\frac{1}{N} + \frac{N\,[\ln(x) - \ln(\bar{x})]^2}{S_{xx}}} \qquad (17)$$

where y = dependent variable equal to sand flux

a, b = power law coefficients presented in Table 6

x = independent variable $V - V_*$, where V and V_* are as defined previously

$t_{\alpha/2}$ = t-statistic for 95 percent confidence interval

$\bar{x}$ = average x, where x is as defined above

$S_{xx} = N \Sigma x^2 - (\Sigma x)^2$, for $x = 1$ to N

94. The 95 percent confidence interval is used in the next section to determine whether certain test conditions were significantly affecting rates of sand transport in the tank.

Independent variables influencing sand transport

95. Two interesting facets that emerged during the tests were explored within time constraints of the project. It was noted that with elapsed time sand in the test section became coarser due to sorting by the flow. Sieve analysis indicated a median grain size of 0.30 mm after approximately 24 runs, compared to 0.23 mm for the originally placed material (Figure 31). The degree to which this sorting decreased quantities collected in the basin was evaluated for one 2.5-min basin test and two 7.5-min basin tests. Between two and eight shovelfuls of the winnowed (coarser) sand in the test section were removed and replaced by the original, finer material. The measured 2.5-min "new sand" flux was 3 percent greater than the flux predicted by a threshold power equation fit to the data set (Figure 32), and the two 7.5-min "new sand" fluxes were 17 and 19 percent less than equation-predicted fluxes (Figure 33). However, these deviations from the equation-predicted fluxes were within the 95 percent confidence limit and, therefore, in the range of experiment variability. The C nozzle measured 32 percent higher fluxes than predicted after three shovelfuls of original sand replaced the winnowed-out material (Figure 34). However, this deviation from the equation-predicted flux was

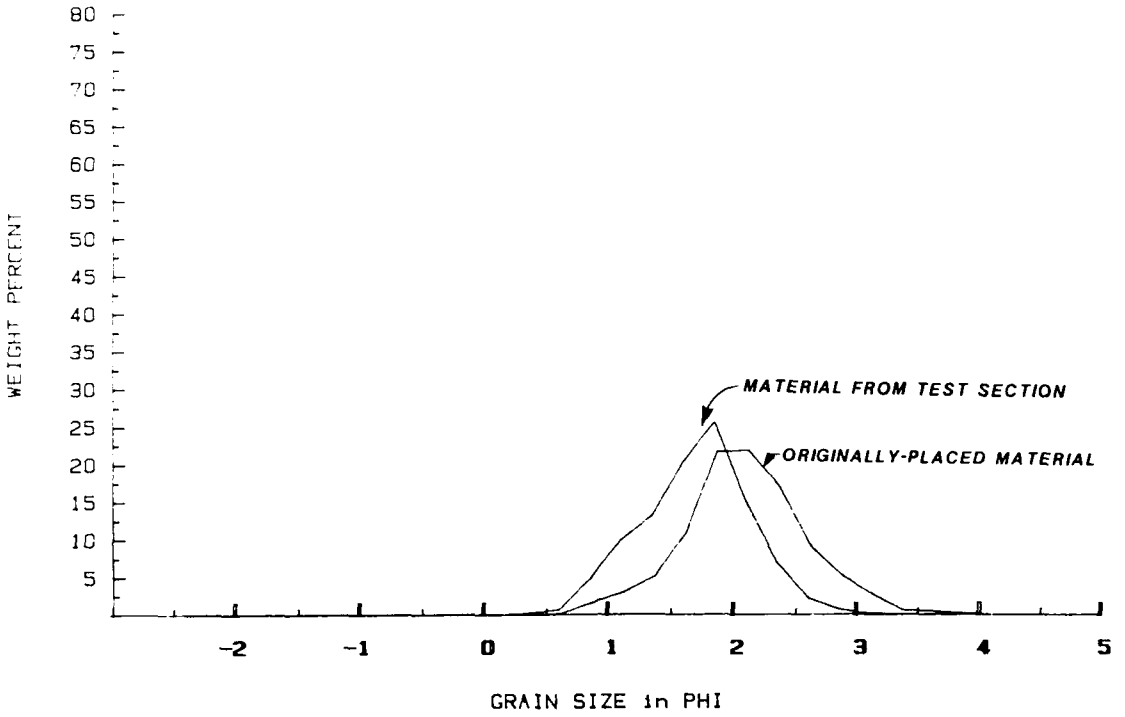

Figure 31. Grain size distributions

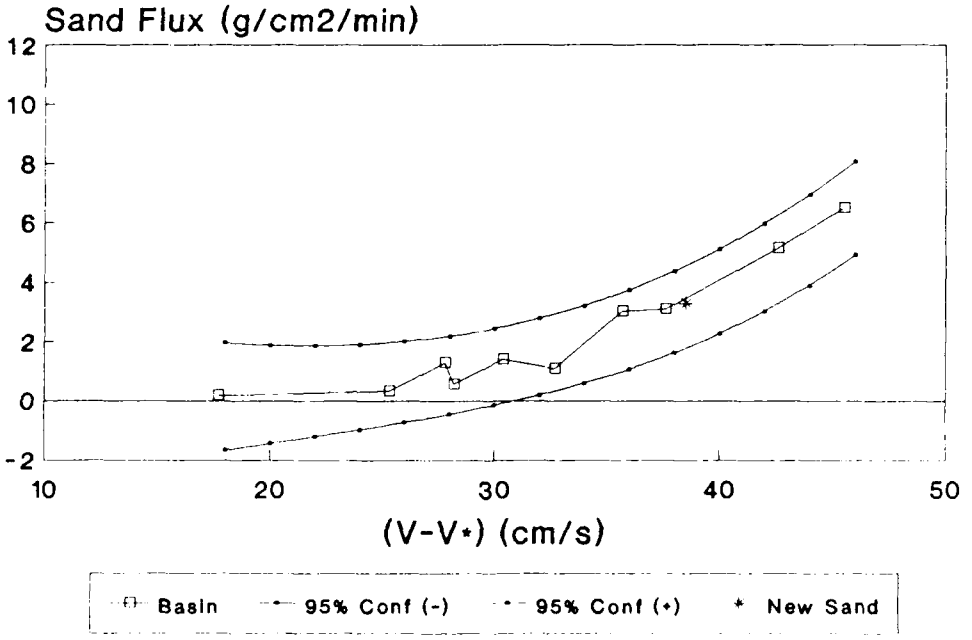

Figure 32. Basin flux for 2.5-min run with "new sand"

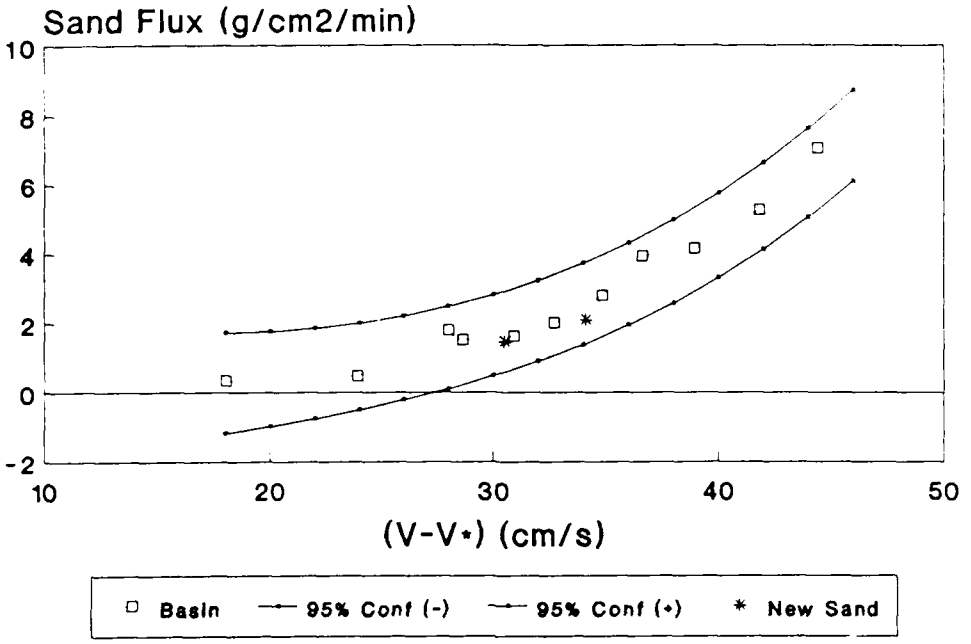

Figure 33. Basin flux for 7.5-min run with "new sand"

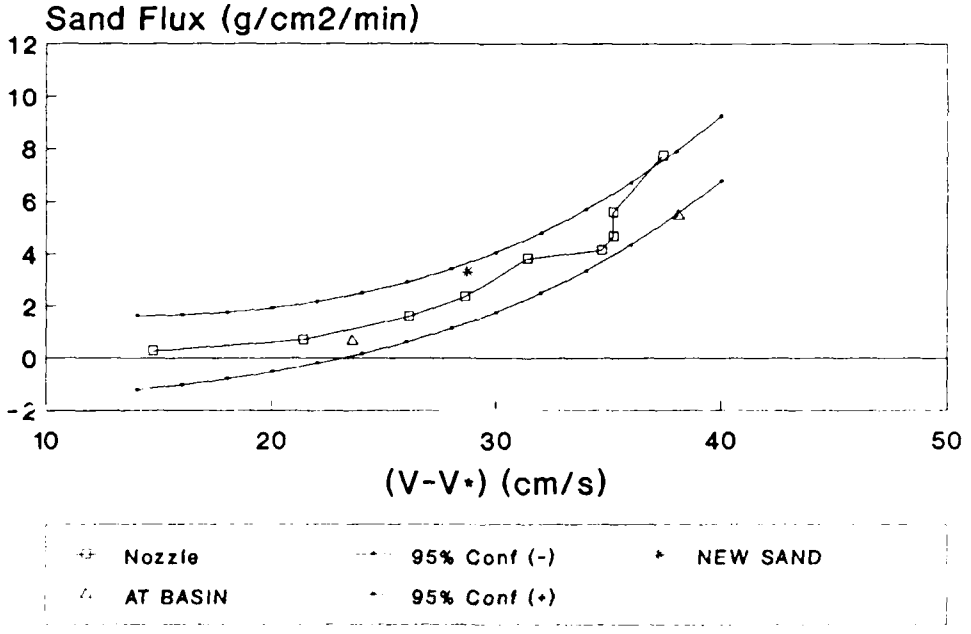

Figure 34. Flux measured with C nozzle

also within the 95 percent confidence interval and, therefore, is considered within the natural range of variability.

96. The second interesting but complicating aspect of the experiment was evaluation of a potential difference between basin-predicted sand transport rates in the central 24.8-cm-wide portion of the tank as compared to the entire width of the tank. A decrease in the sand transport rate might occur near the walls of the tank due to side wall friction; an increase in sand transport could occur in the far side of the tank due to the slight non-uniformity of the flow field established in the hydraulic efficiency experiment (see Part III). The differences (Diff.) between center- and full-width basin transport rates were evaluated for two 2.5-min and four 7.5-min basin tests (Table 9). Individual basin collection cloths extending through the first two basins were placed in the center (24.8 cm wide), near, and far (both 21.3 cm wide) "subbasin" sections of the tank. "Center" subbasin fluxes were consistently higher than those calculated for the entire width of the basin, averaging 11.4 percent higher. "Far" subbasin fluxes were also higher than those calculated for the entire width of the basin, in agreement with the trend of the non-uniform lateral flow speed distribution of the tank (Part III). The difference between "center" and total sand fluxes generally increased with midflow speed, as would be expected if the side wall boundary layer increased with flow speed.

97. The basin threshold power equation was modified to account for the increasing sand flux in the center portion of the tank using Equation 15, with the following additional empirical equation:

$$F = F_1 = 2.06(10^{-5}) \ (V_{mid} - 28)^{3.37}$$

$$F_2 = 5.03(10^{-6}) \ (V_{mid} - 28)^{3.78} \qquad (18)$$

where

F_1 = basin flux, $V_{mid} < 58$ cm/sec (g/cm^2/min)

V_{mid} = midflow speed, cm/sec

F_2 = basin flux, $V_{mid} \geq 58$ cm/sec (g/cm^2/min)

Table 9

Sand Fluxes in Center, Near, and Far Subbasin Sections of Tank

V_{mid} (cm/sec)	Testing Time (min)	Sand Flux g/cm²/min						
		Total	Near	Diff.	Center	Diff.	Far	Diff.
58.0	7.5	1.49	1.56	0.07	1.52	0.03	1.39	-0.10
59.8	7.5	1.93	1.60	-0.33	1.99	0.06	2.19	0.26
60.0	2.5	1.36	1.04	-0.32	1.39	0.03	1.63	0.27
66.1	7.5	4.19	3.68	-0.51	4.54	0.35	4.28	0.09
68.7	2.5	4.42	3.38	-1.04	5.28	0.86	4.44	0.02
69.2	7.5	4.98	3.83	-1.15	5.75	0.77	5.23	0.25
Avg				-0.55		0.35		0.13

98. The modified basin flux for a 5-min test and equation-predicted nozzle fluxes with the 95 percent confidence limits are presented in Figure 35.

Ambient Sand Transport Rate

99. The curve labeled "5-min Basin" in Figure 35 represents the basin transport fluxes to which the nozzle transport fluxes should, in principle, be calibrated. However, although the C nozzle-predicted sand transport fluxes are comparable to the basin transport fluxes at lower midflow speeds, as much as 45 percent higher values of flux were obtained with the C nozzle at higher speeds. There are at least five possible explanations for this discrepancy.

a. The C nozzle produced an increased flow speed in its vicinity, thereby collecting more sand than was actually being transported (similar to the H-S sampler).

b. The cloths used to collect sand in the basins were not sufficiently secured and allowed material to be lost from adjacent sections of cloth.

c. Sand transport at the basins was less than transport in the vicinity of the trap testing area.

d. Greater flow speeds caused increased suspended sand transport, which was not collected in the basins.

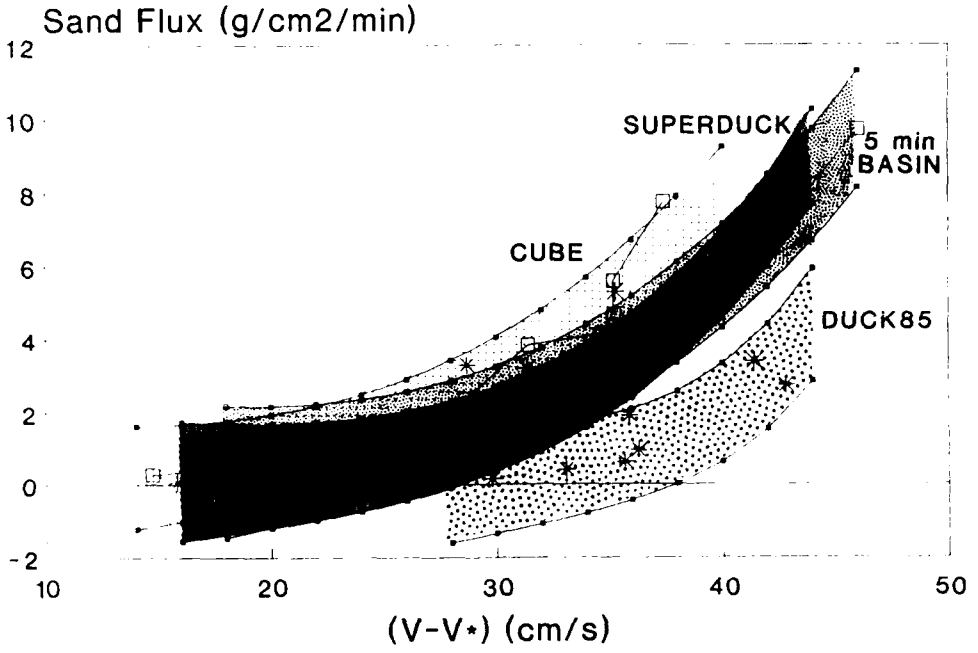

Figure 35. Modified basin flux for 5-min test and power threshold fit nozzle fluxes

e. Sand transport during all trap testing was greater than during basin tests due to an unknown systematic experimental error.

Each of the above-listed possibilities is discussed below.

a. The C nozzle increased flow speed in its vicinity. Because the hydraulic tests indicated an average hydraulic efficiency for the C nozzle of 0.95, this theory does not appear tenable. In addition, characteristics observed for the H-S pressure-difference nozzle (i.e., material moving from sides of the nozzle into the mouth; nozzle burying itself in test section) were not observed during testing of the C nozzle.

b. Loss of sand through basin cloths was significant. Loss of sand through adjacent basin cloths could have occurred, although a 45 percent loss of sand (approximately 1,100 g for 2.5-min and 4,300 g for 7.5-min basin tests) would have resulted in an obvious residue at the bottom of the basins after the cloths were removed (which was not found). Loss of sand through adjacent basin cloths could have occurred to some degree; however, this factor cannot account for the entire discrepancy.

c. Sand transport at the basin was less than at the trap testing area. To evaluate this effect, two runs were made with the C nozzle placed at the first basin for midflow speeds equal to 51.6 and 66.1 cm/sec. The sand flux for the bottom C nozzle at the basin for the two tests was less (48 and 19 percent, respectively) than equation-predicted fluxes for the same flow rate (Figure 34). The test at the higher flow condition was approximately equal to the lower 95 percent confidence limit, indicating that sand flux at the basin did vary significantly (with 95 percent confidence) than sand flux at the trap testing area, at least at the higher flow condition. The differences between C nozzle fluxes measured at the basin and predicted fluxes using the modified 5.0-min basin threshold power equations (Equations 15 and 18) indicate that the C measurements at the basin were within the 95 percent confidence interval for the basin data.

d. Suspended material passed over the basins at the higher flow speeds. A qualitative evaluation of basin efficiency presented in a previous section (see "Evaluation of basin efficiency") concluded that the basins were highly efficient. The quantities of sand collected above the bottom C nozzle for the 51.6-cm/sec midflow speed test described in c were greater (4.1 percent) than observed for the C nozzle data set (Table 5). However, the 66.1-cm/sec midflow speed test percentage of suspended sand was not significantly greater (1.7 percent), contrary to an expected increase in suspended sand at higher flow speeds. Apparently, the 4.1 percent of suspended sand collected above the bottom nozzle during the lower flow speed test is an anomaly. Sand samples from both nozzle and basin tests were sieved to provide some indication of whether the C nozzle did collect finer material (hence suspended sand) that was not collected in the basins. The median grain size for the bottom C nozzle for five samples analyzed was 0.29 mm, equal to the median grain size for the SUPERDUCK nozzle and larger than the median grain size for the DUCK85 nozzle (0.27 mm) and basin (0.26 mm). A larger median grain size for the C nozzle would indicate that the nozzle did create a pressure difference, collecting more material than was actually being transported. The H-S sampler created local flow speeds greater than the ambient flow speed and therefore was able to entrain and collect larger-sized material (median grain size for H-S = 0.33 mm). However, sand collected in midflow C nozzles was also coarser than that collected in the SUPERDUCK midflow nozzles (C = 0.26 mm; SUPERDUCK = 0.19 mm), indicating that the sand in the test section was generally coarser during the C nozzle tests which were conducted near the end of the experiment program.

e. Sand transport during all trap tests was higher than during basin tests due to a systematic error. As discussed in item c above, one test conducted with the C nozzle located at the basin gave sand transport rates less than that of the C nozzle tests at the trap testing area. Therefore, a systematic error did not occur

exclusively for the trap tests, as a large difference was measured with the same trap nozzle at two different locations.

100. One theory that may explain the discrepancies in sand flux measured at the trap testing area compared to fluxes at the basin (see item c) is that the trap testing area was located in the test section such that flow conditions had not equilibrated with the sand bed. Large eddies potentially caused by the transition from the test section ramp to the sand bed at the upflow end of the tank may have entrained more material, thereby creating an artificially high transport rate at the trap testing area (Figure 36). At the far end of the test section, the basin could have been outside the "equilibrium length" of the test section where sand transport had reached an equilibrium state as the eddies were reduced. If this were the case, the 2.4- by 0.67-m area between the trap testing area and basin area would have increased in elevation by sand deposition. The wet-weight density of sand used in the experiment program was calculated as 3.42 g (wet)/cm^3 using the density of quartz sand (2.65 g (dry)/cm^3) and the relationship between wet and dry weight determined empirically (0.78 g (dry)/1.0 g (wet)). Using fluxes obtained with the C nozzle at the basin and predicted fluxes for the same flow rate, and assuming that the accreting sand would settle out evenly over the 2.4- by 0.67-m area, the increase in bed elevation calculated using the wet weight density would have been too slight to observe (0.02 and 0.04 cm). Even the 45 percent discrepancy between the C nozzle and basin fluxes at the highest flow speed would have created only a small increase in elevation (0.06 cm).

Decision on Ambient Sand Transport Rate

101. It is concluded that the basin sampler, possibly partially due to the nonequilibrium length of the test section, did not provide an adequate measure of the ambient sand transport rate. Therefore, fluxes measured with the bottom C nozzle were used as a standard measure of the ambient sand transport rate. It is recognized that by using sand fluxes obtained with the C nozzle as the measure of ambient transport that the original standard of

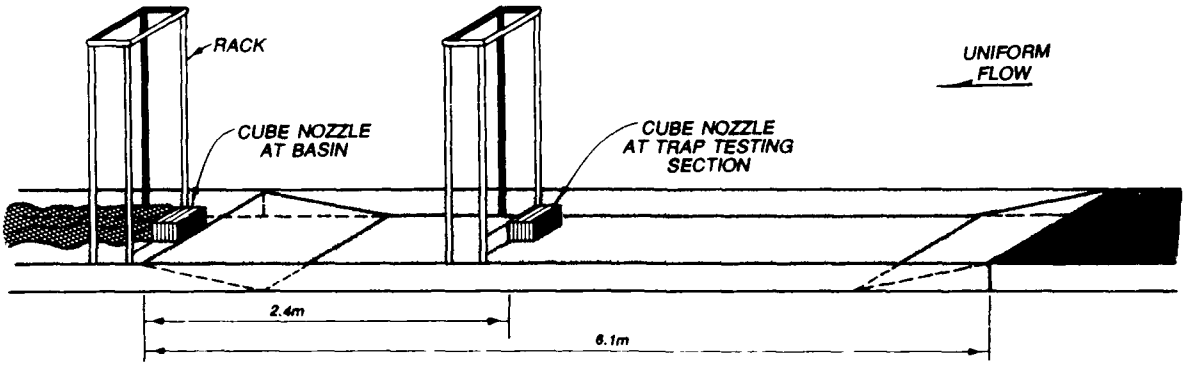

Figure 36. Sketch for discussing the hypothetical disequilibrium of sand flux due to length of test section

measurement has been rejected. In considering all possible reasons for the discrepancy between sand fluxes obtained with the basin sampler and C nozzle, it has been decided that the likeliest source of the incongruity is the pit sampler. In the following, sand-trapping efficiencies for the SUPERDUCK and DUCK85 nozzles have been calculated using the C nozzle flux equal to the ambient sand transport flux.

Sand-Trapping Efficiency Results

102. Tests conducted with midflow speeds greater than 60 cm/sec resulted in a flat-bed sand transport condition, which is most like the mode of transport occurring in the surf zone. Lower midflow speeds resulted in well-developed migrating ripples, which are not characteristic of the surf zone. All nozzles were fully tested in the 60 to 66 cm/sec range of midflow speeds. Therefore, for the purpose of determining nozzle sand-trapping efficiency, equations were developed to describe nozzle flux for the 60 to 66 cm/sec range of midflow speeds as follows:

Cube: $F = 0.00424\ e^{0.1124\ V}$; $r^2 = 0.74$ (19)

SUPERDUCK: $F = 0.4540\ V - 25.026$; $r^2 = 0.76$ (20)

DUCK85: $F = 4.047\ \ 10^{-27}\ \ V^{14.55}$; $r^2 = 0.95$ (21)

103. Sand-trapping efficiencies for the DUCK85 and SUPERDUCK nozzles were calculated by integrating each equation from 60 to 66 cm/sec, giving the area beneath each equation (Figure 37).

Cube:

$$A_{CU} = \int_{60}^{66} (0.004353\ \ e^{Vmid\ \ 0.1123})\ dV$$

$$= \frac{0.004353}{0.1123}\ (e^{(66)0.1123} - e^{(60)0.1123})$$

$$= 31.5$$

SUPERDUCK:

$$A_{SD} = \int_{60}^{66} (0.4540\ \ V_{mid} - 25.03)\ dV$$

$$= \frac{0.4540}{2.0}\ (66^2 - 25.03\ (66))$$

$$- \frac{0.4540}{2.0}\ (60^2 - 25.03\ \ (60))$$

$$= 21.4$$

DUCK85:

$$A_{D85} = \int_{60}^{66} (3.055\ 10^{-27} V_{mid}^{14.62})\ dV$$

$$= \frac{3.055\ \ 10^{-27}}{15.62}\ (\ 66^{15.62} - 60^{15.62})$$

$$= 4.00$$

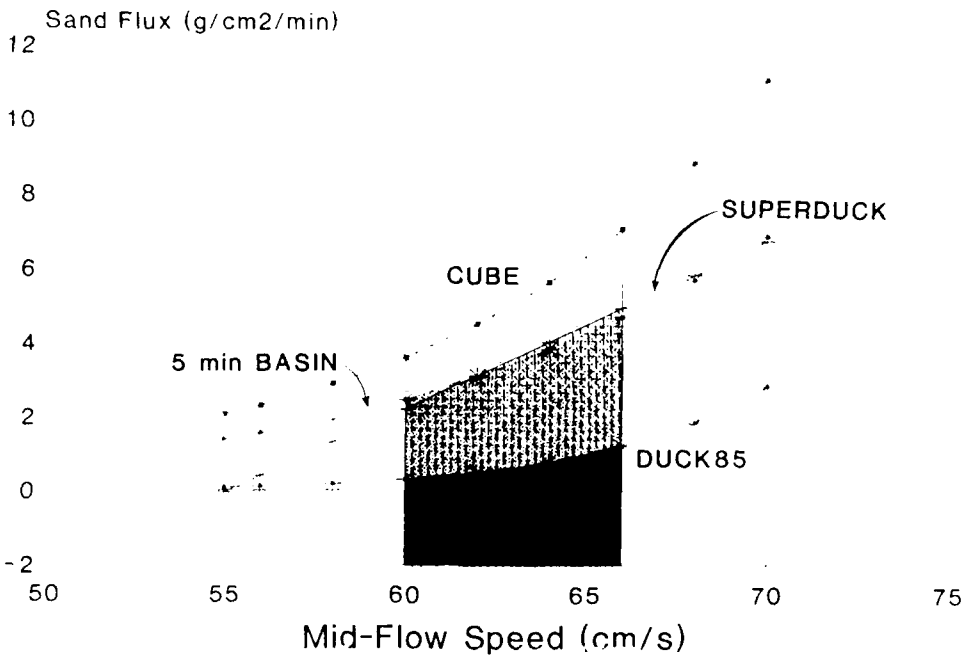

Figure 37. Area beneath each nozzle rate prediction used to calculate sand-trapping efficiency

104. The areas below the upper and lower 95 percent confidence limits were calculated, and the sand-trapping efficiency E_s and corresponding maximum error ϵ were computed as follows:

$$E_s \pm \epsilon = \frac{A_{TR}}{A_{CU}} \left\{ 1 \pm \left[\frac{(A_{uTR} - A_{lTR})}{2\ A_{TR}} + \frac{(A_{uCU} - A_{lCU})}{2\ A_{CU}} \right] \right\} \qquad (22)$$

where

A_{TR} = area below SUPERDUCK or DUCK85 equation

A_{CU} = area below Cube equation

A_{uTR} = area below upper confidence limit equation (either SUPERDUCK or DUCK85 equation)

A_{lTR} = area below lower confidence limit equation (either SUPERDUCK or DUCK85 equation)

A_{uCU} = area below upper confidence limit equation (Cube equation)

A_{lCU} = area below lower confidence limit equation (Cube equation)

105. The measure of error ϵ represents the area between the confidence limits of a particular curve normalized by the area below the curve. This analysis is, perhaps, oversophisticated since the number of points on which to base the calculations is very limited. The confidence bands are wide, most likely resulting in overestimates in the measure of error.

106. Average sand-trapping efficiencies and standard deviations for on-bed and off-bed nozzles are presented in Table 10. On-bed sand-trapping efficiencies and corresponding standard deviations were calculated for the DUCK85, SUPERDUCK, and C nozzles as 0.13 ± 0.50, 0.68 ± 0.51, and 1.00 (by definition), respectively. Off-bed sand-trapping efficiencies and standard deviations for each nozzle were assumed to be equivalent to values for midflow hydraulic efficiencies in this flow range. On-bed sand-trapping efficiencies for the H-S nozzle were estimated from Figure 30 at 1,000 percent. Sand fluxes obtained with a particular nozzle type should be divided by either the near-bottom or midflow sand-trapping efficiency (depending on the nozzle elevation) to obtain an estimate of the true sand flux.

Table 10

Sand-Trapping Efficiencies and Standard Deviations

Nozzle Type	Near-Bottom E_s	Midflow E_s
DUCK85	0.13+/-0.50	0.92+/-0.024
SUPERDUCK	0.68+/-0.51	1.02+/-0.013
CUBE	1.00 (by definition)	1.00+/-0.015
H-S	10.00	---

107. If the basin sampler had been used as the measure of ambient sand transport, the on-bed sand-trapping efficiencies and corresponding standard deviations for the DUCK85, SUPERDUCK, and C nozzles would be 0.19 ± 0.77, 1.02 ± 0.83, and 1.50 ± 1.03, respectively.

108. Both the hydraulic and sand-trapping efficiency tests indicate that the C nozzle has hydraulic and sand-trapping efficiencies closest to unity among the 23 streamer trap nozzles examined in this experiment program.

109. Hydraulic efficiencies determined for the H-S sampler confirm earlier results appearing in the literature (Druffel et al. 1976). However, sand-trapping efficiencies for the H-S sampler were higher than the 150 to 175 percent that has been stated in the literature for sand-sized material (Helley and Smith 1971, Emmett 1980). Results from the present experiment program reinforce previous studies recommending that the H-S sampler not be used for material finer than 0.25 mm and at sites where material can also be transported in suspension (Emmett 1980). Because of its self-burying characteristic, sediment-flow conditions in which the H-S sampler can be used may be very limited.

PART V: FIELD EFFICIENCY TESTS

110. The streamer trap has performed successfully in two major field data collection projects as well as in smaller scale field experiments. In particular, longshore sand transport rate measurements were made at DUCK85 (Mason, Birkemeier, and Howd 1987) and SUPERDUCK projects. These projects were named for the village of Duck, North Carolina, located near the Field Research Facility (FRF) of the Coastal Engineering Research Center. Use of the streamer trap in data collection to be conducted on Lake Michigan during September 1988 (Great Lakes '88 (GL88)) is also planned.

111. Two types of longshore sand transport data have been collected with the streamer trap: the distribution of longshore transport across the surf zone using a spatial sampling method (SSM) (Kraus and Dean 1987), and the variation of longshore transport through time at a point using a temporal sampling method (TSM) (Kraus, Gingerich, and Rosati 1988). SSM runs involved simultaneous deployment of traps on a line through the surf zone, resulting in the measurement of vertical and cross-shore distributions of longshore sand transport. During the data collection projects performed at the FRF, typically 7 to 10 traps were placed on a line crossing the surf zone for a 5- to 10-min data collection period. TSM runs resulted in vertical distributions of sand transport at a point over an extended period (typically 30 min to 1 hr). A single streamer trap typically collected transport data for a 5- to 10-min period at a particular point in the surf zone, then it was replaced with another trap positioned at the same general location for a similar time interval.

112. During the DUCK85 and SUPERDUCK data collection projects, tests were conducted to evaluate the behavior of the streamer trap in the prototype. An indication of trap reliability was assessed by comparing sand transport rates collected with two closely-spaced traps. These so-called "consistency" tests involved measuring sand transport with two traps positioned approximately 1 m apart both in the cross-shore and longshore directions. In addition, qualitative characteristics of nozzle behavior in the surf zone were noted during the consistency tests and the TSM and SSM runs.

113. Part V gives an overview of the type of data collected during the DUCK85 and SUPERDUCK field data collection projects and discusses both qualitative observations and quantitative comparisons between closely spaced traps. Tests of various streamer trap nozzles planned for the GL88 data collection project are also presented.

Overview

114. During the DUCK85 and SUPERDUCK data collection projects, a total of 45 transport rate data collection runs/tests was made. These runs consisted of 15 SSM, 11 TSM, one rip current run, and 17 consistency tests. An example of data collected during an SSM run is presented in Figure 38. Figure 39 presents data collected during a TSM run, in which sand transport was sampled at one location through time over approximately a 1-hour period. The data in Figures 38 and 39 have been adjusted using values of sand-trapping efficiencies presented in Part IV, differing from results previously presented (Kraus 1987, Kraus and Dean 1987).

115. During field use of the trap, qualitative observations of trap and nozzle behavior in the surf zone were made. Scour was observed to appear intermittently at the mouths of the DUCK85 and SUPERDUCK bottom nozzles. No measurements were made of the scour pattern, however. The trap proved to be fairly stable in the surf zone and could be "righted" quickly if tipped during the passage of a wave. The streamers moved with the current and oscillatory motion of the waves and occasionally would wrap around the trap legs if the longshore current speed was not sufficiently great. However, the trap operator could easily keep the streamers untangled and aligned with the direction of the longshore current. Additional discussion of field use of the streamer trap has been presented in Part II.

Consistency Tests

116. Tests were conducted with two closely spaced traps placed in the surf zone, collecting sand moving either longshore or offshore in the throat

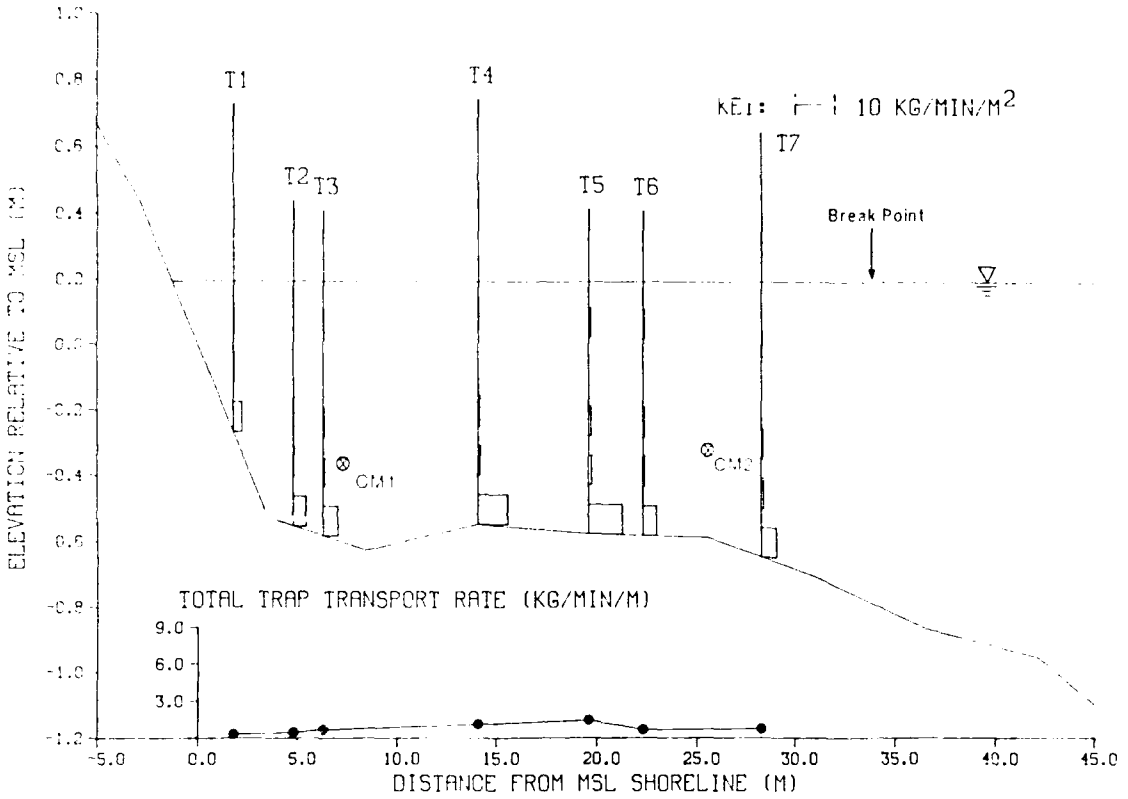

Figure 38. Example SSM data set

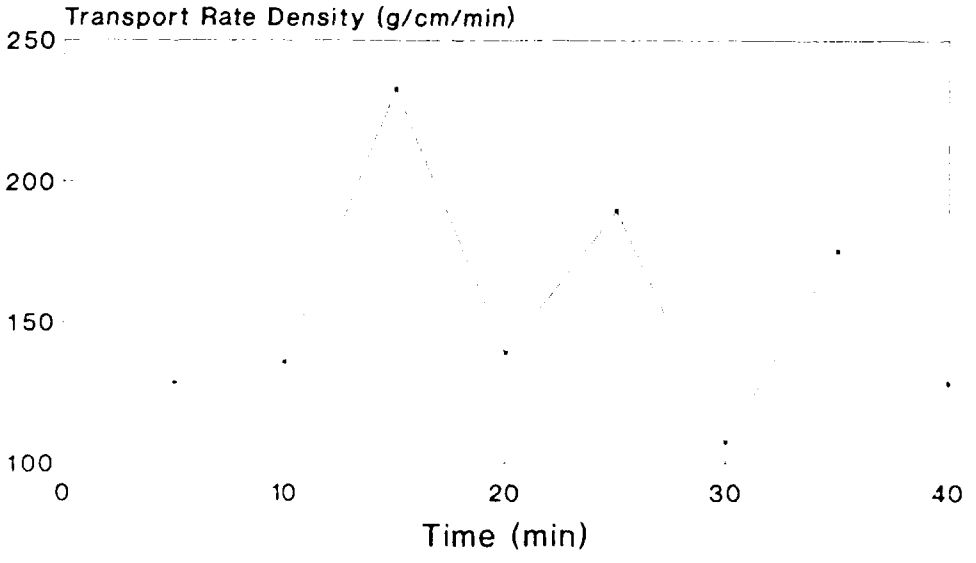

Figure 39. Example TSM data set

of a rip current. The purpose of the tests was to quantify the reliability and reproducibility of results from the streamer trap. Both DUCK85 and SUPERDUCK nozzles were used in the consistency tests. Traps were positioned with one located approximately 1 m offshore and 1 m downflow (seaward trap) of the other (shoreward trap), such that collection of trap-induced transport would be minimal (Figure 40).

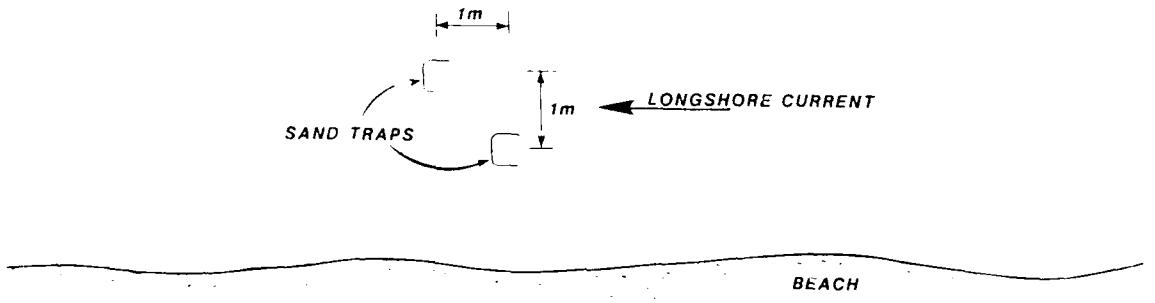

Figure 40. Consistency test arrangement

117. Kraus (1987) presented two example consistency tests of ten tests conducted during the DUCK85 field data collection program, one showing nearly equal vertical distributions of transport and the other showing greatly differing distributions. Based on the ten consistency tests conducted during DUCK85, Kraus tentatively concluded that the different transport rates measured by closely spaced traps is most likely an accurate representation of the transport rate and that the transport rates actually differed by the margins measured with the traps.

118. Figures 41 through 50 and Figures 51 through 57 present vertical flux profiles measured with the DUCK85 and SUPERDUCK nozzles, respectively. Agreement between the DUCK85 shoreward and seaward traps is generally good, with the greatest difference occurring at the bottom nozzle. The discrepancy between the two bottom nozzle fluxes may be due to a difference in scour at the bed between the two traps. However, the bottom nozzle flux for the shoreward trap is less than that of the seaward trap for 7 out of 10 cases, indicating that the difference observed at the bottom nozzle may also have

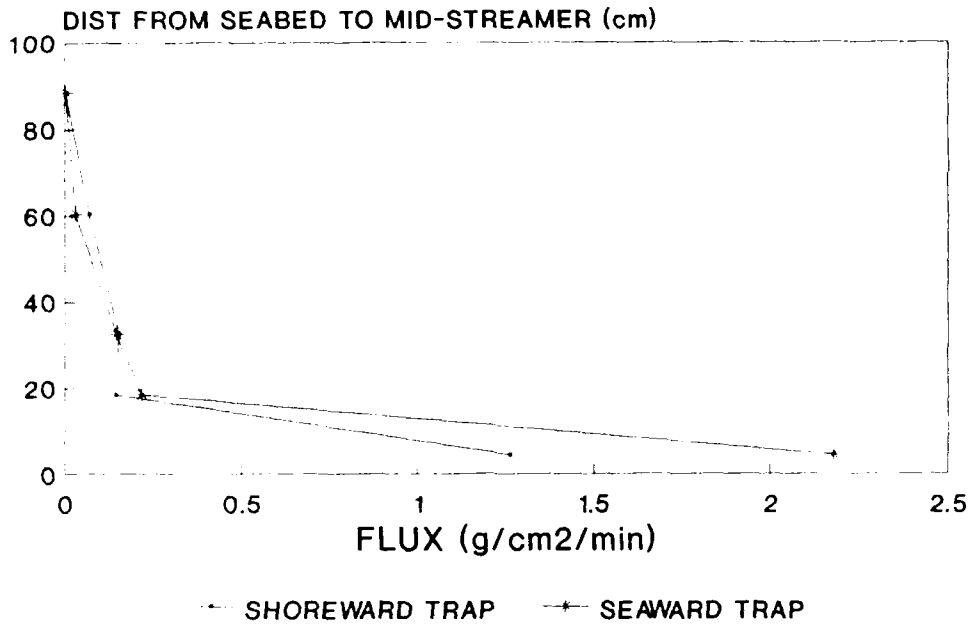

Figure 41. Run 2-1, DUCK85 consistency test (9-4-85)

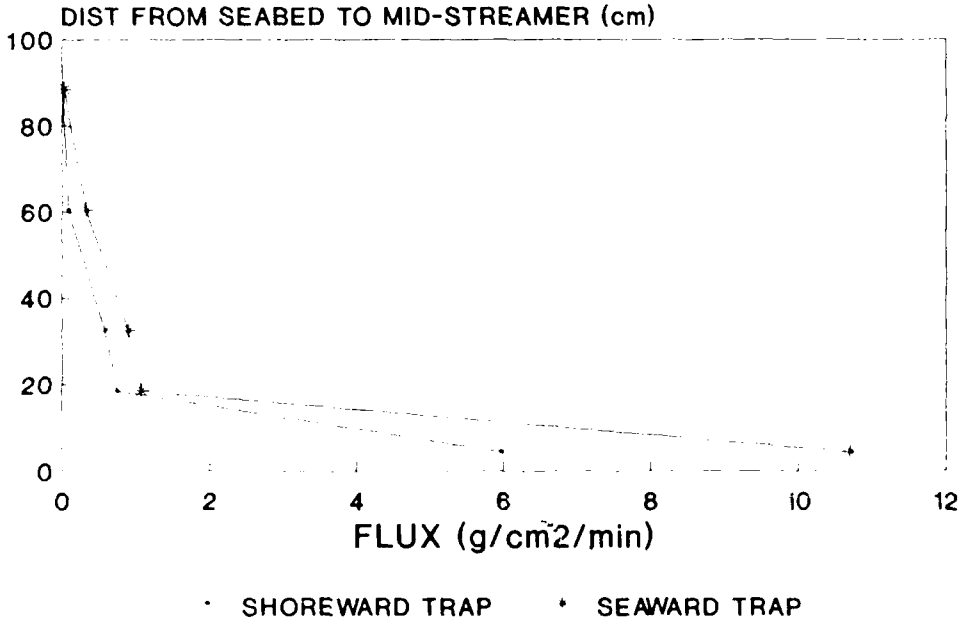

Figure 42. Run 2-2, DUCK85 consistency test (9-4-85)

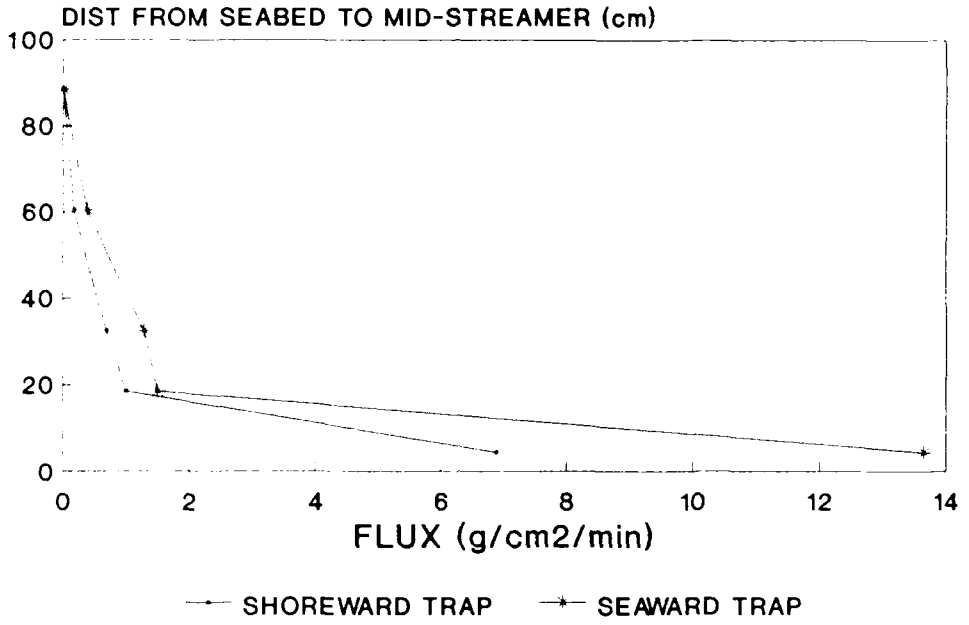

Figure 43. Run 1, DUCK85 consistency (9-7-85)

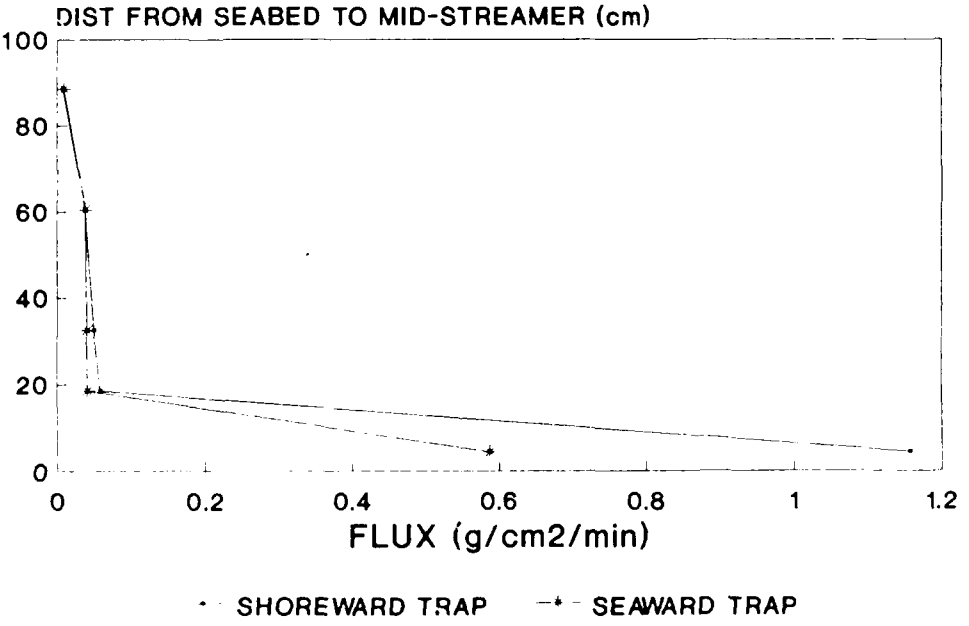

Figure 44. Run 4, DUCK85 consistency test (9-7-85)

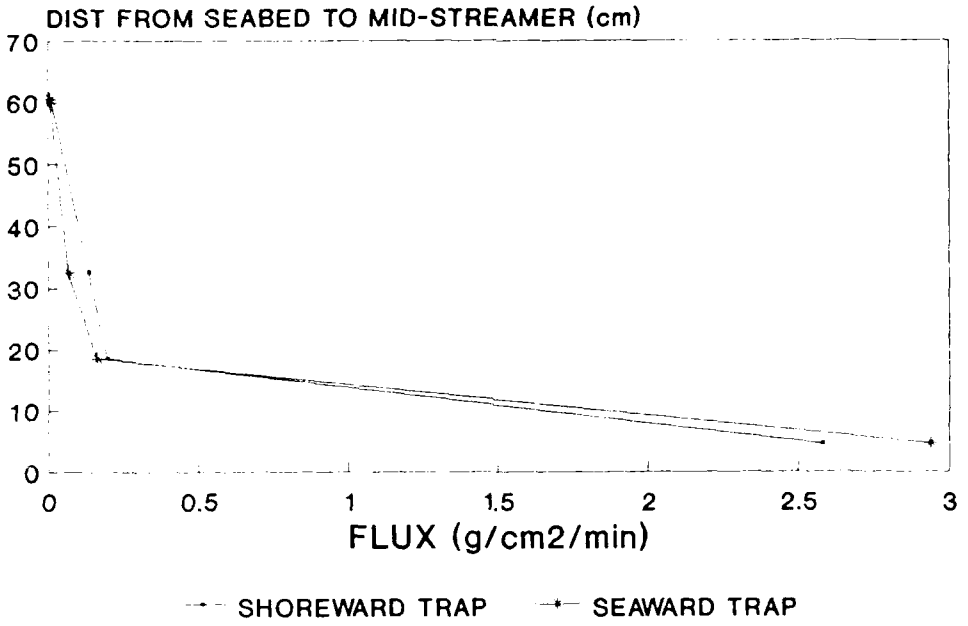

Figure 45. Run 5, DUCK85 consistency test (9-9-85)

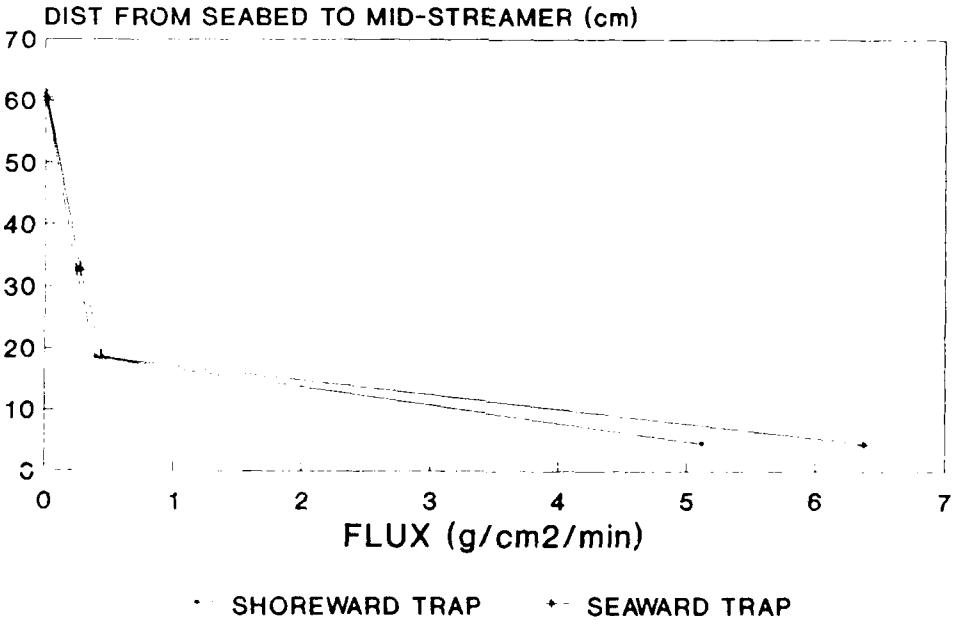

Figure 46 Run 6, DUCK85 consistency test (9-9-85)

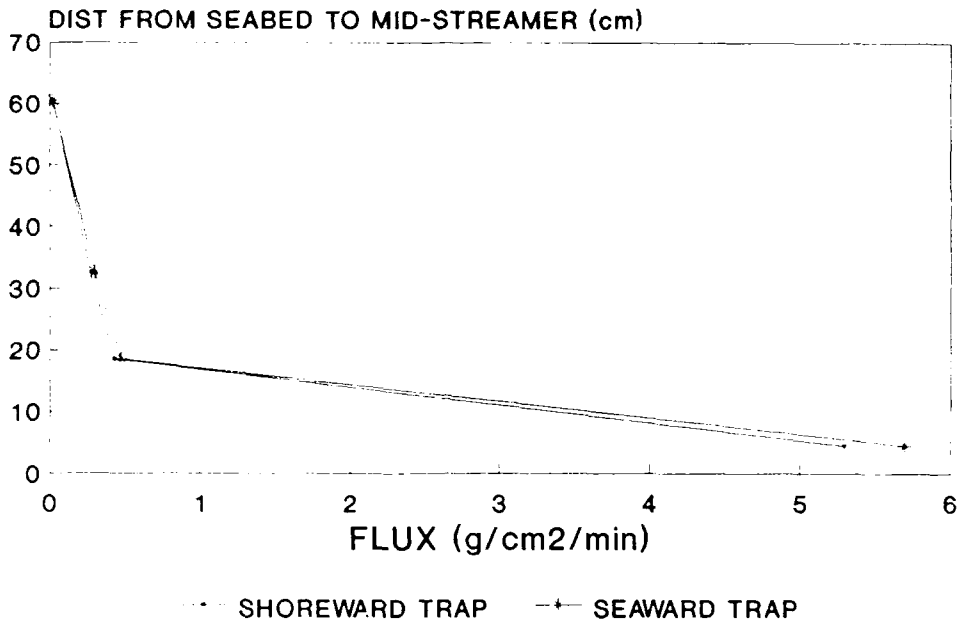

Figure 47. Run 7, DUCK85 consistency test (9-9-85)

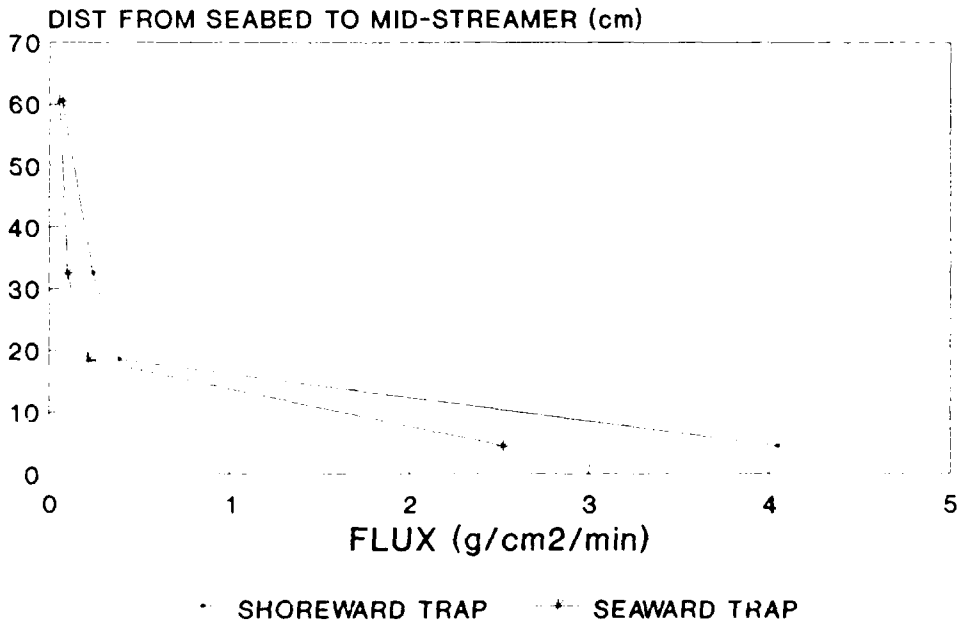

Figure 48. Run 8, DUCK85 consistency test (9-9-85)

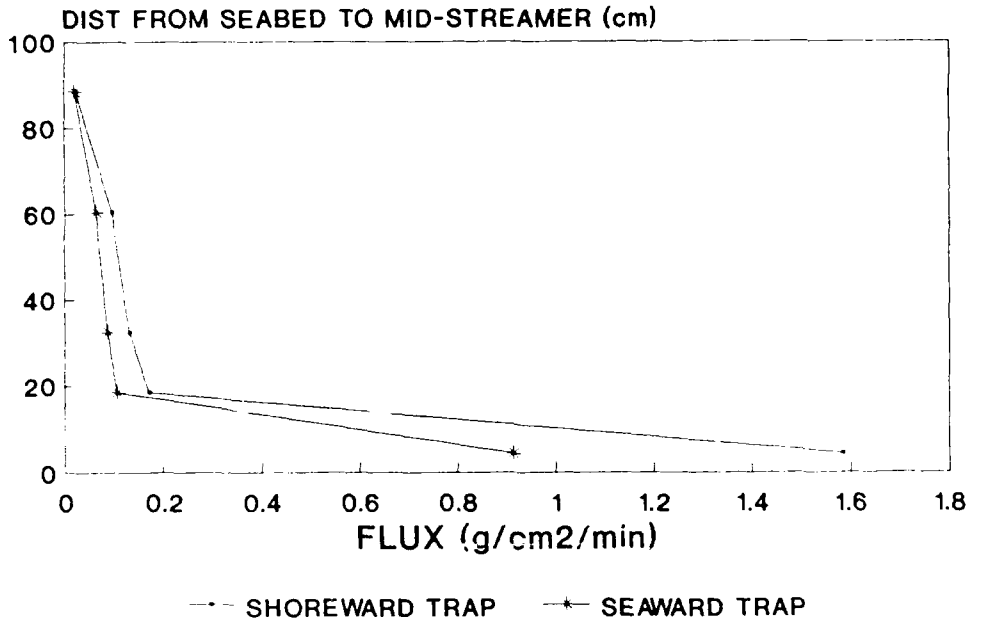

Figure 49. Run 9, DUCK85 consistency test (9-9-85)

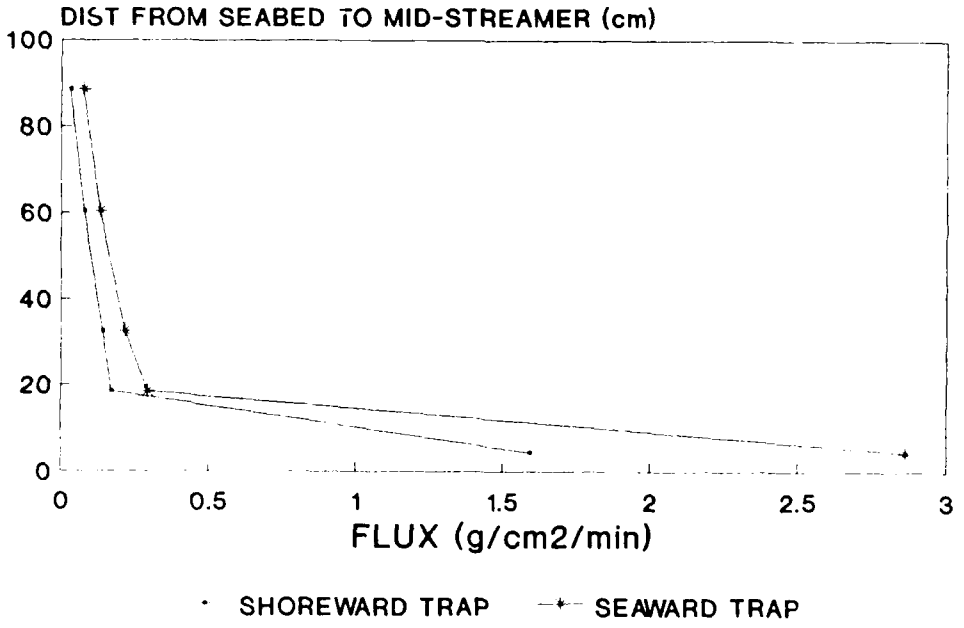

Figure 50. Run 10, DUCK85 consistency test (9-9-85)

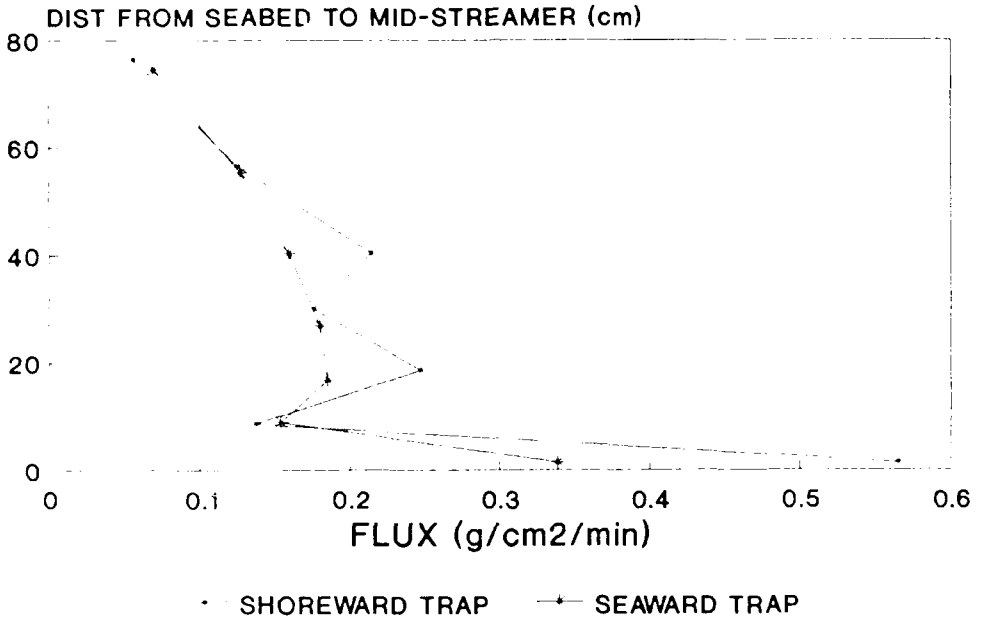

Figure 51. Run 23, SUPERDUCK consistency test (9-16-85)

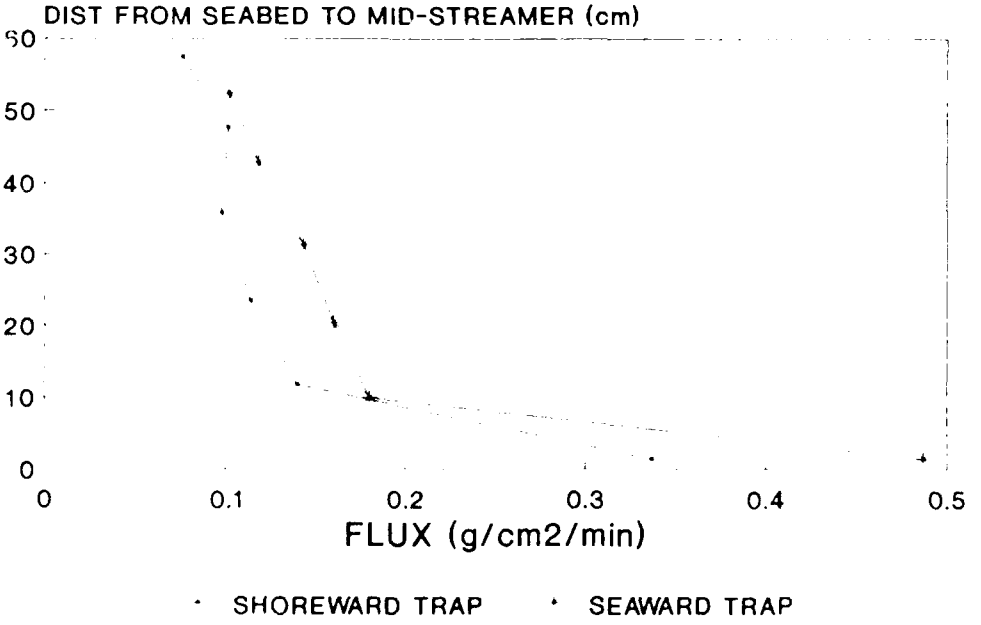

Figure 52. Run 24, SUPERDUCK consistency test (9-16-86)

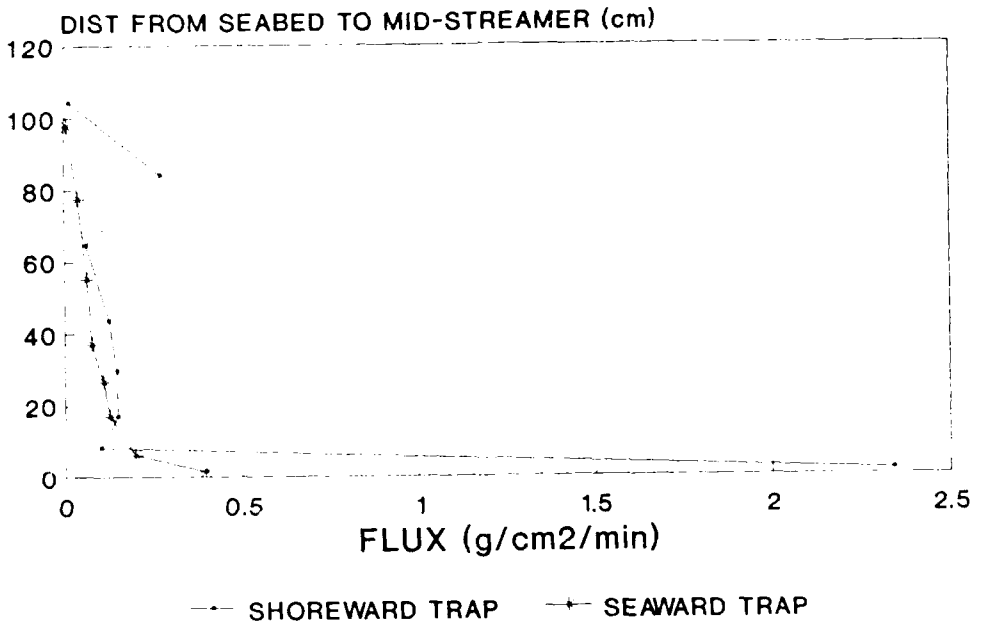

Figure 53. Run 34-1, SUPERDUCK consistency test (9-20-86)

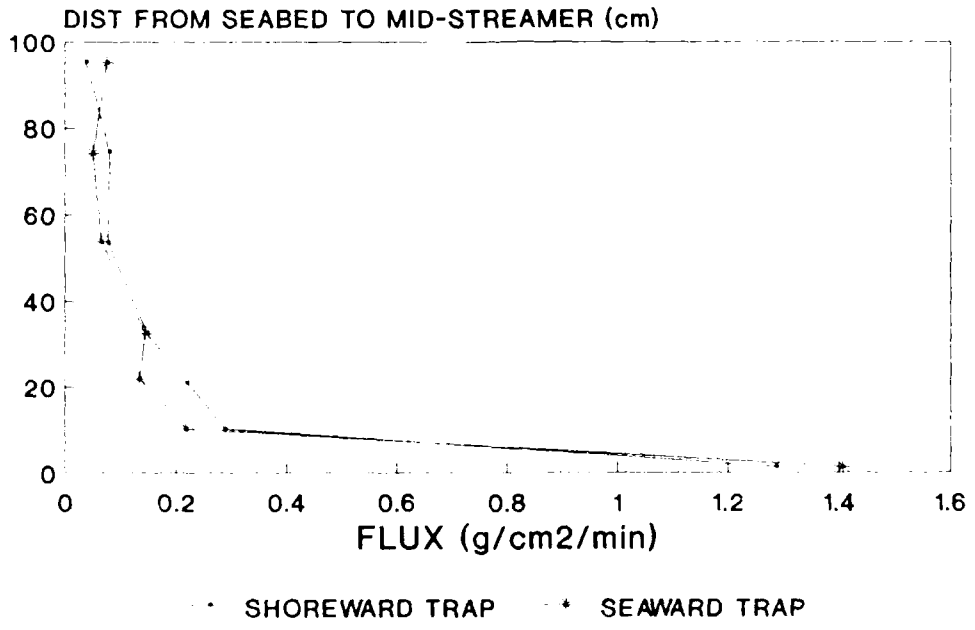

Figure 54. Run 34-2, SUPERDUCK consistency test (9-20-86)

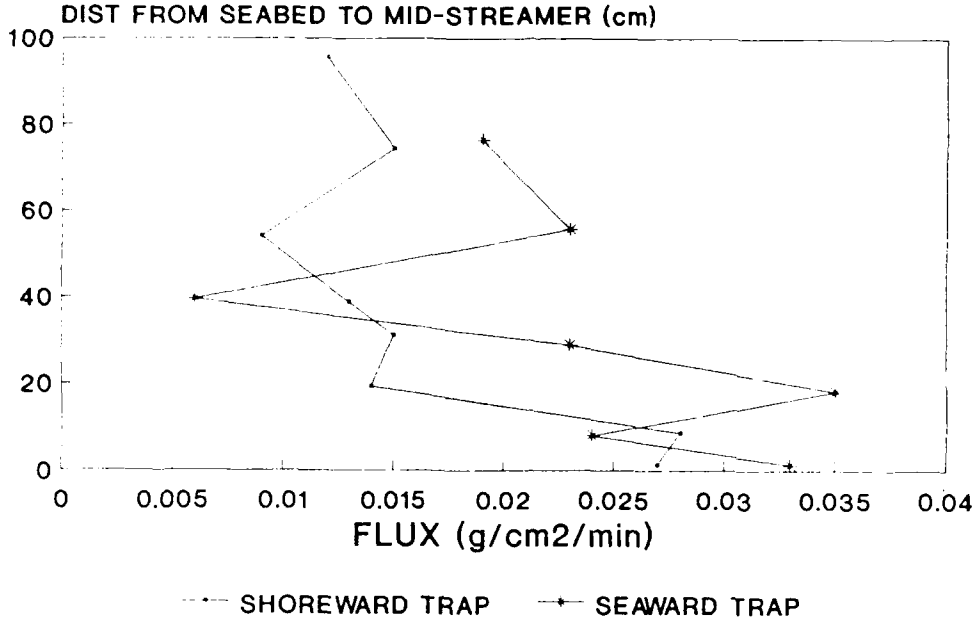

Figure 55. Run 35, SUPERDUCK consistency test (9-21-86)

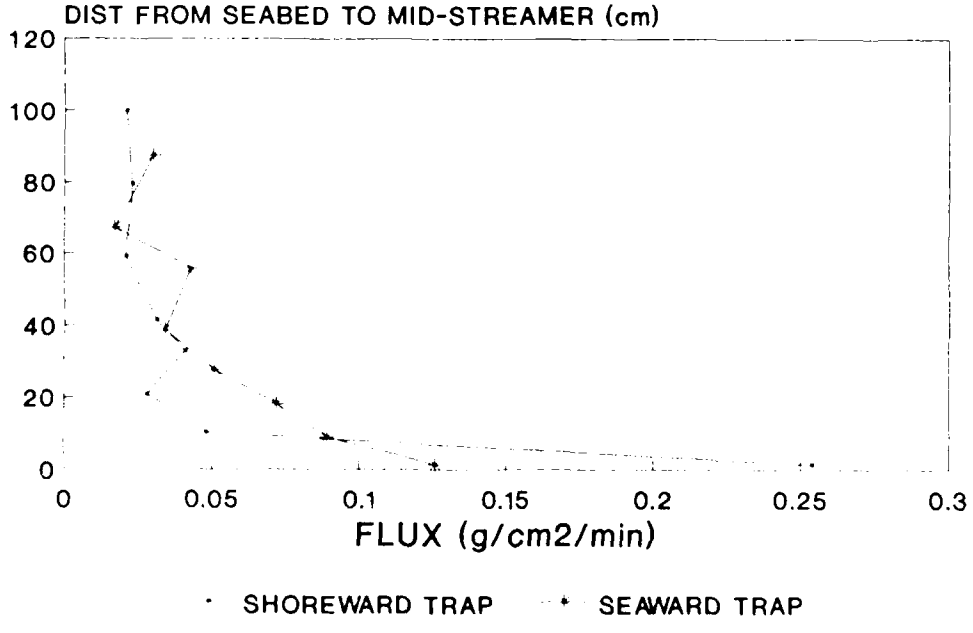

Figure 56. Run 37-1, SUPERDUCK consistency test (9-21-86)

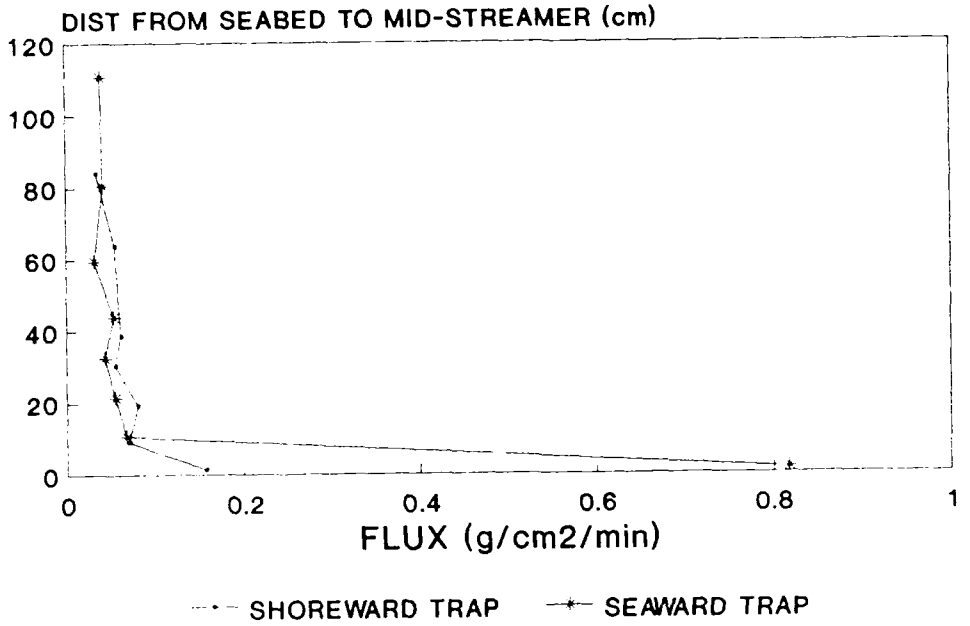

Figure 57. Run 37-2, SUPERDUCK consistency test (9-21-86)

depended on trap location. The majority of the DUCK85 consistency runs were conducted in the feeder of a rip current where the flow was steady and strong.

119. The vertical distributions of sand flux measured with the SUPERDUCK nozzle varied more between the shoreward and seaward traps than was observed with the DUCK85 nozzle. However, wave conditions were different, with clean swell occurring during DUCK85 and more choppy wind waves during SUPERDUCK. Figure 55 shows the run with poorest agreement between seaward and shoreward traps measured during a very low transport condition.

120. Integration of the measured fluxes through the water column gives the total transport rate density for that trap. Table 11 summarizes the total transport rate density data for the 17 consistency tests conducted both at DUCK85 and SUPERDUCK field data collection programs. Fluxes were adjusted using the values of sand-trapping efficiency determined in Chapter 4. The consistency ratio gives a measure of consistency between the shoreward and seaward traps. If it is assumed that the transport rate is uniform over a distance of approximately 2 to 3 m in a plane normal to the flow, then results

Table 11

Comparison of Transport Rate Density Measured with Two Closely Spaced Traps

Run No.	Date	Nozzle	Transport Rate Density, g/(cm/min) Shoreward Trap	Seaward Trap	Consistency Ratio* %
2-1	9-4-85	DUCK85	21.8	32.1	68
2-2	9-4-85	"	94.1	166.7	57
1	9-7-85	"	112.5	215.9	52
4	9-7-85	"	16.4	9.5	58
5	9-9-85	"	35.4	37.5	94
6	9-9-85	"	69.6	85.5	81
7	9-9-85	"	72.8	78.7	93
8	9-9-85	"	58.3	35.3	61
9	9-9-85	"	26.5	16.0	60
10	9-9-85	"	26.4	46.7	57
23	9-16-86	SUPERDUCK	14.2	11.9	84
24	9-16-86	"	7.8	9.6	81
34-1	9-20-86	"	19.2	8.6	45
34-2	9-20-86	"	18.9	17.4	92
35	9-21-86	"	1.4	1.7	82
37-1	9-21-86	"	4.1	4.2	98
37-2	9-21-86	"	5.5	9.5	58

* "Consistency Ratio %," a measure of consistency, is calculated by dividing the lower value of the transport rate density for a particular run (seaward or shoreward trap) by the higher value for a particular run (seaward or shoreward trap) and then multiplying by 100.

presented in Table 11 indicate a consistency for the DUCK85 nozzle from 50 to 90 percent and a consistency for the SUPERDUCK nozzle from 50 to 100 percent (values rounded off to first significant number).

121. Trap reproducibility can also be quantified by mathematically describing the vertical flux. Values of sand flux corresponding to a particular elevation were represented with linear, exponential, and power law least square fits. The equations were developed using the distance from the seabed to midstreamer Z as the independent variable and sand flux F as the dependent variable as follows:

$$\text{Linear:} \quad F = aZ + b \tag{23}$$

$$\text{Exponential:} \quad F = ae^{Zb} \tag{24}$$

$$\text{Power:} \quad F = aZ^{b} \tag{25}$$

where a and b are empirically determined coefficients with dimensions consistent with variables in the equation. The coefficients and resulting squared correlation coefficient for each data set are presented in Table 12.

122. As presented in Table 12, the vertical distribution of sand flux has the highest squared correlation coefficient for either an exponential or power-law relationship. Out of the 20 DUCK85 vertical distributions examined, 11 are best described with an exponential fit, and 9 are best described with a power-law fit. Of the 14 SUPERDUCK vertical distributions of sand flux, 10 have the highest squared correlation coefficient with a power-law fit, 3 best fit an exponential relationship, and 1 is best described linearly. The majority (14 out of 17) of the shoreward and seaward consistency test data sets have similar coefficients and are described by the same type of equation. This favorable comparison between the form of the vertical flux data measured with closely spaced traps indicates that the streamer trap and nozzles are indeed consistent and provide reproducible measurements of the transport rate.

Future Study

123. Consistency tests between streamer traps with C, SUPERDUCK, and DUCK85 nozzles (and the H-S sampler) will be conducted at the GL88 field data collection project. A C trap and another nozzle trap will be deployed in either the longshore current, if it is sufficiently strong, or next to a shore-perpendicular structure where the longshore current is expected to be concentrated and deflected offshore. Many tests will be conducted to give an indication of the test variability and ultimately a measure of relative nozzle efficiency for a field condition. In addition, the development of scour through time at each bottom nozzle will be quantified.

124. Tests with a streamer trap (C, SUPERDUCK, and DUCK85 nozzles) near an Optical Backscatter Sensor (OBS) (see Appendix A) in the surf zone are also planned for GL88. Comparisons between trap-measured and OBS sediment transport fluxes will give a quantitative indication of consistency between the streamer trap (for nozzles collecting suspended material) and electronic instrumentation.

Table 12

Mathematical Equations Describing the Vertical Distribution of Sand Flux for Two Closely Spaced Traps

Run No.	Date	Coefficients*	Type of Equation: Linear** Shore	Linear** Sea	Exponential** Shore	Exponential** Sea	Power** Shore	Power** Sea
2-1	9-4-85	a	-0.01	-0.02	1.01	1.51	15.30	49.20
	(DUCK85)	b	0.74	1.22	-0.05	-0.06	-1.50	-1.80
		r^2	0.49	0.45	0.85	0.95	0.77	0.91
2-2	9-4-85	a	-0.05	-0.09	5.50	7.67	171.00	166.70
	(DUCK85)	b	3.46	6.06	-0.07	-0.06	-1.88	-1.64
		r^2	0.50	0.47	0.96	0.90	0.85	0.84
1	9-4-85	a	-0.06	-0.11	6.89	15.6	179.80	475.10
	(DUCK85)	b	4.05	7.82	-0.07	-0.74	-1.81	-1.94
		r^2	0.51	0.48	0.93	0.85	0.80	0.69
4	9-7-85	a	-0.01	-0.01	0.39	0.22	7.11	2.35
	(DUCK85)	b	0.62	0.32	-0.04	-0.03	-1.39	-1.13
		r^2	0.41	0.42	0.74	0.76	0.91	0.87
5	9-9-85	a	-0.04	-0.04	2.29	2.32	48.70	88.50
	(DUCK85)	b	1.82	2.03	-0.09	-0.10	-1.86	-2.17
		r^2	0.56	0.54	0.92	0.93	0.91	0.96
6	9-9-85	a	-0.08	-0.09	5.91	5.84	167.80	149.00
	(DUCK85)	b	3.61	4.47	-0.10	-0.09	-2.11	-1.98
		r^2	0.57	0.56	0.92	0.92	0.84	0.90
7	9-9-85	a	-0.08	-0.08	4.82	5.56	103.30	123.00
	(DUCK85)	b	3.75	4.04	-0.09	-0.09	-1.87	-1.91
		r^2	0.57	0.57	0.93	0.93	0.91	0.89
8	9-9-85	a	-0.06	-0.04	2.72	1.40	35.50	19.80
	(DUCK85)	b	2.88	1.77	-0.07	-0.06	-1.47	-1.46
		r^2	0.57	0.55	0.87	0.79	0.98	0.98
9	9-9-85	a	-0.01	-0.01	0.76	0.42	8.57	4.00
	(DUCK85)	b	0.90	0.52	-0.04	-0.03	-1.20	-1.09
		r^2	0.46	0.46	0.81	0.78	0.92	0.93

(continued)

* Dimensions of coefficients a and b are consistent with variables in equation.

** Underlined values indicate the highest squared correlation coefficient for each data set.

Table 12 (concluded)

Run No.	Date	Coeffi-cients*	Type of Equation: Linear** Shore	Linear** Sea	Exponential** Shore	Exponential** Sea	Power** Shore	Power** Sea
10	9-9-85	a	-0.01	-0.03	0.72	1.13	8.33	12.80
	(DUCK85)	b	0.90	1.60	-0.04	-0.03	-1.19	1.14
		r^2	0.46	0.44	0.81	0.75	0.96	0.97
23	9-16-86	a	-0.004	-0.003	0.36	0.26	0.60	0.38
	(SUPERDUCK)	b	0.36	0.25	-0.02	-0.02	-0.41	-0.30
		r^2	0.49	0.64	0.66	0.78	0.64	0.73
24	9-16-86	a	-0.004	-0.006	0.24	0.33	0.37	0.53
	(SUPERDUCK)	b	0.25	0.35	-0.02	-0.02	-0.37	-0.41
		r^2	0.62	0.59	0.76	0.75	0.98	0.98
34-1	9-20-86	a	-0.011	-0.003	0.47	0.29	2.24	0.73
	(SUPERDUCK)	b	0.85	0.24	-0.03	-0.03	-0.95	-0.72
		r^2	0.26	0.63	0.70	0.92	0.83	0.77
34-2	9-20-86	a	-0.008	-0.009	0.56	0.42	1.84	1.56
	(SUPERDUCK)	b	0.65	0.65	-0.03	-0.03	-0.77	-0.75
		r^2	0.43	0.43	0.83	0.62	0.97	0.95
35	9-21-86	a	-0.0001	-0.0002	0.02	0.03	0.03	0.04
	(SUPERDUCK)	b	0.02	0.03	-0.01	-0.01	-0.23	-0.19
		r^2	0.49	0.26	0.49	0.14	0.69	0.22
37-1	9-21-86	a	-0.001	-0.001	0.08	0.10	0.24	0.18
	(SUPERDUCK)	b	0.12	0.10	-0.02	-0.02	-0.57	-0.42
		r^2	0.33	0.73	0.52	0.75	0.91	0.77
37-2	9-21-86	a	-0.001	-0.004	0.11	0.14	0.17	0.62
	(SUPERDUCK)	b	0.11	0.31	-0.01	-0.02	-0.31	-0.68
		r^2	0.55	0.25	0.72	0.36	0.88	0.85

PART VI: CONCLUSIONS AND RECOMMENDATIONS

Conclusions

125. The objectives of this study were to evaluate and improve upon the hydraulic and sand-trapping characteristics of the streamer trap nozzle for use in the nearshore zone. Twenty-three variations of the streamer trap nozzle were initially evaluated to determine their hydraulic characteristics, and three streamer trap nozzles with near-optimum hydraulic efficiencies were subsequently tested to qualitatively and quantitatively determine their sand-trapping characteristics. The H-S sampler, a pressure-difference riverine sediment trap extensively reported on in the literature, was also tested in both the hydraulic and sand-trapping phases of the experimental program for comparison with both streamer trap nozzle results and reported efficiencies.

126. One hundred and seventeen hydraulic and 101 sand-trapping efficiency tests were performed. Both the hydraulic and sand-trapping tests were conducted in a unidirectional flow tank with the objective of simulating the longshore current in the surf zone. Hydraulic testing of the nozzles involved measuring flow speed at the nozzle and then repeating the measurements for the same flow condition at the same location in the tank without the nozzle in place. By dividing the flow speed in the nozzle by the ambient (without nozzle) flow speed, a measure of hydraulic efficiency was obtained for the particular flow condition. For nozzles with near-optimal hydraulic efficiencies, measurements were made for four flow conditions (midflow speeds equal to 22, 43, 59, and 74 cm/sec) with one nozzle located at the bed or at the midflow elevation, and with two nozzles in place (one at the bed and the other at a midflow elevation).

127. The sand-trapping tests primarily consisted of measuring ambient sand flux (with a pit sampler) for a range of midflow speeds (ranging from 46 to 74 cm/sec) and comparing values of ambient flux to nozzle-predicted sand flux. Sand with a median grain size of 0.23 mm was placed in a test section built into the testing tank. Because of a presumed disequilibrium of sand transport between the trap testing section and the pit sampler, measurements of ambient transport were not comparable to the nozzle-predicted sand flux.

As a result, sand fluxes measured with one nozzle (the C nozzle), observed to have no effect on the movement of sand near the mouth and with a near-unity on-bed hydraulic efficiency (0.96), were assumed to represent the ambient sand flux. Values of sand-trapping efficiency for the near-bed position were calculated for the 60 to 66 cm/sec range of flow speeds which produced the flat-bed sand transport condition most like the surf zone. At lower flow speeds, large sand ripples formed and moved in the direction of flow. This type of bedform is unique to the surf zone. Because sand transport occurred for the most part in a 5-cm-high layer above the bed, nozzles located off the bed collected small amounts of sand. Values of sand-trapping efficiency for the off-bed nozzle position were taken to be equal to the hydraulic efficiencies for a similar midflow speed.

128. Main conclusions from this study are as follows:

a. The streamer trap nozzle previously used in the DUCK85 field data collection project performed well in an off-bed position, with an off-bed sand-trapping efficiency equal to 0.92 (standard deviation 0.02). Significant scour occurred at the bottom of the nozzle when it was located near the bed, and the on-bed sand-trapping efficiency was calculated as 0.13 (maximum error equal to 0.50).

b. The SUPERDUCK nozzle, used in a field data collection project conducted at Duck, North Carolina, in 1986, had an off-bed sand-trapping efficiency equal to 1.02 (standard deviation 0.01). Behavior of the nozzle near the bed was judged to be fair, with scour occurring approximately half the testing period. The on-bed sand-trapping efficiency was calculated as 0.68 (maximum error equal to 0.51).

c. The C-type nozzle was observed to have no effect on sand movement in the region upflow of the nozzle. Small bedforms moving in the direction of flow were observed to enter unobstructed into the nozzle mouth. The off-bed sand-trapping efficiency was calculated as 0.93 (standard deviation 0.02), and the on-bed sand-trapping efficiency was, by definition, 1.00.

d. The pressure-difference H-S sampler had values of hydraulic efficiency ranging from 1.20 at a midflow position to 1.48 when located at the bed. These values are slightly smaller than values quoted in the literature (1.54 (Druffel et al. 1976)); however, testing flow speeds were lower in the present experiment program, and efficiency was observed to increase with flow speed. The sampler in the sand-trapping phase of the experiment distorted the normal patterns of sand movement in the tank. The H-S sampler increased the

flow speed at the nozzle mouth to such a degree that it buried itself during a 5-min testing period. Sand was observed to move upflow from the rear of the sampler to be collected in the sampler bag. A sand-trapping efficiency of 10.0 was calculated from two measurements. The H-S sampler is not recommended for use in the nearshore zone where sand-sized particles are present.

e. Tests employing two closely spaced streamer traps in the surf zone gave comparable results, both in the magnitude of sand transport and in the shape of the sand flux vertical distribution. If it is assumed that the transport rate was uniform over a distance of approximately 2-3 m in a plane normal to the flow, then the DUCK85 nozzle was from 50 to 90 percent consistent, and the SUPERDUCK nozzle was from 50 to 100 percent consistent.

Recommendations

129. Based on the results of this study, it is concluded that the streamer trap is an accurate and reliable apparatus for measuring rates and vertical distributions of sand transport in the nearshore zone. The SUPERDUCK and C streamer trap nozzles were judged to have fair to excellent sand-trapping efficiencies. Qualitative observations of nozzle behavior on the bed indicated that scour may occur at the lower lip of the SUPERDUCK nozzle for approximately half of the testing period. It is recommended that the testing period not extend past the 5- to 10-min interval presently employed. Behavior of the C nozzle at the sand bed was observed to be ideal in the laboratory tests. The sand-trapping efficiencies developed in this study can correct for the effects of scour, although it is cautioned that the sand-trapping efficiencies pertain strictly to unidirectional flow.

130. A more extensive laboratory calibration program could be conducted to better simulate wave-induced turbulence in the surf zone and more fully explore the relationship between nozzle size and efficiency. A wider unidirectional flow tank could be slightly modified to house a wave paddle that could introduce an oscillatory motion perpendicular to the direction of flow, similar to that which exists in the surf zone. If funding allowed, different types of apparatus and instruments used to measure flow speed and ambient sand transport could be employed to obtain more accurate measurements. The relationship between the length of the test section and the rate of sand transport

at a section should be fully investigated and a test section planned such that trap testing location and ambient measurement location have similar sand transport characteristics. An extensive set of various nozzles could be evaluated to optimize nozzle size and shape, for which the present study provides much guidance.

131. Similarly, a field experiment could be conducted with various types of sediment transport instruments (optical backscatter sensors, pit samplers, Kana sampler, etc. (see Appendix A)) to evaluate the performance of the streamer trap relative to other measurement devices. The streamer trap provides an easy, inexpensive, and reliable method of making measurements in the nearshore zone within certain limitations, primarily wave height. However, more developmental work both in the laboratory and field would refine and lend understanding to trap characteristics for more complicated flow conditions. Optimization and use of the streamer trap would greatly benefit the furtherance of quantitative sand transport studies in the nearshore and in rivers.

REFERENCES

Anderson, J. 1987. "Field Evaluation of a Marine Sediment Trap," Report No. UCB/HEL-87/04, University of California, Berkeley, CA.

Basinski, T., and Lewandowski, A. 1974. "Field Investigation of Suspended Sediment," Proceedings of the 14th Coastal Engineering Conference, American Society of Civil Engineers, pp 1096-1108.

Beach, R. A., and Sternberg, R. W. 1987. "The Influence of Infragravity Motions on Suspended Sediment Transport in the Inner Surf Zone," Proceedings of Coastal Sediments '87, American Society of Civil Engineers, pp 913-928.

Bijker, E. W. 1971. "Longshore Transport Computations," Proceedings of American Society of Civil Engineers, Vol 97, No. WW4, pp 687-701.

Bosman, J. J., van der Velden, E. T. J. M., and Hulsberger, C. H. 1987. "Sediment Concentration Measurement by Transverse Section," Coastal Engineering, Vol 11, pp 353-370.

Brenninkmeyer, B. M. 1973. "Synoptic Surf Zone Sedimentation Patterns," unpublished Ph.D. Dissertation, University of Southern California, 274 p.

Brenninkmeyer, B. M. 1974. "Mode and Period of Sand Transport in the Surf Zone," Proceedings of the 14th Coastal Engineering Conference, American Society of Civil Engineers, pp 812-827.

Brenninkmeyer, B. M. 1976. "In Situ Measurements of Rapidly Fluctuating, High Sediment Concentrations," Marine Geology, Vol 20, pp 117-128.

Brown, C. B. 1950. "Sediment Transportation," Chapter 12, Engineering Hydraulics, ed. H. Rouse, John Wiley and Sons, Inc., New York, NY.

Bruno, R. O., Dean, R. G., and Gable, C. G. 1981. "Longshore Transport Evaluations at a Detached Breakwater," Proceedings of the 17th Coastal Engineering Conference, American Society of Civil Engineers, pp 1453-1475.

Caldwell, J. M. 1956. "Wave Action and Sand Movement Near Anaheim Bay, California," Technical Memo. No. 68, Beach Erosion Board, US Army Engineer Waterways Experiment Station, Vicksburg, MS.

Coakley, J. P., Saville, H. A., Pedrosa, M., and Larocque, M. 1979. "Sled System for Profiling Suspended Littoral Drift," Proceedings of the 16th Coastal Engineering Conference, American Society of Civil Engineers, pp 1764-1775.

Crickmore, B. A., and Aked, R. F. 1975. "Pump Samplers for Measuring Sand Transport in Tidal Waters," Hydraulic Research Publication, Department of Environment, Wallingford, England, pp 311-326.

Downing, J. P., Jr. 1981. "Particle Counter for Sediment Transport Studies," Journal of Hydraulics Division, Vol HY11, pp 1455-1465.

Downing, J. P. 1984. "Suspended Transport on a Dissipative Beach," Proceedings of the 19th Coastal Engineering Conference, American Society of Civil Engineers, pp 1765-1781.

Downing, J. P., Sternberg, R. W., and Lister, C. R. B. 1981. "New Instrumentation for the Investigation of Sediment Suspension Processes in the Shallow Marine Environment," Marine Geology, Vol 42, pp 19-34.

Druffel, L., Emmett, W. W., Schneider, V. R., and Skinner, J. V. 1976. "Laboratory Hydraulic Calibration of the Helley-Smith Bedload Sediment Sampler," United States Geological Survey Open-File Report 76-752, US Government Printing Office, Washington, DC.

DuBoys, P. 1879. "Le Rohne et les Rivieres a Lit Affouillable," Annales des Ponts et Chaussees, Series 5, Vol 18, pp 141-195.

Ehrenberger, R. 1931. "Direct Bedload Measurements on the Danube at Vienna and their Results to Date," Translation No. 39-20, US Army Engineer Waterways Experiment Station, Vicksburg, MS.

Einstein, A. H. 1937. "Calibrating the Bedload Trap as Used in the Rhine," Bauzeitung, Vol 110, No. 12. Translation, Soil Conservation Service, California Institute of Technology, Pasadena, CA.

Einstein, A. H. 1944. "Bed-Load Transportation in Mountain Creek," Soil Conservation Service, Technical Bulletin No. 55.

Emmett, W. W. 1976. "Bedload Transport in Two Large, Gravel-Bed Rivers, Idaho and Washington," Proceedings of Third Federal Inter-Agency Sedimentation Conference, Denver, CO, pp 4-104 - 4-114.

Emmett, W. W. 1980. "A Field Calibration of the Sediment-Trapping Characteristics of the Helley-Smith Bedload Sampler," US Geological Survey Professional Paper 1139, US Government Printing Office, Washington, DC.

Emmett, W. W. 1981. "Measurement of Bed Load in Rivers," Erosion and Sediment Transport Measurement, Proceedings of the Florence Symposium, International Association for Hydraulic Research Publication No. 133, pp 3-15.

Emmett, W. W., Leopold, L. B., and Myrick, R. M. 1983. "Some Characteristics of Fluvial Processes in Rivers," Proceedings of the Second International Symposium on River Sedimentation, Nanjing China, Water Resources and Electric Power Press, pp 730-754.

Emmett, W. W., and Thomas, W. A. 1978. "Scour and Deposition in Lower Granite Reservoir, Snake and Clearwater Rivers near Lewiston," Journal of Hydraulic Research, Vol 16, No. 4, pp 327-345.

Fairchild, J.C. 1972. "Longshore Transport of Suspended Sediment," Proceedings of the 13th Coastal Engineering Conference, American Society of Civil Engineers, pp 1069-1088.

Fukushima, H., and Kashiwamura, M. 1959. "Drift Sand and its Measurement (4th Report)," Proceedings of 6th Conference on Coastal Engineering in Japan, Japanese Society of Civil Engineers, pp 57-62.

Fukushima, H. and Mizoguchi, Y. 1958. "Field Investigation of Suspended Littoral Drift," Coastal Engineering in Japan, Vol 1, pp 131-134.

Graf, W. H. 1984. Hydraulics of Sediment Transport, Water Resources Publications, Littleton, CO.

Greer, M. N., and Madsen, O. S. 1978. "Longshore Sediment Transport Data: A Review," Proceedings of the 16th Coastal Engineering Conference, American Society of Civil Engineers, pp 1563-1576.

Hallermeier, R. J. 1982. "Oscillatory Bedload Transport - Data Review and Simple Formulation," Continental Shelf Research, Vol 1, No. 2, pp 159-190.

Hanes, D. M., and Huntley, D. A. 1986. "Continuous Measurements of Suspended Sand Concentration in a Wave Dominated Nearshore Environment," Continental Shelf Research, Vol 6, No. 4, pp 585-596.

Hanes, D. M., and Vincent, C. E. 1987. "Detailed Dynamics of Nearshore Suspended Sediment," Proceedings of Coastal Sediments '87, American Society of Civil Engineers, pp 285-299.

Hanes, D. M., Vincent, C. E., Huntley, D. A., and Clarkey, T. L. In press. "Acoustic Measurements of Suspended Sand Concentration in the C2S2 Experiment at Stanhope Lane, Prince Edward Island," Marine Geology.

Hattori, M. 1969. "The Mechanics of Suspended Sediment due to Standing Waves," Coastal Engineering in Japan, Vol 12, pp 69-80.

Hattori, M. 1971. "A Further Investigation of the Distribution of Suspended Sediment Concentration due to Standing Waves," Coastal Engineering in Japan, Vol 14, pp 73-82.

Helley, E. J., and Smith, W. 1971. "Development and Calibration of a Pressure-Difference Bedload Sampler," US Geological Survey Open-File Report No. 73-108, Menlo Park, CA.

Hom-ma, M., and Horikawa, K. 1962. "Suspended Sediment Due to Wave Action," Proceedings of the 8th Coastal Engineering Conference, American Society of Civil Engineers, pp 168-193.

Hom-ma, M., Horikawa, K., and Sonu, C. J. 1960. "A Study of Beach Erosion at the Sheltered Beaches of Katasai and Kamakura, Japan," Coastal Engineering in Japan, Vol 3, pp 101-122.

Hom-ma, M., Horikawa, K., and Kashima, R. 1965. "A Study on Suspended Sediment Due to Wave Action," Coastal Engineering in Japan, Vol 8, pp 85-103.

Horikawa, K., ed. 1988. Nearshore Dynamics and Coastal Processes, University of Tokyo Press, Tokyo, Japan, and University of Columbia Press.

Horikawa, K., Watanabe, A., and Katori, S. 1983. "Sediment Transport Under Sheet Flow Condition", Proceedings of the 18th Coastal Engineering Conference, American Society of Civil Engineers, pp 1335-1352.

Hotta, S. 1988. "Vertical Distribution of Sand Transport Rate by Wind," Abstracts, 21st Coastal Engineering Conference, American Society of Civil Engineers, pp 109-110.

Hubbell, D. W. 1964. "Apparatus and Techniques for Measuring Bedload," Geological Survey Water-Supply Paper 1748, US Government Printing Office, Washington, DC.

Hubbell, D. W., Stevens, H. H., Jr., Skinner, J. V., and Beverage, J. P. 1985. "New Approach to Calibrating Bed Load Samplers," Journal of Hydraulic Engineering, Vol 111, No. 4, pp 677-694.

Hubbell, D. W., Stevens, H. H., Jr., Skinner, J. V., and Beverage, J. P. 1987. "Laboratory Data on Coarse-Sediment Transport for Bedload-Sampler Calibrations," United States Geological Survey Water-Supply Paper 2299, US Government Printing Office, Washington, DC.

Huntley, D. A., and Hanes, D. M. 1987. "Direct Measurement of Suspended Sediment Transport," Proceedings of Coastal Sediments '87, American Society of Civil Engineers, pp 723-737.

Inman, D. L. 1949. "Sediment Trap Studies of Suspended Material near the Surf Zone," Scripps Institution of Oceanography Quarterly Progress Report to US Army Corps of Engineers, Beach Erosion Board, No. 2, pp 5-6.

Inman, D. L. 1978. "Status of Surf Zone Sediment Transport Relationships," Proceedings of Workshop on Coastal Sediment Transport with Emphasis on the National Sediment Transport Study, University of Delaware, Sea Grant Report DEL-SG-16-78, pp 9-20.

Inman, D. L., and Bowen, A. J. 1963. "Flume Experiments on Sand Transport by Waves and Currents," Proceedings of the 8th Coastal Engineering Conference, Council on Wave Research, pp 137-150.

Inman, D. L., Zampol, J. A., White, T. E., Hanes, D. M., Waldorf, B. W., and Kastens, K. A. 1980. "Field Measurements of Sand Motion in the Surf Zone," Proceedings of the 17th Coastal Engineering Conference, American Society of Civil Engineers, pp 1215-1234.

Interagency Committee on Water Resources. 1940a. "A Study of Methods Used in Measurement and Analysis of Sediment Loads in Streams, Report No. 1, Field Practice and Equipment used in Sampling Suspended Sediment," St. Paul Engineer District Sub-Office, Hydraulics Laboratory, University of Iowa, Iowa City, IA.

Interagency Committee on Water Resources. 1940b. "A Study of Methods Used in Measurement and Analysis of Sediment Loads in Streams, Report No. 2, Equipment for Sampling Bed Load and Bed Material," St. Paul Engineer District Suboffice, Hydraulics Laboratory, University of Iowa, Iowa City, IA.

Interagency Committee on Water Resources. 1963. "Measurement and Analysis of Sediment Loads in Streams, Report No. 14, Determination of Fluvial Sediment Discharge," 151 p.

Jaffe, B. E., Sternberg, R. W., and Sallenger, A. H. 1984. "The Role of Suspended Sediment in Shore-Normal Beach Profile Changes," Proceedings of the 19th Coastal Engineering Conference, American Society of Civil Engineers, pp 1983-1996.

James, C. P., and Brenninkmeyer, B. M. 1971. "Sediment Entrainment Within Bores and Backwash," Geoscience and Man, Volume XVIII, pp 61-68.

Jansen, R. H. J. 1978. "The In Situ Measurement of Sediment Transport by Means of Ultrasound Scattering," Delft Hydraulics Laboratory Publication No. 203, Delft, The Netherlands.

Johnson, C. W., Engleman, R. L., Smith, J. P., and Hanson, C. L. 1977. "Helley-Smith Bed Load Samplers," Journal of the Hydraulics Division, Proceedings of the American Society of Civil Engineers, Vol 103, No. HY10, pp 1217-1221.

Kalinske, A. A. 1942. "Criteria for Determining Sand Transportation by Surface Creep and Saltation," Transactions, American Geophysical Union, Part II, Washington, DC, pp 639-643.

Kana, T. W. 1976. "A New Apparatus for Collecting Simultaneous Water Samples in the Surf Zone," Journal of Sedimentary Petrology, Vol 46, No. 4, pp 1031-1034.

Kana, T. W. 1977. "Suspended Sediment Transport at Price Inlet, S.C.," Proceedings of Coastal Sediments '77, American Society of Civil Engineers, pp 366-382.

Kana, T. W., Ward, L. G., and Johnson, H. M. 1980. Suspended Sediment and Sand Transport at Duck, North Carolina, Contract DACW72-78-M-0865, Final Report, US Army Engineer Waterways Experiment Station, Coastal Engineering Research Center, Vicksburg, MS.

Katori, S 1982. "Measurement of Sediment Transport by Streamer Trap," Report of the 6th Cooperative Field Investigation, Nearshore Environment Research Center, Report No. 16, TR-81-2, Tokyo, Japan, pp 138-141 (in Japanese).

Katori, S. 1983. "Measurement of Sediment Transport by Streamer Trap," Report of the 7th Cooperative Field Investigation, Nearshore Environment Research Center, Report No. 17, TR-82-1, Tokyo, Japan, pp 110-117 (in Japanese).

Katori, S., Sakakiyama, T., and Watanabe, A. 1984. "Measurement of Sand Transport in a Cross Unidirectional-Oscillatory Flow Tank," Coastal Engineering in Japan, Vol 27, pp 193-203.

Kilner, F. A. 1977. "Measurement of Suspended Sediment in the Surf Zone," Proceedings of the 15th Coastal Engineering Conference, American Society of Civil Engineers, pp 2045-2059.

Klingeman, P. C., and Emmett, W. W. 1982. "Gravel Bedload Transport Processes," Chapter 7, Gravel-Bed Rivers, John Wiley and Sons, Inc., New York, NY, pp 141-179.

Komar, P. D., and Inman, D. L. 1970. "Longshore Sand Transport on Beaches," Journal of Geophysical Research, Vol 75, No. 30, pp 5914-5927.

Kraus, N. C. 1987. "Application of Portable Traps for Obtaining Point Measurements of Sediment Transport Rates in the Surf Zone," Journal of Coastal Research, Vol 3, No. 2, pp 139-152.

Kraus, N. C., and Dean, J. L. 1987. "Longshore Sand Transport Rate Distributions Measured by Trap," Proceedings of Coastal Sediments '87, American Society of Civil Engineers, pp 881-896.

Kraus, N. C., and Nakashima, L. 1986. "Field Method of Determining Rapidly the Dry Weight of Wet Sand Samples," Journal of Sedimentary Petrology, Vol 56, No. 4, pp 550-551.

Kraus, N. C., and Nakashima, L. 1987. "Field Measurement of a Rip Current: Fluid and Sediment Movement," EOS, Vol 68, No. 44, pp 1311-1312.

Kraus, N. C., Gingerich, K. J., and Rosati, J. D. 1988. "Toward an Improved Empirical Formula for Longshore Sediment Transport," Proceedings of the 21st Coastal Engineering Conference, American Society of Civil Engineers, pp 1182-1196.

Kraus, N. C., Gingerich, K. J., and Rosati, J. D. 1989. "DUCK85 Sand Trap Experiments," Technical Report, US Army Engineer Waterways Experiment Station, Coastal Engineering Research Center, Vicksburg, MS.

Kraus, N. C., Gingerich, K. J., and Rosati, J. D. In preparation. "SUPERDUCK Data Report," Technical Report, US Army Engineer Waterways Experiment Station, Coastal Engineering Research Center, Vicksburg, MS.

Kraus, N. C., Isobe, M., Igarashi, H., Sasaki, T. O., and Horikawa, K. 1982. "Field Experiments on Longshore Sand Transport in the Surf Zone," Proceedings of the 18th Coastal Engineering Conference, American Society of Civil Engineers, pp 969-988.

Lee, K. K. 1975. "Longshore Currents and Sediment Transport in West Shore of Lake Michigan," Water Resources Research, Vol 11, No. 6, pp 1029-1032.

Leonard, J. E. and Brenninkmeyer, B. M. 1979. "Periodicity of Suspended Sand Movement During a Storm," Proceedings of the 16th Conference on Coastal Engineering, American Society of Civil Engineers, pp 1744-1763.

Locher, F. A., Glover, J. R. and Nakato, T. 1976. "Investigation of the Operating Characteristics of the Iowa Sediment Concentration Measuring System," Technical Paper No. 76-6, US Army Engineer Waterways Experiment Station, Vicksburg, MS.

Madsen, O. S., and Grant, W. D. 1976. "Quantitative Description of Sediment Transport by Waves," Proceedings of the 15th Coastal Engineering Conference, American Society of Civil Engineers, pp 1093-1142.

Mason, C., Birkemeier, B., and Howd, P. 1987. "An Overview of DUCK85, A Nearshore Processes Experiment," Proceedings of Coastal Sediments '87, American Society of Civil Engineers, pp 818-833.

Meyer-Peter, E. 1937. "Discussion of an Instrument for the Measurement of the Bedload in Rivers," International Association of Hydraulic Structures Research, First Meeting, Berlin, Germany, pp 109-110 (Translation from Iowa University Institute of Hydraulic Research).

Meyer-Peter, E., and Muller, R. 1948. "Formulas for Bed-Load Transport," Report on Second Meeting of International Association for Hydraulic Research, Stockholm, Sweden, pp 39-64.

Miller, I., and Freund, J. E. 1985. Probability and Statistics for Engineers, Prentice-Hall, Inc., Englewood Cliffs, NJ.

Nagata, Y. 1961. "Balance of the Transport of Sediment due to Wave Action in Shoaling Water, Surf Zone, and on Foreshore," Records of Oceanography Works in Japan, Vol 6, pp 53-62.

Nagata, Y. 1964. "Deformation of Temporal Patterns of Orbital Wave Velocity and Sediment Transport in Shoaling Water, Breaker Zone, and on Foreshore," Journal of the Oceanographic Society of Japan, Vol 20, pp 57-70.

Nakato, T., Locher, F. A., Glover, J. R., and Kennedy, J. F. 1977. "Wave Entrainment of Sediment from Rippled Beds," Proceedings, American Society of Civil Engineers, Vol 103, No. WW1, pp 83-100.

Nielsen, P. 1979. "Some Basic Concepts of Wave Sediment Transport," Series Paper No. 20, Technical University of Denmark, Lyngby, Denmark.

Nielsen, P. 1983. "Entrainment and Distribution of Different Sand Sizes Under Water Waves," Journal of Sedimentary Petrology, Vol 53, No. 2, pp 423-428.

Nielsen, P., Green, M. O., and Coffey, F. C. 1982. "Suspended Sediment Under Waves," Coastal Studies Unit Technical Report No. 82-6, Department of Geography, University of Sydney, 157 p.

Noda, H. 1962. "Suspension of Sediment Due to Wave Action," Proceedings of 14th Conference on Coastal Engineering in Japan, Japanese Society of Civil Engineers, pp 306-314.

Novak, P. 1957. "Bed Load Meters-- Development of a New Type and Determination of their Efficiency with the Aid of Scale Models," Transactions, International Association of Hydraulic Research, 7th General Meeting, Vol 1.

Pickrill, R. A. 1986. "Sediment Pathways and Transport Rates through a Tide-Dominated Entrance, Rangaunu Harbour, New Zealand," Journal of Sedimentology, Vol 33, pp 887-898.

Reid, I., Layman, J. T., and Frostick, L. E. 1980. "The Continuous Measurement of Bedload Discharge," Journal of Hydraulic Research, Vol 18, No.3, pp 243-249.

Rosati, J. D., and Kraus, N. C. 1988. "Hydraulic Test of the Streamer Sediment Trap," Journal of Hydraulics Division, Vol 114, No. 12, pp 1527-1532.

Sawamoto, M., and Yamashita, T. 1986. "Sediment Transport Rate Due to Wave Action." Journal of Hydroscience and Hydraulic Engineering, Vol 4, pp 1-15.

Shamov, G. I. 1935. "Brief Information Regarding the Results of Laboratory Tests of Silt Samplers," Science Research Institute Hydrotechnics, Translation No. 114, California Univ., Mechanical Engineering Department, Berkeley, CA.

Shen, H. W. 1971. River Mechanics, Vols I and II, H. W. Shen Publishing Co., Ft. Collins, CO.

Shields, A. 1936. "Anwendung der Aenlichkeitsmechanik und der Turbulenzforschung auf die Geschiebebewegung," Mitteilungen der Preussischen Versuchsanstalt fur Wasserbau und Schiffbau, Berlin, Germany, Translated to English by W. P. Ott and J. C. van Uchelen, California Inst. of Technology, Pasadena, CA.

Shore Protection Manual. 1984. 4th ed., 2 vols, US Army Engineer Waterways Experiment Station, Coastal Engineering Research Center, US Government Printing Office, Washington, DC.

Simons, D. B., Richardson, E. V., and Nordin, C. F.(Jr.). 1965. "Bedload Equation for Ripples and Dunes," Geological Survey Professional Paper 462-H, US Government Printing Office, Washington, DC.

Sleath, J. F. A., 1984. Sea Bed Mechanics, John Wiley and Sons, New York, NY.

Southard, J. B. 1971. "Representation of Bed Configurations in Depth - Velocity-Size Diagrams," Journal of Sedimentary Petrology, Vol 41, No. 4, pp 903-915.

Staub, C., Svendsen, I. A., and Jonsson, I. G. 1983. "Measurements of the Instantaneous Sediment Suspension in Oscillatory Flow by a New Rotating-Wheel Apparatus," Progress Report 58, Institute of Hydrodynamics and Hydraulic Engineering, Technical University of Denmark, pp 41-49.

Sternberg, R. W., Cacchione, D. A., Drake, D. E., and Kranck, K. 1986a. "Suspended Sediment Transport in an Estuarine Tidal Channel Within San Francisco Bay, CA," Marine Geology, Vol 71, pp 237-258.

Sternberg, R. W., Johnson II, R. V., Cacchione, D. A., and Drake, D. E. 1986b. "An Instrument System for Monitoring and Sampling Suspended Sediment in the Benthic Boundary Layer," Marine Geology, Vol 71, pp 187-189.

Sternberg, R. W., Shi, N. C., and Downing, J. P. 1985. "Field Investigations of Suspended Sediment Transport in the Nearshore Zone," Proceedings of the 19th Coastal Engineering Conference, American Society of Civil Engineers, pp 1782-1798.

Subcommittee On Sedimentation. 1963. A Study of Methods Used in Measurement And Analysis of Sediment Loads in Streams, Report No. 14, St. Anthony Falls Hydraulic Laboratory, Minneapolis, Minn., US Government Printing Office, Washington, DC.

Tamura, T., and Hanes, D. M. 1986. "Laboratory Calibration of a 3 Megahertz Acoustic Concentration Meter to Measure Suspended Sand Concentration," Technical Report No. 86-004, University of Miami, Rosenstiel School of Marine and Atmospheric Science, Miami, FL.

Thornton, E. B. 1969. "A Field Investigation of Sand Transport in the Surf Zone," Proceedings of the 11th Coastal Engineering Conference, American Society of Civil Engineers, pp 335-351.

Thornton, E. B. 1972. "Distribution of Sediment Transport Across the Surf Zone," Proceedings of the 13th Coastal Engineering Conference, American Society of Civil Engineers, pp 1049-1068.

Thornton, E. B., and Morris, W. D. 1977. "Suspended Sediments Measured within the Surf Zone," Proceedings of Coastal Sediments '77, American Society of Civil Engineers, pp 655-668.

US Army Corps of Engineers, Beach Erosion Board. 1933. Interim Report, 15 April 1933, unpaged.

US Army Engineer Waterway Experiment Station. 1935. "Studies of River Bed Materials and Their Movement, with Special Reference to the Lower Mississippi River," Paper 17, Vicksburg, MS.

Vanoni, V. A., ed. 1977. Sedimentation Engineering, American Society of Civil Engineers, New York, NY.

Wantanabe, A. 1988. "Numerical Model of Beach Topography Change," Chapter III, Nearshore Dynamics and Coastal Processes, ed. K. Horikawa, University of Tokyo Press, Tokyo, Japan.

Waslenchuk, D. G. 1976. "New Diver-Operated Bedload Sampler," Journal of the Hydraulics Division, Vol 102, No. HY6, pp 747-757.

Watts, G. M. 1953. "Development and Field Tests of a Sampler for Suspended Sediment in Wave Action," TM-34, US Army Engineer Waterways Experiment Station, Vicksburg, MS.

White, F. H. 1979. Fluid Mechanics, McGraw-Hill Book Company, New York, NY.

Yalin, M. S. 1963. "An Expression for Bed-Load Transportation," Journal of Hydraulics Division, Vol 89, pp 49-59.

Young, R. A., Merrill, J. T., Clarke, T. L. and Proni, J. R. 1982. "Acoustic Profiling of Suspended Sediments in the Marine Bottom Boundary Layer," Geophysical Research Letters, Vol 9, No. 3, pp 175-178.

Zampol, J. A. and Waldorf, D. W. In press. "Measuring Sediment Dynamics: Discrete Sampling of Bedload and Suspended Load," Chapter 5A, NSTS Monograph, ed. R.J. Seymour, Pergamon Press, New York, NY.

APPENDIX A: LITERATURE REVIEW OF SEDIMENT TRAPS AND SAMPLING DEVICES

Introduction

1. This appendix presents a review of riverine and coastal apparatus for measuring sediment transport. The chapter is organized with an introduction and general discussion, description of various types of riverine suspended and bed-load traps, and description of coastal suspended, bed-load, and total load measuring techniques. Riverine devices are discussed fi t because their development preceded the development of coastal apparatus, and the flow environment is simpler than that of the coastal zone.

2. The first field measurements of entrained sediment were conducted in rivers and streams (Subcommittee on Sedimentation 1963). Sedimentation and erosion in the riverine environment created navigational and structural problems for the ancient civilizations of China, Mesopotamia, and Egypt. However, the earliest documented study was performed in 1808-1809 and concerned measurements of suspended sediment on the Rhone River, France. Suspended sediment is defined as sediment which is supported by the surrounding fluid during its entire motion. Sediment is kept in suspension by a turbulent-velocity component of the flow, and its concentration varies through time both vertically and horizontally. Unfortunately, measurement techniques and apparatus employed in the earliest studies were not recorded. The first documented technique for measuring suspended sediment, dating from the 1800's, made use of ordinary pails to sample the concentration of sediment near the surface. The sample was assumed to represent the mean of the vertical suspended sediment at that point (Inter-Agency Committee on Water Resources 1940b).*

3. A bed-load sampler was first developed in 1898 and used in the Nicaragua Canal (Inter-Agency Committee on Water Resources 1940a). Bed load is defined as that part of the solids load of the stream which is supported by the bed, rolling, skipping, or sliding along the bottom, and moving in con-

---

* References cited in the Appendix can be found in the list of references at the end of the main text.

tinuous or near-continuous contact with the bed. The sum of the suspended and bed-load quantities is termed the "total load." Bed-load transport is even more sporadic than that of suspended load, varying cyclically with the movement of bedforms (Ehrenberger 1931, Einstein 1937, Hubbell et al. 1987). Therefore, short-term measurements of bed load are not likely to be representative of an average transport at a particular point. Development of bed-load samplers lagged behind that of suspended load samplers for three reasons. First, bed load is more difficult to sample than suspended load; the sampler must rest on or near the bed and collect sediment without disturbing material on the bed. Bed material is defined as that material which composes the river bed and may have arrived there as the result of previous suspended and/or bed-load movement. Second, samplers were usually developed to collect data on specific rivers, and many highly utilized rivers have beds composed of finer grained material, the majority of which is usually transported as suspended load. Finally, designing a bed-load trap that collects only bed load (excluding suspended load) is difficult.

4. Sediment samplers have traditionally been classified as either bed-load or suspended load measuring devices; however, the boundary between material moving as bed load and suspended load is not well defined and varies with time, location, and nature of the material. Therefore, bed-load traps may collect some suspended material, and suspended load samplers, if close to the bed, may collect material moving along the bed.

5. An ideal sediment sampler collects the quantity and size distribution of sediment flowing through a particular area during a time period equivalent to the quantity and size distribution of sediment that would have passed through that area in that time period had the sampler not been there. An ideal sampler has the following characteristics:

a. Shape and size that minimize flow disturbance.

b. Flow speed at the intake equal to the ambient (undisturbed) speed at that point.

c. Proper vertical and horizontal orientation during the sampling period.

6. Two quantities commonly used in evaluation and calibration of sediment samplers are the hydraulic efficiency E_h and the sediment-trapping

efficiency E_s. The hydraulic efficiency, defined by Equation A1, is the ratio of the average velocity in the sampler nozzle V_t (in units of distance per time) to the average velocity for the same flow condition at the same vertical and horizontal location without the sampler V_o (in units of distance per time):

$$E_h = \frac{V_t}{V_o} \tag{A1}$$

The trapping efficiency, defined by Equation A2, is the ratio of the trap-measured sediment transport rate q_t (weight per width and time or equivalent units) to the actual sediment transport rate for the same flow condition at the same vertical and horizontal location without the sampler q_o (weight per width and time or equivalent units):

$$E_s = \frac{q_t}{q_o} \tag{A2}$$

An ideal sampler has hydraulic and sediment-trapping efficiencies equal to 1.0, or 100 percent. Both field and laboratory tests are necessary to fully evaluate the hydraulic and sediment-trapping efficiencies of a sampler for various flow conditions and sediment characteristics.

7. Most suspended load samplers yield the suspended load transport rate q_{ss} (weight of sediment per unit time and width) from the product of the concentration of sediment C (parts of sediment per parts of water) in a water-sediment sample and the water discharge q (volume per unit time and width):

$$q_{ss} = C\ q \tag{A3}$$

For this relationship to accurately predict the suspended load transport rate, sediment must be moving at the same velocity (speed and direction) as the flow, and both C and q must be steady in time. A time-averaging procedure could also be used as these quantities vary with time. Because material near the bed travels more slowly than the flow speed, Equation A3 is not valid near

the bed. Suspended sediment transport rates can also be calculated from the weight of sediment collected w_s, the width of the active collection element Δw, and the measurement time Δt:

$$q_{ss} = \frac{w_s}{\Delta w \, \Delta t} \tag{A4}$$

8. The bed-load transport rate q_b (units of weight per unit time and width) can be calculated from the weight of bed load collected g_b (units of weight), width of the sampler nozzle Δw (units of length), and sampling time interval Δt (units of time):

$$q_b = \frac{g_b}{\Delta w \, \Delta t} \tag{A5}$$

Riverine Measurement Apparatus

Suspended load samplers

9. Riverine suspended sediment samplers can be classified generally as instantaneous, integrating, or indirect measuring (continually recording). Each category of sampler is defined and discussed below.

a. Instantaneous capture samplers. After being lowered to a specified depth in a horizontal or vertical position, these samplers collect a water-sediment mixture when triggered. Four types of instantaneous samplers, as described by the Inter-Agency Committee on Water Resources (1963), are listed below. All of these samplers measure the concentration of sediment in the fluid and yield a suspended sediment transport rate using the flow velocity. Because of the variation in suspended sediment transport through time and location, many samples must be collected to assure that the calculated transport rates and suspended sediment distributions will be representative.

(1) Ordinary Vertical Pipe Sampler
Ordinary vertical pipe samplers consist of a cylinder with valves on the ends of the pipe that close when triggered. As the open sampler is lowered to a specified depth, the water-sediment mixture flows upward into the cylinder. The valves then close when the sampler stops at

the desired position. The simplicity of the sampler made it popular from the mid-1800's to the 1940's, but several inherent problems have discouraged its use. Disadvantages of such a sampler include excessive disturbance to the flow caused by the cylinder and excessive intermixing of the sample with water and sediment above the sampling point. In addition, the samples are not sufficiently time-integrated to give a representative mean of the sediment concentration. An example of this type of sampler is the Riesbol pipe sampler shown in Figure A1. It consists of a 2-in-diameter (5.1-cm) pipe with variable length (suggested length is approximately equal to the river depth). For use of the sampler, the base plate is placed on the stream bed, and the pipe is dropped from the surface, enclosing the sample as it hits the base plate. The sampler was used from 1874-79 on the Ganges Canal in India and was considered to give an average suspended sediment sample for the depth of stream (Inter-Agency Committee on Water Resources 1940a).

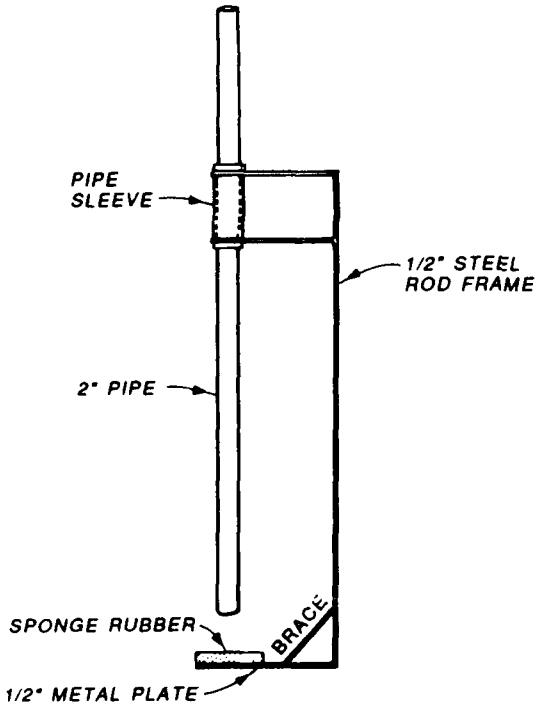

APPROXIMATELY TO SCALE 1:10

Figure A1. Riesbol ordinary vertical pipe suspended sampler (from Inter-Agency Committee on Water Resources 1940a)

(2) Instantaneous Capture Vertical Sampler

An instantaneous capture vertical sampler is similar to an ordinary vertical pipe sampler in that it consists of a vertical cylinder that collects a sample when triggered. However, the instantaneous capture vertical sampler cylinder is shorter and operates by sealing the cylinder

against a flat plate. In this way, an instantaneous point sample of suspended sediment can be collected. The objective in designing such a sampler is to minimize flow disturbance prior to sampling. However, the degree to which such a sampler disturbs the flow does not appear to have been investigated, and the sampler is not recommended for use near the river bed. An example of an instantaneous capture vertical sampler is the Eakin sampler shown in Figure A2. The sampler consists of a cylinder that is held above a lower disk prior to sampling by a catch mechanism. A messenger weight, released from above, triggers the cylinder which falls onto the base plate, thereby collecting the sample. A more streamlined version of this sampler with multiple sampling capability is shown in Figure A3. A similar multiple instantaneous vertical sampler that has recently been used to measure suspended sediment transport in the nearshore coastal zone is the Kana sampler (Kana 1976). This sampler is discussed in detail in the section entitled "Coastal Suspended Sediment Samplers."

(3) Instantaneous Capture Horizontal Sampler
Instantaneous capture horizontal samplers consist of horizontal cylinders with flaps on each end that can be closed when the sampler reaches the desired sampling point. Water and sediment flow through the cylinder as it is being lowered to a particular depth. Advantages of this type of sampler include its simple design and mechanism, the capability to sample close to the river bed, and the capability to use the sampler in varying depth streams. Multiple samples through the depth must be collected to measure a representative average suspended sediment concentration. The degree to which the sampler disturbs the flow has not been investigated, but is believed to be minimal. An example of an instantaneous horizontal sampler is the Leitz sampler, shown in Figure A4, consisting of a brass cylinder 1 ft (30.5 cm) in length and 3 in. (7.6 cm) in diameter with disk doors that swing shut when released.

(4) Bottle Sampler
Bottle samplers are the simplest of suspended sediment samplers and consist of a standard container such as a milk bottle or fruit jar. This type of sampler is lowered to a sampling point, and the water-sediment mixture fills the container displacing the air. Advantages of these samplers are that they are simple in design and easily facilitate the transport of individual samples to the laboratory. Disadvantages of bottle samplers outweigh the advantages and include: excessive disturbance to the flow, inter-

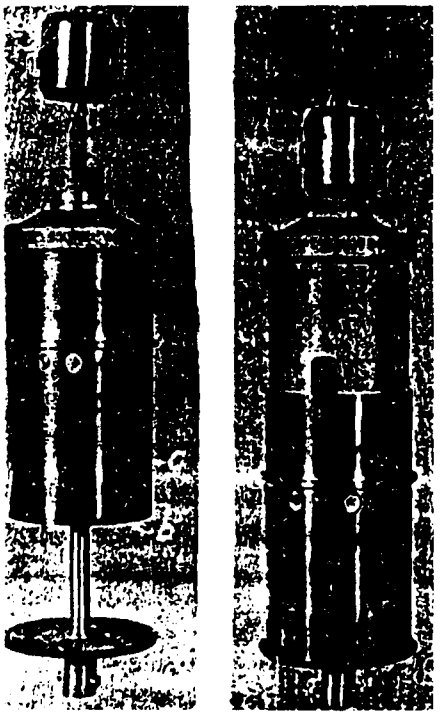

Figure A2. Eakin instantaneous capture vertical suspended sediment sampler; open (left) and shut (right) (from Inter-Agency Committee on Water Resources 1940a)

Figure A3. Eakin multiple instantaneous capture vertical suspended sediment sampler; open (left) and shut (right) (from Inter-Agency Committee on Water Resources 1940a)

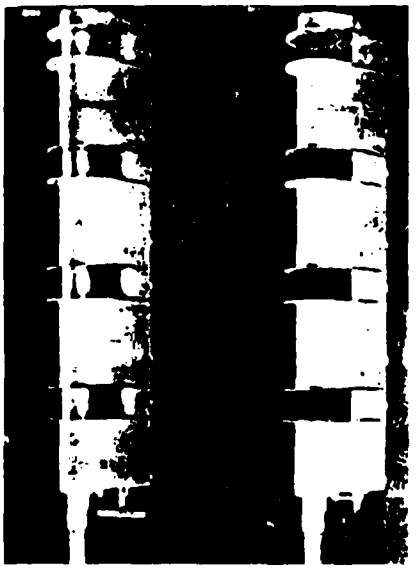

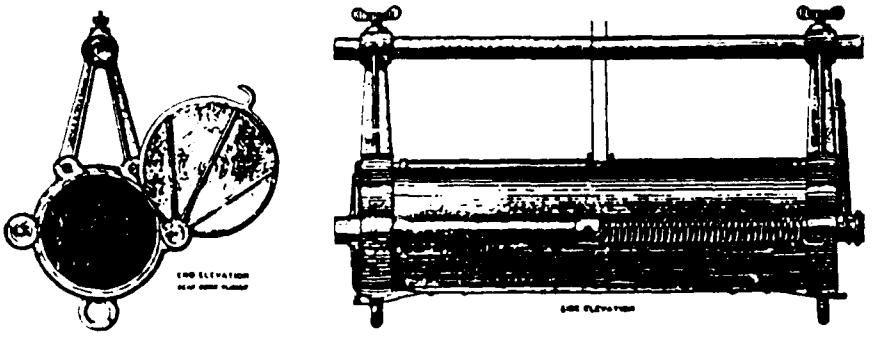

Figure A4. Leitz instantaneous capture horizontal suspended sediment sampler end elevation (left) and side elevation (right) (from Inter-Agency Committee on Water Resources 1940a)

mixing of the collected sample with sediment from other depths during descent and ascent of the sampler (unless immediately closed), non-uniform filling rate of the sampler, and unsuitability for sampling in shallow streams and near the river bed. Bottle samplers were used to obtain sediment concentrations in the nearshore zone of the north New Jersey coast in the early 1930's (Morrough P. O'Brien, personal communication 1986).

b. Integrating samplers. Integrating samplers collect a sample over a period of time or through a depth. The quantity of sediment is then averaged by the time period or distance to obtain a representative sample.

(1) Time- and depth-integrating samplers
Time- and depth-integrating samplers consist of a container such as a milk bottle with a valve so that air can escape as the sample is being collected. The container is held in a streamlined shell to weight the sampler and control its horizontal attitude. Both laboratory and field tests have been conducted for certain versions of these samplers to ensure that the flow velocity at the sampling point is

equal to the intake velocity. Reduction of the bias of the flow either into or away from the sampler assures that a representative sample can be collected. Point-integrating samplers are held at a specified depth for a period of time, thereby collecting a time-integrated sample. These samplers can be lowered to the design depth and then activated to begin sampling. Depth-integrating samplers are lowered from the surface to the bed and returned at a constant rate. The collected sample represents an average concentration for the river depth. An example of a point-integrating sampler is the Anderson-Einstein sampler shown in Figure A5. The Anderson-Einstein sampler consists of a pint milk bottle with water intake and air-exhaust tubes to facilitate sampling. A point-integrating sampler that measures the quantity of sediment entering the apparatus rather than the sediment concentration is the Delft bottle (Jarocki 1963, as referenced in Graf 1984). This sampler consists of an entrance pipe, 0.022 m in diameter, that expands to 0.31 mm in diameter; in the rear is a cover plate with holes. As the water-sediment mixture enters the sampler, the expanding pipe causes the mixture velocity to decrease, and the sediment is expected to settle out in the inner chamber while the fluid exits through the rear holes. This sampler is illustrated in Figure A6.

(2) Pumping Sampler

Pumping samplers pump a water-sediment mixture at a particular point through a pipe or hose. In principle, the intake velocity can be adjusted to be equal to the fluid velocity, and a representative sample of any volume can be obtained. However, adjustment of the pump velocity to equal the fluid velocity is very difficult. An average concentration for a particular depth can be measured by collecting a sample over a period of time. Several coastal studies that have used pumping samplers are discussed in the "Coastal Suspended Sediment Apparatus" section. Disadvantages of pumping samplers include: the pumping rate must be continually regulated as the flow velocity varies; large suspended sediment particles tend to settle in the pipe, necessitating higher pumping velocities; the depths at which the sampler can be used are limited by resistance of the hose/pipe to fluid currents and by vacuum capability of the pump; and the bulkiness of the sampler limits portability.

c. Indirect-measuring (or continually recording) samplers.

These samplers measure some phenomena occurring as a result of sediment transport. Three types of such devices have been identified by Graf (1984) and are described below.

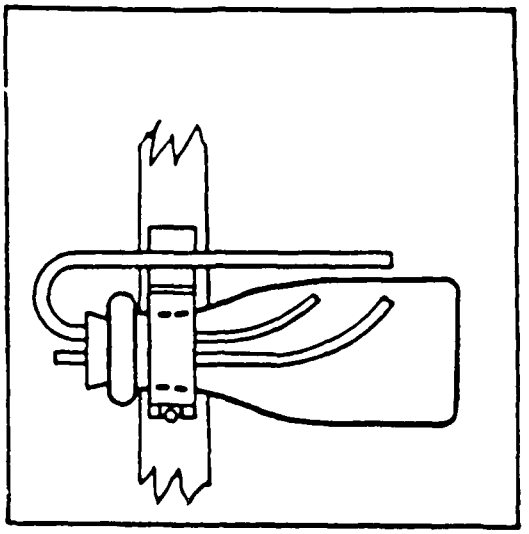

Figure A5. Anderson-Einstein point-integrating suspended sediment sampler (from Inter-Agency Committee on Water Resources 1940a)

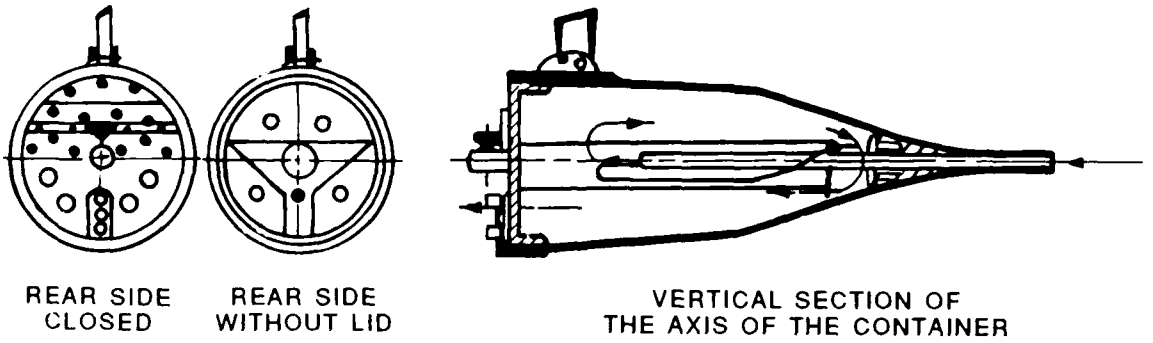

Figure A6. Delft bottle point-integrating suspended sediment sampler (from Graf 1984)

(1) Transparency indicator
As volume of suspended sediment increases, the transparency of the water decreases. This type of instrument measures the decrease in fluid transparency through which suspended sediment concentration may be inferred. A disadvantage of such a device is that it must be calibrated for every situation because of the variability of fluid, sediment, and lighting. However, such a device could be designed to minimize flow disturbance, thereby accurately measuring the quantity of suspended material. Coastal instrumentation using this principle are discussed in detail in the "Coastal Suspended Sediment Apparatus" section.

(2) Resistance indicator
This type of instrument measures the variation in resistance as sediment passes through an aperture.

(3) Ultrasonic indicator
The attenuation of sound waves passing through a fluid-sediment mixture varies as the quantity of sediment increases and decreases. With calibration, this type of instrument can indirectly measure the concentration of suspended sediment.

Bed-load samplers

10. Methods available for measuring bed-load transport can be classified as either direct or indirect. These methods and the types of riverine samplers associated with each are discussed below.

a. Direct-measuring bed-load samplers. These samplers consist of a container or excavated region into which sediment moving along the bed is deposited. Because of the cyclic nature of bed-load transport as bedforms pass a fixed point, the quantity of sediment collected with a bed-load trap depends on the location of the sampler at the start of sampling relative to the bedform. Four types of direct-measuring samplers for riverine use were identified by Hubbell (1964) and Graf (1984), and are described below.

(1) Box or basket sampler
Box or basket samplers consist of a rectangular frame with screen material on all sides except the front and, possibly, the top. These samplers rest on the bed and collect sediment during a sampling period; then they can be retrieved and the sample retained for later analysis. An example of a basket trap designed to collect large-grained sediment is the Nesper sampler (Figure A7). This sampler has a bottom of loosely woven iron rings that conforms to the shape of the bed. Einstein (1937) measured sediment-trapping efficiencies of this sampler ranging from 0.9 to

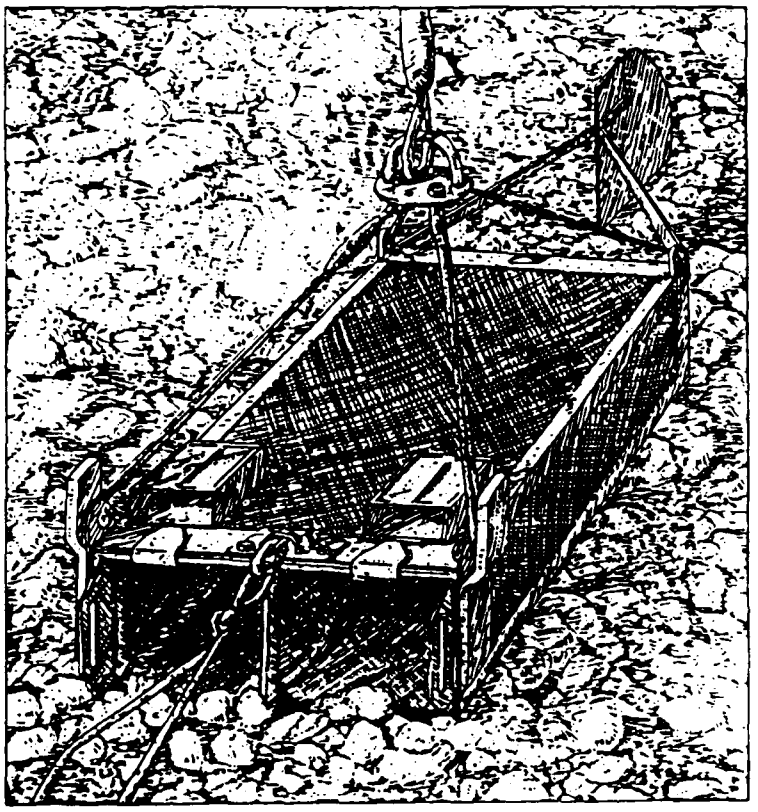

Figure A7. Nesper basket bed-load sampler (from Hubbell 1964)

0.2, depending on particle size and bed-load transport rate. In general, a basket sampler has a sediment-trapping efficiency of about 0.45 (Hubbell 1964). Box and basket-type samplers were popular prior to 1940 and were used to check the validity of various predictive relationships for bed-load transport rates (Hubbell 1964).

(2) Pan or tray samplers

Pan or tray samplers consist of an entrance ramp leading to a slot or slots. Sediment that has rolled, slid, or skipped up the ramp is retained in the sampler. An example of the pan or tray sampler is the Polyakov sampler, shown in Figure A8. Shamov (1935) found that the Polyakov sampler sediment-trapping efficiency for flow speeds from 1.3 to 1.75 ft/sec (39.6 to 53.3 cm/sec) was about 0.46; the sediment-trapping efficiency of the sampler decreased at flow velocities greater than 2.1 ft/sec (64 cm/sec). Several versions of these samplers were developed, with varying ramp designs and numbers of slots. Shamov reports

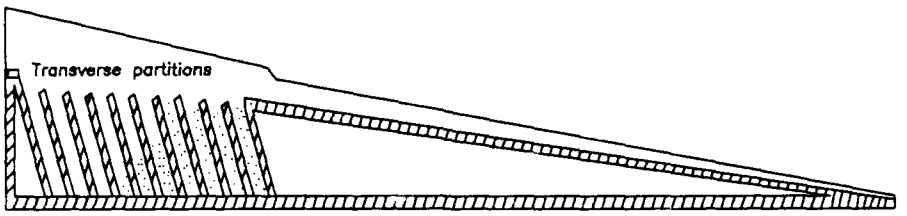

Figure A8. Polyakov pan bed-load sampler (from Hubbell 1964)

efficiencies ranging from 0.38 to 0.75. Certain versions of the sampler were observed to mound bed-load material in front of the ramps, thereby decreasing the sediment-trapping efficiency.

(3) Pressure-difference samplers

Pressure-difference samplers are usually composed of a rigid expanding nozzle attached to a removable mesh bag in which sediment collects. The concept of these samplers is to compensate for changes in flow resistance as might result from the collected sediment and sampler by constructing the sampler walls such that they diverge towards the rear. The larger exit area creates a pressure decrease which increases the fluid/sediment speed at the entrance of the sampler. A removable mesh bag is attached to the nozzle to allow collection and removal of the sample. The pressure-difference sampler is the only direct-measuring bed-load device that is extensively used in the U.S. One of the earliest pressure-difference samplers and the precursory device to the Helley-Smith sampler (a popular present-day pressure-difference sampler) was the Arnhem or Dutch sampler (Figure A9) (Hubbell 1964). This sampler is held next to the bed and directly into the flow with a large frame. The sampler itself is composed of a rigid rectangular expanding entrance nozzle and a 0.2- to 0.3-mm removable mesh bag. The sediment-trapping efficiency for the Arnhem sampler is approximately 0.70 (Meyer-Peter 1937). Pressure difference samplers recently developed for riverine bed-load measurements include the "VUV" sampler (Novak 1957, Lee 1975, Pickrill 1986) and the Helley-Smith

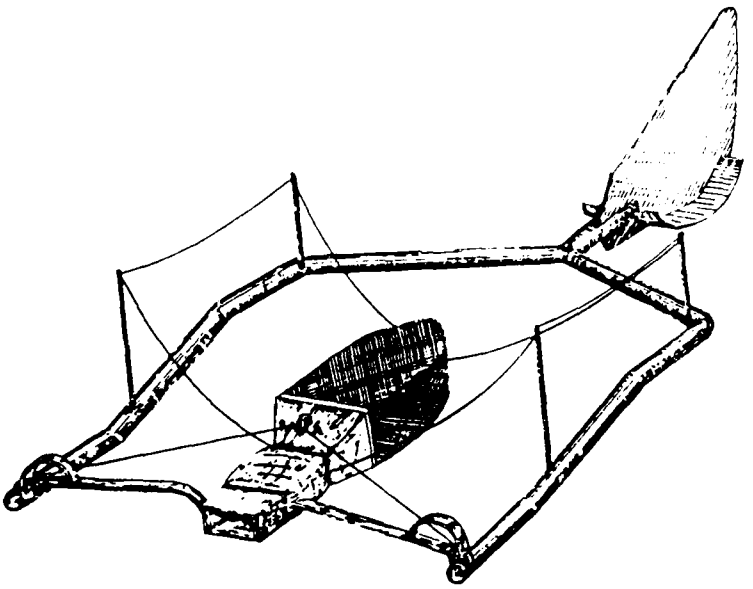

Figure A9. Arnhem (Dutch) pressure-difference bed-load sampler (Hubbell 1964)

Sampler (Helley and Smith 1971; Druffel et al. 1976; Emmett 1976; Johnson et al. 1977; Emmett and Thomas 1978; Emmett 1980; Emmett 1981; Emmett, Leopold, and Myrick 1983). The VUV bed-load sampler was developed in 1957 based on the Goncarov and Karolyi types of samplers. The sampler consists of a full metal streamlined exterior with a wire mesh on the rear top part of the apparatus to facilitate flow exiting the sampler. The shape of the sampler was designed to compensate for the resistance of the apparatus. Novak (1957) measured the hydraulic and sediment-trapping efficiencies of several types of samplers, including the VUV, S (mesh), Karolyi, Nesper (Figure A7), and Ehrenberger. Hydraulic efficiencies of the VUV and Karolyi samplers were calculated at 1.0 and 0.8, respectively. Ambient sediment trapping efficiencies were measured in a flume using a pit sampler. Conclusions from the experiment were as follows: (a) sediment trapping efficiency of the VUV sampler may increase slightly with grain size; (b) all samplers retain representative samples; (c) efficiency may increase slightly as flow increases; and (d) the hydraulic efficiency only gives a qualitative measure of sediment-trapping efficiency. Sediment-trapping efficiencies for the samplers were as follows: VUV sampler, 0.70; S(mesh) sampler, 0.65; Karolyi, 0.45; Nesper, 0.40; and Ehrenberger, 0.60 Lee (1975) and Pickrill (1986) used the VUV sampler in the coastal environment, and their studies are discussed in the coastal section. The Helley-Smith sampler, perhaps the most extensively studied sediment

trapping apparatus, is a pressure-difference device developed in 1971 for use in measuring bed-load transport on natural streams carrying coarse sediments (Helley and Smith 1971). The sampler is similar in design to the Arnhem or Dutch sampler (Figure A9), and consists of a removable mesh bag attached to an expanding nozzle (Figure A10). Helley and Smith (1971) hydraulically calibrated the sampler in a 60-ft (18.3-m) recirculating flume and noted that speeds in the sampler at 4 inches (10.2 cm) in front of the sampler were consistently higher than ambient speeds, and that they tended to increase as the ambient flow speed increased. Ambient bed-load transport rates were calculated by subtracting measured suspended transport rates from total load transport rates. A concentration sampler was used to measure the suspended material, and a splitter 1/2 in. (1.3 cm) in width was used to measure the total load. The splitter is a device at the end of a flume that retains the water-sediment mixture as it traverses the width of the flume. The quantities of sediment collected by the sampler, determined in a recirculating flume, were found to vary considerably, with the variation in samples equal in most cases to the mean value of collected sediment. However, the bed-load transport rates inferred from collected quantities of sediment were in reasonable agreement predictions from the Meyer-Peter and Muller bed-load equation for coarse sediments (0.4 to 30 mm). For sand-sized material, the studies suggested that over-registration as high as 50 percent might occur. The sampler was very stable in high flows, but it tended to scoop up bed-load material as it was lowered to sampling position. An extensive hydraulic calibration of the sampler was conducted by Druffel et al. (1976) for various entrance-to-exit ratio versions of the device. Druffel et al. (1976) calculated hydraulic efficiencies from 1.06 to 1.54 as the exit-entrance area ratios increased from 1.00 to 2.62. They recommended and continued testing the version with the hydraulic efficiency equal to 1.54. Filling of the sampler bag up to 40 percent did not decrease efficiency; however, particles close to the diameter of the mesh collection bag (0.2 mm) did decrease efficiency, presumably because of mesh clogging. The sediment-trapping efficiency of the sampler was evaluated in the field using the East Fork River, Wyoming, conveyor belt sampler to measure the ambient bed-load transport rate (Figure A11)(Emmett 1980). A large data set with a 1,000-fold range in measured transport rates was obtained. Emmett (1980) concluded that the Helley-Smith sediment-trapping efficiency for material 0.5 to 16 mm in diameter is 100 percent. For material sized from 0.25 to 0.5 mm, the sampler was 175 percent efficient; the comparably

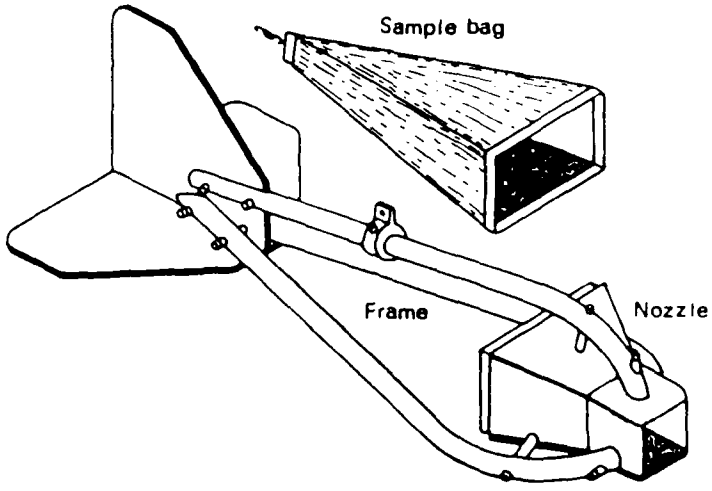

Figure A10. Helley-Smith bed-load sampler (from Druffel et al. 1976)

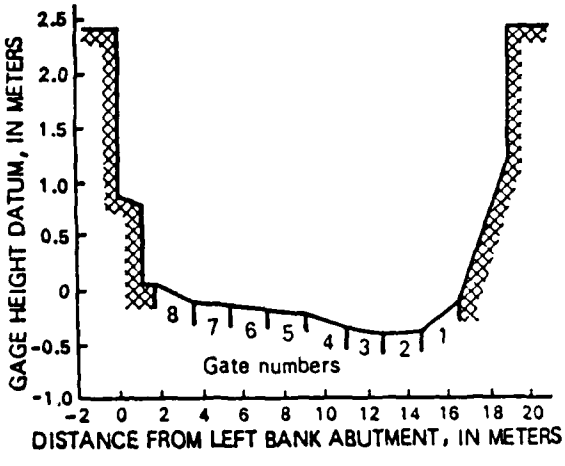

Figure A11. Cross-sectional view of East Fork River, Wyoming slot bed-load sampler (after Emmett 1980)

higher efficiency was attributed to collection of suspended material in the sampler. For material with a diameter greater than 16 mm, the sampler was 70 percent efficient. Emmett (1980) recommends that the sampler not be used for material finer than 0.25 mm and at sites where bed-load material can also be transported as suspended sediment.

(4) Slot or pit samplers

Slot or pit samplers consist of an excavated region in the stream bed from which sediment collected during a time period can be retrieved and the bed-load transport rate estimated. A recent use of this sampling method was made by Emmett (1980) to calibrate the Helley-Smith sampler in the field. Emmett used a series of eight gates above a conveyor belt built into the river bed (Figure A11) and therefore was able to continuously measure the quantity and size distribution of the bed-load material. This sampling method has been shown to have a sediment-trapping efficiency of 100 percent if the slot widths are from 100 to 200 times the grain diameter (Einstein 1944). Other pit samplers developed for riverine use include the Birkbeck Bed-load Sampler (Reid, Layman, and Frostick 1980), the Waslenchuk portable pit sampler (Waslenchuk 1976), the vortex tube system permanently installed at Oak Creek, Oregon, and the conveyor belt system permanently installed at East Fork, Wyoming (Klingeman and Emmett 1982). Pit samplers that use an excavated region to collect sediment are considered the ideal type of sampler because they do not introduce apparatus that may disturb the flow regime. However, this type of sampler is usually costly to install, site permanent, and requires periodic emptying. The Birkbeck Bed-load Sampler (Reid, Layman, and Frostick 1980) consists of a sediment-collection box inside a precast concrete liner. The inner box is free to move up and down inside the liner, and rests on a rubber pressure cushion that responds to the continually varying masses of water and collected sediment (Figure A12). River stage data can be collected simultaneously with the variation of fluid pressure in the cushion; therefore, instantaneous differences in cushion pressure head can be related proportionally to the mass of sediment in the trap. The sampler is recommended for coarse-grained alluvial channels because of the tendency for finer grained materials to settle on the pressure pillow and inhibit function of the device. Six of the samplers were installed at Turkey Brook in England. Bed-load sediment transport values corresponded well with predictions from the Meyer-Peter and Muller bed-load transport equation. The primary advantage of the Birkbeck Bed-load sampler is that sediment transport can be continually recorded. The Waslenchuk portable pit sampler

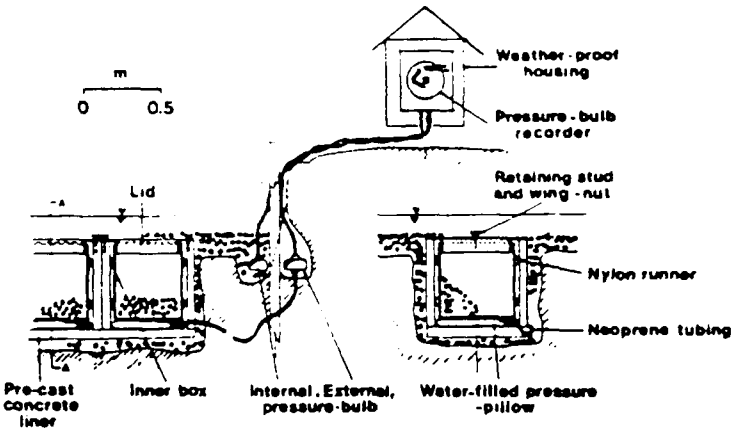

Figure A12. Birkbeck bed-load sampler (from Reid, Layman, and Frostick 1980)

consists of a wedge-shaped pan that can be inserted into the bed by divers during low to moderate flows. The sampler induces flow separation at the leading edge of the pan; a sieve-mesh screen contains sediment as flow exits the trap. The trap was installed in a section of the Ottawa River, Ottawa, Canada. Sediment transport rates inferred from use of the sampler were compared with the dune-tracking method of calculating sediment transport. Values compared well at two of three stations. The author contributes discrepancies at the other station to (a) the cyclic nature of sediment transport and the short sampling times inherent in this type of sampler, and (b) the non-angularity of dunes at that station, an assumption in the dune-tracking method. Laboratory experiments were conducted in two flumes. The first flume was exactly the width of the sampler and indicated that the trap had a sediment-trapping efficiency equal to or greater than 0.85. The ambient rate of sediment transport was calculated using the weight of sediment in the tail water without the sampler in use. The width of the second flume was twice that of the sampler; therefore, for a sediment-trapping efficiency of 1.0, the weight of material caught by the sampler would equal the weight of material in the tail

water. The experiments in the wider flume indicated a sediment-trapping efficiency for the sampler equal to 1.0. Velocity profiles taken upstream from the sampler and directly above the sampler were nearly identical, indicating that the sampler did not adversely affect the flow regime. The vortex tube system operating since 1969 at Oak Creek, Oregon develops vortex flow to move fluid and sediment through a flume. The bed load is removed to an off-channel pit where it is measured and returned to the creek. The vortex flume is continually operated; sampling can be continual or intermittent. The authors state that the trapping efficiency for coarse sand and large particles is 1.0 for all flow regimes. For lower flows, trapping efficiencies are also 1.0 for finer sediments; at higher flow regimes, finer sediments are transported as suspended material. Sampling intervals range from a few minutes to several hours, depending on the magnitude and rate-of-change of discharge. The East Fork, Wyoming, conveyor-belt bed-load sampler began operation in 1973 (Figure A11). The bed-load sampler basically consists of a concrete trough permanently embedded into the river bed. Eight gates in the trough allow all or part of the sampler to be closed. Beneath the gates is a continuous rubber belt adjacent to a series of belts that eventually carries sediment entering the trough to a weighing scale. Sediment, after being weighed, is returned to the river downstream.

b. Indirect-measuring samplers. Similar to suspended sediment in direct-measuring devices, indirect-measuring samplers measure some associated characteristic of sediment movement. Three types of indirect-measuring samplers have been developed for riverine bed-load transport, and they are discussed below.

(1) Acoustic sampler

Acoustic samplers measure the sound created by particle collisions with the bed material and consist of an underwater microphone, located some distance above the bed, and an amplifier and recorder. One type of acoustic sampler is the Beauvert Laboratory hydrophonic detector, consisting of a microphone mounted on a triangular base plate which rests on the bed (Graf 1984). The sound of interparticle collisions and of the particle impact on the base plate are amplified and recorded. Disadvantages associated with this type of sampler include: (a) the apparatus can only be used with larger sized material because of the weak sound level produced by finer sediments; (b) large instruments, while resting on the bed, may significantly alter the flow; and (c) the results provide only qualitative bed-load transport information (Graf 1984).

(2) Ultrasonic sampler
These samplers measure sediment concentration using high-frequency ultrasonic sound waves. A transmitter and receiver of sound waves are located some distance above the bed such that the material moving as bed load passes between them. Different amounts of ultrasonic wave energy are absorbed, depending on the concentration of sediment. Graf (1984) reports that reliable results have been produced with these types of samplers. However, several assumptions are inherent when using the method: (a) the size distribution of the bed load is identical to the bed material; (b) the bed load is traveling at the velocity of flow (this assumption does not hold for regions near the bed); (c) the bed-load transport rate is directly proportional to the concentration of sediment and the fluid velocity; (d) suspended sediment entering the sampling region has the same ultrasonic absorption properties as the bed load; and (e) the hydraulic and sediment-trapping efficiencies of the sampler are close to 1.0.

(3) Tiltmeter
Tiltmeter samplers measure the ground tilt resulting from the passage of water and sediment, thereby estimating the total sediment load when the water-stage data are removed. Hubbell (1964) describes limited use of a tiltmeter sampler. He also discusses several questionable assumptions inherent for operation of the tiltmeter method.

11. Other methods used in estimating the rate of riverine bed-load transport include: using flow velocity, bed-load grain size, and other parameters in analytical formulae; tracking the size and movement of bedforms through time; and documenting grain movement with high-speed photography.

Nearshore Zone Measurement Apparatus

12. Instruments designed to measure nearshore and surf zone sediment transport have only recently been developed and used in the field. Probably the earliest documented use of a sediment-measurement apparatus in the surf zone was by the U.S. Army Corps of Engineers Beach Erosion Board (1933); brass cylinders of known volume were opened at varying depths along a pier to collect a water-sediment mixture. More recently, a multitude of coastal apparatus have been developed, from simple devices very similar to early riverine samplers, to indirect devices that measure the transmission of light, absorption or backscatter of radiation, and absorption of sound. This section

will discuss types of coastal measurement apparatus and studies associated with each.

Suspended load apparatus

13. Devices developed to measure suspended load in the nearshore zone, similar to riverine suspended sediment samplers, can be classified as either instantaneous, integrating, or indirect-measuring.

a. Instantaneous. Instantaneous bulk (in situ) samplers are similar to the riverine Eakin multiple samplers (Figure A3) consisting of a vertical array of cylinders that collect a bulk water-sediment sample when triggered. An in situ sampler developed by Kana (1976, 1977; Kana, Ward, and Johnson 1980) for use in the surf zone consists of five 2-liter acrylic tubes with hinged doors mounted vertically on a 2-m-long pole (Figure A13). When the sampler is thrust into the bed, a foot-pad assembly triggers hinged doors that close the acrylic tubes, and samples are collected in approximately 0.5 sec. Surf zone studies have been conducted at Price Inlet, South Carolina, and Duck, North Carolina, with a line of samplers spaced across the width of the surf zone. Trap operators hold the device above the water level until the passage of the wave crest, at which time the sampler is thrust into the bed. The bulk samples can then be carried in the sampler back to the beach. Tests are conducted to determine the degree to which sampler operation suspends additional sediment. Samples are taken by gently placing the sampler on the bed and compared with violently "pole vaulting" the device to collect samples. The size distributions and quantities of suspended sediment were not significantly different, indicating that operation of the sampler does not place sediment in suspension. Tests with two samplers in close proximity also gave results in close agreement, indicating that the samplers are consistent (Kana 1976). Suspended sediment transport measured with the samplers at Price Inlet, South Carolina, was 95 percent of that predicted by the Coastal Engineering Research Center (CERC) formula (Shore Protection Manual 1984) (Kana 1977); storm measurements at Duck, North Carolina, agreed with the CERC formula, whereas post-storm transport rates were 30 percent of the predicted quantities (Kana et al. 1980). The use of a similar sampler called the "water coring" device is slightly different: the sampler is held in the surf zone prior to triggering, allowing water and sediment to flow freely through the chambers until samples are collected. Motion pictures of the sampler with confetti to

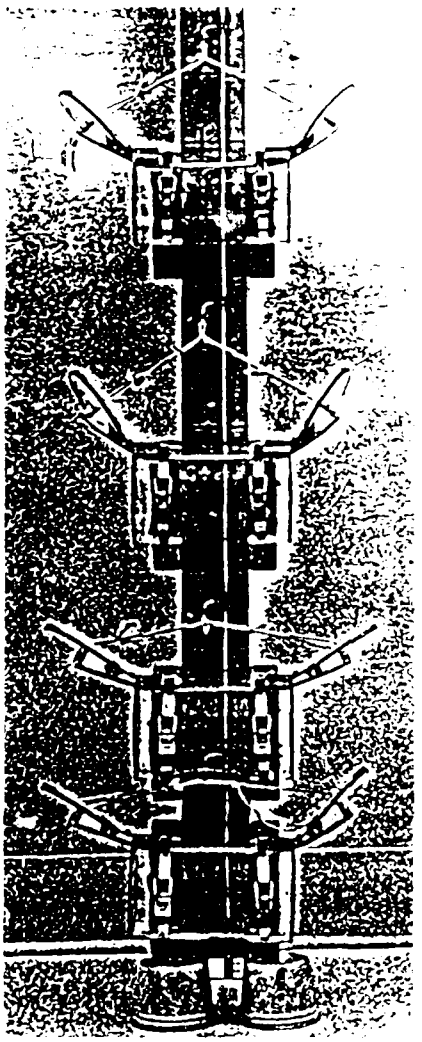

Figure A13. Kana in-situ bulk suspended sediment sampler (from Kana, Ward, and Johnson 1980)

trace water motion indicated that the sampler caused the least disturbance to the water column when compared to instantaneous samplers that suck water into chambers (Zampol and Waldorf in press). This device has been used at Torrey Pines Beach near San Diego, California, to measure the concentration of tracer in the water column (Inman 1978, Inman et al. 1980). Disadvantages of the in situ bulk sampler are: (a) a large volume of a water-sediment mixture must be collected to obtain a significant quantity of sediment; (b) because the device samples instantaneously, many samples must be collected to give a representative distribution of suspended sediment; and (c) fluid velocity measurements must be known at the location and instant of sampling to determine a sediment transport rate.

b. Time-integrating.

(1) Sample bags

Many types of vertically mounted sample bag traps have been developed for use in the surf zone (Inman 1949, Hom-ma, Horikawa, and Sonu 1960; Nagata 1961, 1964; James and Brenninkmeyer 1971; Katori 1982; Kraus 1987). The streamer trap investigated in the present study is a type of vertically mounted sample bag apparatus; however, because both bed and suspended load are collected to yield the vertical distribution of the total load, this device is discussed in the "Total Load" section. One type of suspended sample bag trap, developed by James and Brenninkmeyer (1971), consists of a 1-cm-diameter nozzle connected to a 3.25-cm tube collection area with stainless steel mesh screen at the rear (Figure A14). Sediment entering the nozzle is deposited in the tube while water passes through the mesh. Five of the tubes are vertically arranged at 7-cm intervals, mounted on a galvanized steel pipe. The steel pipe has 1-cm-diameter holes drilled at the same elevations as the tubes such that the trap can begin sampling when the steel pipe is rotated. Various geometric designs of the sampler were tested in a circulating flume; the chosen design was shown to create little turbulence. This device was used to measure the distribution of suspended sediment in bores and backwash at Nauset Light Beach on Cape Cod, Massacnusetts. Disadvantages of this type of apparatus include: (a) the sampler nozzle may disturb the flow; (b) the apparatus may induce scour at the bed, thereby increasing the quantity of sediment in suspension; and (c) sediment with nominal grain size smaller than the mesh diameter passes through the sampler.

(2) Bamboo samplers

Inexpensive bamboo samplers consisting of a bamboo pole with small holes at intervals and concrete blocks at the base to weight the apparatus have been used in the surf zone to measure the vertical distribution of suspended sediment (Fukushima and Mizoguchi 1958, Fukushima and Kashiwamura 1959, Hom-ma and Horikawa 1962, Noda 1962, Basinski and Lewandowski 1974). Bamboo samplers, because they are light and buoyant, tend to move with both the wind and waves. Sediment is deposited in the hollows between joints. Fukushima and Mizoguchi (1958) deployed 5-m-high bamboo samplers along the coast of Hokkaido in Japan. The samplers were removed from the surf zone after a week or so, and the bamboo poles cut into lengths of about 1 m for

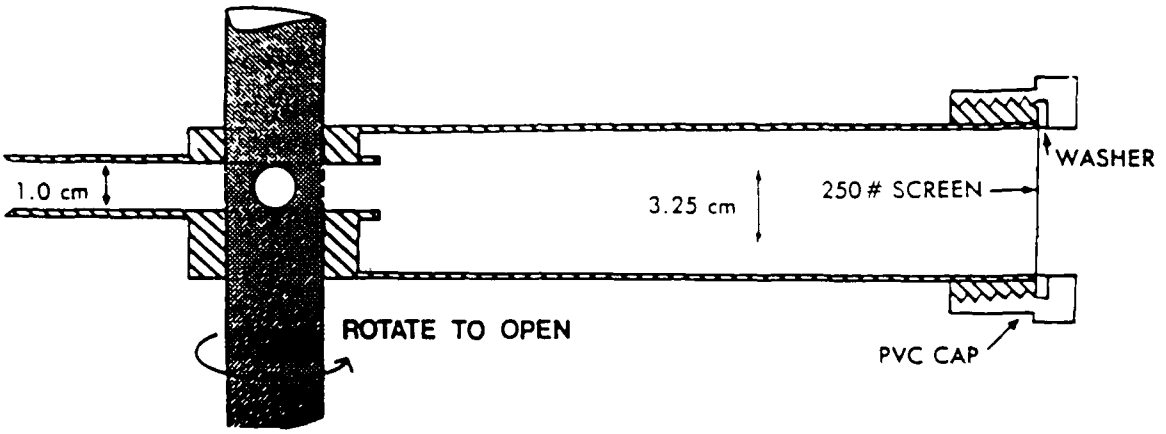

Figure A14. James and Brenninkmeyer suspended sample bag trap (from James and Brenninkmeyer 1971)

analysis of the sediment. These types of samplers have several disadvantages which include: (a) the movement of the bamboo pole varies the elevation at which samples are collected, and erratically affect the hydraulic and sediment-trapping efficiencies; (b) the concrete base will induce scour; and (c) the effects of orifice opening and collection area on the hydraulic and sediment-trapping efficiencies are unknown.

(3) Pumping/siphon samplers

Nearshore pumping samplers are very similar to riverine pumping samplers, consisting of a nozzle and hose through which a water-sediment mixture is pumped. Watts (1953) developed and tested in the laboratory and field a sampler that pumps a sediment-laden mixture at a point, sieves the sediment, and discharges the water back into the ocean (Figure A15). Efficiency curves for the sampler with a vertically-oriented 1/2 in. (1.3 cm) nozzle were developed based on maximum orbital velocity of the waves; the sampler had an average efficiency of 94 percent if the orbital velocity of the wave varied from 0 to 5 ft/sec (1.5 m/sec).

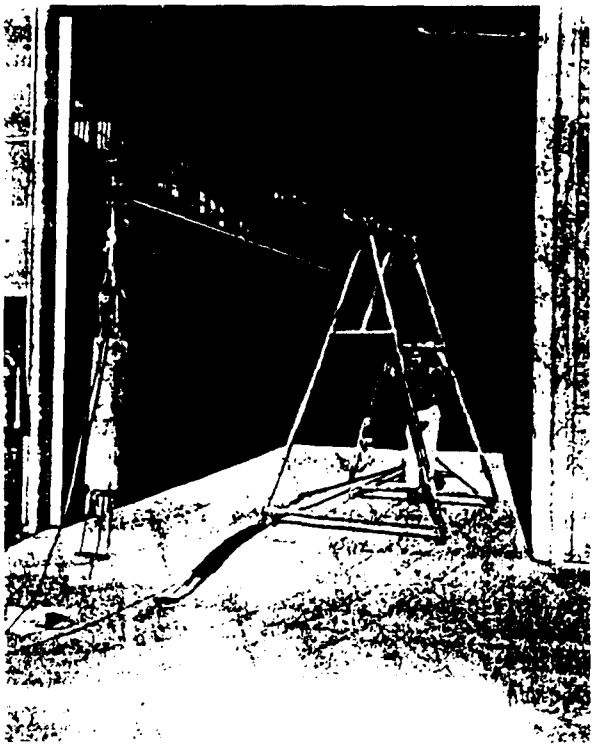

Figure A15. Pumping suspended sediment sampler (from Watts 1953)

Samples were collected across the surf zone from a pier at Crystal Pier near San Diego, California; organic material tended to clog the nozzle and resulted in only 71 percent of the samples being used in data analysis. In addition, the sampler could only be deployed from a pier. Thornton (1972) combined a pump with bed-load sediment traps in the nearshore and surf zone at Fernandina Beach, Florida. The traps sampled for 15 min, then doors on the bed-load traps were shut and the collected sediment pumped out for approximately 5 min. The bed-load traps tended to clog, however, and get buried in heavy wave conditions. Thornton estimated the efficiency of the system from 40 to 100 percent. Fairchild (1972) collected suspended sediment samples for approximately 3 minutes in the New Jersey surf zone and North Carolina nearshore zone using a tractor-mounted pump sampler. Crickmore and Aked (1975) made a series of point measurements above the bed in an estuary with fine sediment using a vertical array of nozzles feeding to a pump mounted on a boat; the sediment was filtered out of the mixture, while the cumulative water volume was recorded on a volumetric meter. Coakley et al. (1979) measured samples on-offshore and longshore using a

pump mounted on a sled. Visual inspection indicated that the sled did not increase the sediment in suspension; however, if nozzle orientation was reversed, more than double the concentration of sediment was collected. Thornton and Morris (1977) used a series of intake nozzles in the surf zone to calibrate a transmissometer, a light transmission indicator (see below). Bosman, Van Der Velden, and Hulsberger (1987) pumped samples at a speed three times greater than ambient flow speeds, with the nozzle orientation perpendicular to vertical plane of orbital motion. The pumping method of collecting suspended sediment works well when the nozzle is oriented vertically. Disadvantages, however, include: (a) large volumes must be collected to obtain significant quantities of sediment; and (b) the apparatus needs a mounting system such as a pier, boat, or sled. Suction and self-syphoning samplers are types of pumping devices that collect a water-sediment mixture using either suction or the pressure difference between the water surface and nozzle location. Nielsen (1983) and Nielsen et al. (1982) used a self-siphoning sampler in the Eastern Beach, Gippsland, Australia, surf zone that sampled at seven elevations simultaneously (Figure A16). The sampler collected for 3.5 min with an intake velocity of 1.5 m/sec in a 1.2-m water depth; the intake velocity was limited by the pressure difference between the water surface and nozzle locations. Hom-ma and Horikawa (1962) used siphon samplers in the laboratory to measure the vertical distribution of suspended sediment due to wave action. Staub, Svendsen, and Jonsson (1983) describe a rotating-wheel apparatus designed to collect water-sediment mixtures in the turbulent oscillatory flow over a laboratory sand bed. A siphon probe located at a particular elevation above the bed feeds into a rotating wheel outside of the flume with 18 cups in the circumference. The rotation of the wheel is synchronized with the oscillating flow in the flume; in this manner, the concentration of sediment collected in each cup represents one-eighteenth of the wave period. Kilner (1977) used 2-liter preserving jars with a total internal vacuum as handheld samplers for use in wading depths (surf zone). For deeper water, two compressed air samplers were developed using 7-liter compressed air cylinders with a trigger valve connected to an air motor. Disadvantages of the suction/siphon type of sampler are: (a) the intake flow speed with self-siphoning samplers depends on the distance between the probe and water surface; (b) large samples must be obtained to result in significant quantities of sediment; and (c) the flow speed must be known at the probe to calculate sediment transport rates.

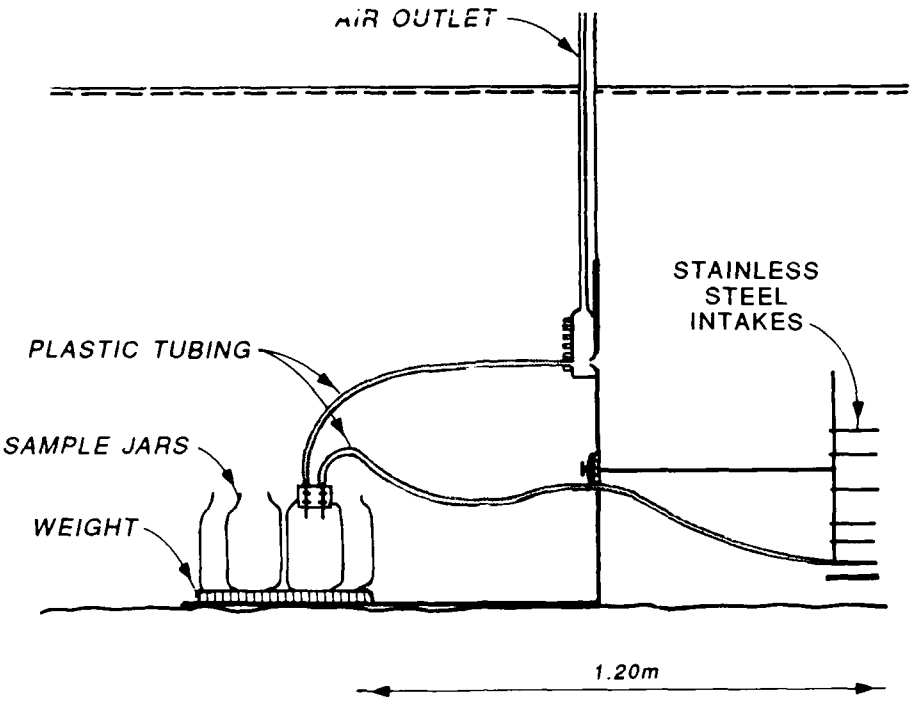

Figure A16. Nielsen self-siphoning suspended sediment sampler (from Nielsen 1983)

c. Instantaneous.

(1) Optical

(a) Transmissometers

Transmissometers, nephelometers, and almometers measure the concentration of suspended sediment by means of transmitted light over a fixed path length. The instruments usually consist of a light source and sensor on separate mounts; as sediment passes between the mounts, an attenuation in light is detected and can be calibrated to indicate the concentration of material in suspension. The amount of light transmitted through sediment-laden water depends on the distance between the source and sensor, sediment grain size and shape, fluid opacity, amount of organic material in suspension, amount of natural light, and quantity of air entrained in the fluid. The instruments can be calibrated for the source-to-sensor distance and grain size expected in the field; however, the degree to which the other variables will enter cannot be predicted. Hom-ma, Horikawa, and

Kashima (1965) developed a calibration curve for a photoelectric concentration meter used in the laboratory; the instrument did not appear to disturb the flow or suspended sediment concentration, but accuracy of the meter was found to decrease at higher concentrations of sediment. Thornton and Morris (1977) installed a series of instruments at Torrey Pines, California, including a nephelometer designed to measure the suspended sediment concentration at any one of three elevations in the surf zone. As mentioned previously, three intake nozzles were also in place to sample sediment-laden water and in situ calibrate the nephelometer. The nephelometer was designed with scattered and reference light detectors; therefore, any fluctuations in the light source could be accounted for by a ratio of the two values. Unfortunately, unanticipated line loss in the power cable meant that the excitation line voltage for the nephelometer had to be varied to match the output level of the telemetry /recording system. Absolute calibration of the nephelometer was not possible. In addition, Thornton and Morris (1977) note that the nephelometer may have sensed entrained air in the water column. Brenninkmeyer (1974, 1976) describes the use of almometers in the surf zone. The instruments consist of 64 photo-electric cells opposite a high intensity fluorescent lamp; both parts are encased in a plastic cylinder and mounted on poles that can be placed up to 1 m apart. Leonard and Brenninkmeyer (1979) installed two almometers at Nauset Light Beach, Cape Cod, Massachusetts; data were collected from 2400 and 0600 hours so that sunlight could not affect the incident light sensed by the photocells. Nakato et al. (1977) calibrated and used the Iowa Sediment Concentration Measuring System (ISCMS) (Locher, Glover, and Nakato 1976) in an oscillatory-flow flume. These types of optical instruments have several disadvantages: (a) calibration is dependent on grain size and may vary vertically; (b) almometers using photocells are sensitive to sunlight; (c) bubbles may be interpreted by the instrument as suspended sediment; (d) water opacity and organic material may influence the calibration of the instrument; and (e) scour may be induced by the rods that mount the source and sensor.

(b) Optical Backscattering Sensors (OBS)

An Optical Backscattering Sensor (OBS) radiates a cone of light and detects the intensity of backscattered light. The intensity of backscattered light is a function of sediment concentration and grain size; therefore, the instrument can be calibrated in the

laboratory using sediment at the field site. Jaffe, Sternberg, and Sallenger (1984) used a vertical array of OBS sensors originally described by Downing et al (1981) mounted on a sled that moved through the surf zone at Duck, North Carolina. Downing (1984), Sternberg, Shi, and Downing (1985), Hanes and Huntley (1986), Sternberg et al. (1986b), Huntley and Hanes (1987), and Beach and Sternberg (1987) all used either OBS or Miniature Optical Backscatter Sensors (MOBS) in the nearshore or surf zone to measure concentrations of suspended sediment. Sternberg, Shi, and Downing (1985) calibrated the instrument before and after the field experiment in a calibration tank using sand from the site; the instrument response was linear from 0.1 to 150 parts per thousand (ppt) concentration. The introduction of air bubbles in the calibration tank varied the calibration very little. However, suspension of fine sand in the field due to storm drain flooding during a storm increased the background signal levels and obscured the suspension of nearshore sand. Sternberg et al. (1986a) used OBS sensors to measure silty suspended sediment in the bottom boundary layer of a tidal channel within San Francisco Bay, California. The OBS and MOBS sensors can provide an instantaneous and continuous measurement of the suspended sediment concentration in the nearshore and surf zone. The instruments are less sensitive to air entrained in the water column than transmissometers. However, disadvantages associated with the OBS sensor include: (a) the instrument must be calibrated with the grain size of the suspended sediment; (b) if left in the field for an extended period of time, organic growth on the sensors must be removed; (c) fluid velocities must be known at the sensor elevation to calculate sediment transport; and (d) scour may be induced around the sensor mounts.

(c) Radiation Absorption Meter

Basinski and Lewandowski (1974) describe a radiation absorption meter that determines the concentration of suspended sediment in the water column by the absorption of gamma radiation. The apparatus consists of a radioactive source, counter, photomultiplier, input amplifier, discriminator, and output amplifier. The calibration of the instrument depends on the suspended sand concentration, natural gamma radiation, the seawater chemical composition, and the chemical composition of sediment. During use of the instrument in the Baltic Sea, electrochemical corrosion occurred on the internal surface. This instrument has not been widely used. Disadvantages of the device include: (a) fluid velocity must be known at the point of

measurement to calculate a sediment transport rate; (b) calibration varies with grain size, and grain size may vary vertically in the water column; and (c) scour around the mounts may increase suspended sediment concentrations.

(2) Acoustic instruments

Acoustic instruments measure the absorption or backscatter of sound due to sediment entrained in the water column. The acoustic concentration meter (ACM) (Young et al. 1982, Tamura and Hanes 1986, Hanes and Vincent 1987, Hanes et al. in press) senses the intensity of backscattered acoustic energy and can measure the suspended sediment profile up to 200 cm away from the instrument with 1-cm spatial resolution and 0.5-sec temporal resolution. In addition, the instrument measures the location of the bed within 0.5 cm. The instrument works well if air is not entrained in the water column; bubbles are obvious by spikes in the signals (Hanes et al. in press). An ultrasound doppler meter (Jansen 1978) measures the sediment concentration and fluid velocity in the water column. Acoustic instruments are useful for continuous measurement of vertical suspended sediment concentrations. Disadvantages of the instrument include: (a) bubbles, non-sand particles, and organisms in the water column cause scattering of sound, thereby altering the instrument's calibration; (b) calibration of the instrument is dependent on grain size; and (c) a low signal-to-noise ratio exists near the bottom, creating a 1-m "dead zone" between the instrument and bed.

(3) Electrical resistance meters

Hattori (1969, 1971) describes the use of electrodes on the heads of two mounts to detect the number of suspended sediment particles passing through a slit. Electrical resistance between the mounts varies as the concentration of material increases or decreases. Horikawa, Watanabe, and Katori (1983) used an electro-resistance detector close to and within the bed in a laboratory study with sheet-flow to measure the near-bed suspended sediment concentration and bed-load transport. The instrument was calibrated in a cylindrical tank, and instrument response with concentration was linear. These types of instruments have several disadvantages: (a) because of their fragility, they can only be used in the laboratory; and (b) material other than sediment will obscure results.

(4) Photography

Some researchers (e.g., Bijker 1971; Horikawa, Watanabe, and Katori 1983) have used high-speed photography to document and measure the movement of suspended and near-bed sediment. Horikawa, Watanabe, and Katori used a motor-driven 35-mm camera and stroboscopic lamp to record the suspended sediment concentration and particle advection speed in the upper layer of flow in the laboratory. A painted black copper plate located 1 cm into the flume was used as a backdrop; grains passing between the flume wall and the black copper plate were photographed. Disadvantages with this type of measurement tool include: (a) analysis of the photographic data is extremely time-consuming; and (b) the method appears to be applicable only to the laboratory environment.

Bed-load apparatus

14. The number of suspended-sediment instruments available far outnumber the number of bed-load measuring apparatus. Direct measuring bed-load devices include variations of the pit, pressure-difference, and box riverine samplers; the only indirect measuring device is an acoustical instrument.

a. Pit samplers.

Pit samplers in the nearshore coastal zone are nearly identical to those described for riverine use: some sort of collection device rests in an excavated region in the bed. Inman and Bowen (1963) used two pits at either end of a flume to measure the net quantity of sediment transported due to oscillatory flow. The pits consisted of perforated steel sheets placed over an excavated region; sediment fell through the perforations and was retained in the excavated region.

b. Pressure-difference.

The only pressure-difference traps used in the coastal zone have been the VUV sampler, developed for riverine use and discussed in the riverine pressure-difference section. Lee (1975) used an array of VUV samplers through the surf zone to measure the bed-load transport on the west shore of Lake Michigan in Kewaunee County, Wisconsin. Pickrill (1986) used VUV traps across a cross-section of Rangaunu Harbor, New Zealand. Results were corrected for the sediment-trapping efficiency of 0.70, reported by Novak (1957). Measured transport rates were lower than those predicted with relationships presented by Yalin (1963); Pickrill attributes the discrepancy to: (a) migrating bedforms and their location relative to the initial placement of the traps; (b) the use of only one trap; and/or (c) spillage of the samples upon removal because the trap had no doors. Thornton (1969) used bed-load traps at Fernandina Beach, FL.

c. Acoustic.

Downing (1981) describes an acoustic bed-load device that detects the impact of bed-load particles. Bubbles and fine materials such as clay and silt do not have sufficient inertia to be counted as they hit the device; therefore only sand-sized material is detected. The device consists of a "needle" partially embedded in the bed. The Helley-Smith bed-load sampler described in the riverine pressure-difference section was used to calibrate the acoustic bed-load device in a riverine environment; the correlation coefficient between measured and Helley-Smith sampler predicted rates was 0.898. Use of the device is limited to regions with well-sorted material, grain speeds exceeding 0.6 m/sec, and high sediment transport rates. The present study indicates that the Helley-Smith sampler may give unrepresentative high transport rates of sand.

Total load apparatus

15. Instruments developed to measure the total load, both the suspended and bed-load transport in the coastal nearshore or surf zone include a pit sampler developed for use in the nearshore zone and the streamer trap.

a. Pit sampler.

Anderson (1987) placed a marine sampler approximately 6 ft^2 (.56 m^2) in the nearshore zone (50-ft depth) off Carmel Point, California. The trap was made of 1-in. (2.5-cm) marine grade plywood and divided into sections so that transport from each direction could be distinguished (Figure A17). Suspended load was not expected to travel more than 3 ft, and could, in principle, be differentiated from bed-load material by the section in which it settled. Divers measured the quantities of collected sediment. In use of the trap, eddies on the leading edge of the interior of the box tended to resuspend sediment that had already settled. Significant flow disturbance was not observed except around the corners of the trap, where scour occurred. The pit trap became the abode for many animals and began growing seaweed by the third week of installation. In practice, deposition of suspended material could not be distinguished from deposition of bed load.

b. Streamer trap.

The streamer trap consists of vertically mounted mesh collection bags (streamers) attached to nozzles mounted in a metal frame (see Figure 2 in Part I) and is the subject of the main portion of this report. The bottommost streamer rests on the bed and collects both bed and suspended load, whereas, the higher-elevation streamers collect suspended material. Integration of the vertical distribution of sediment transport yields the total longshore sediment transport in the water column. The streamer trap is discussed in detail in Part II.

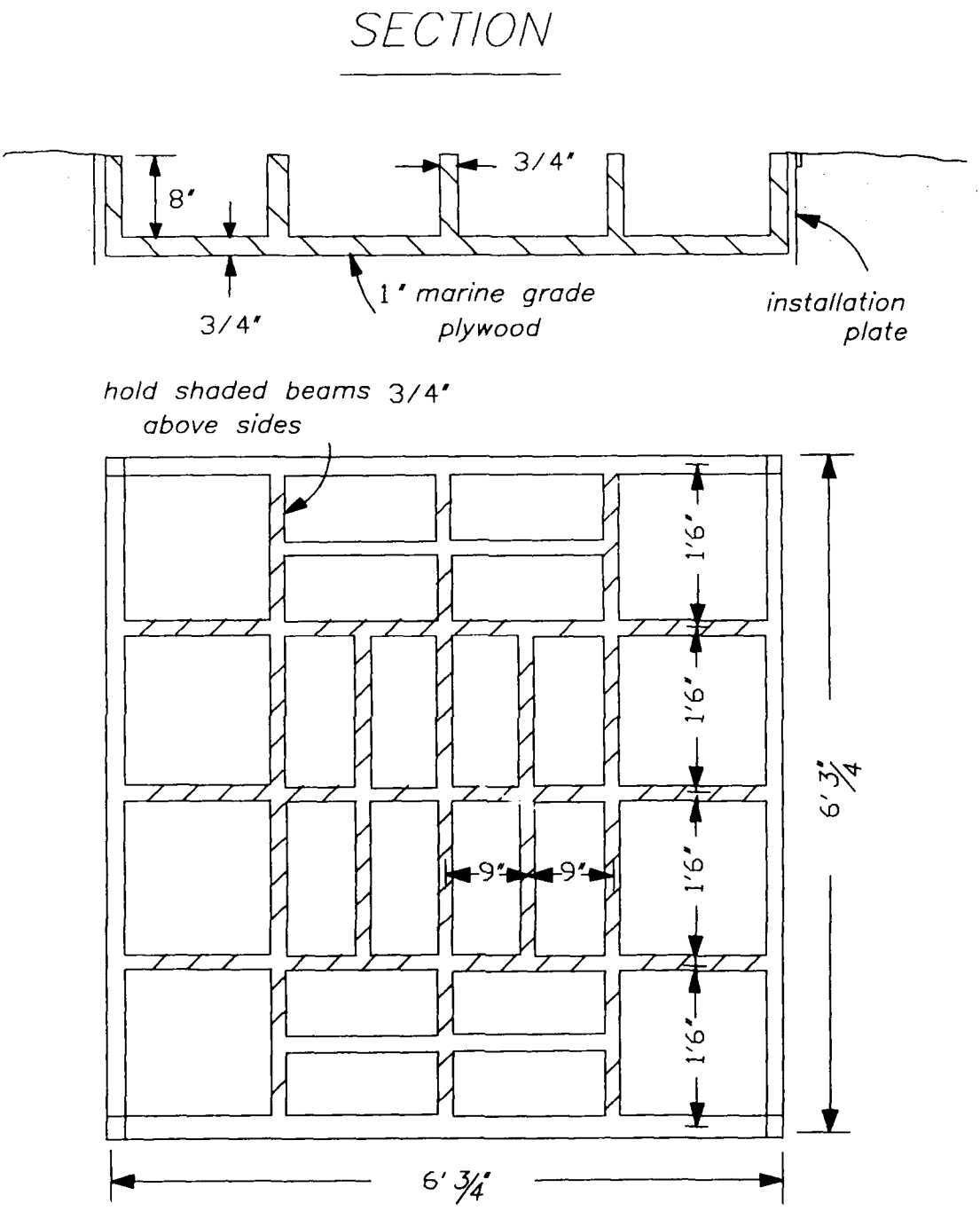

Figure A17. Anderson total load pit sampler (from Anderson 1987)

APPENDIX B: HYDRAULIC TEST DATA

1. This appendix presents tabulated data measured in the hydraulic efficiency tests. Flow speeds were measured at 3 to 9 points in each nozzle (measurement locations referenced in the tabulation are numbered in Figure 16). Tests were conducted with the nozzle at a near-bed elevation (BOT), at a midflow elevation (MID), or with two nozzles (2ST), one at each the near-bed and midflow elevation. For the two-streamer tests (2ST), data were collected first from the upper (midflow) nozzle, followed by measurements at the near-bed nozzle. Measurements were made both with the trap in place (TR) or without the trap (ambient, AM). Tests that were repeated are distinguished by a "-1" and "-2" (e.g., BOT-1, BOT-2) in the table.

2. Values of hydraulic efficiency E_h represent the ratio of trap (TR) to ambient (AM) flow speed (see Equation 7, Part III). The nozzle characteristics examined are defined and discussed in detail in Part III of the main text.

Table B1

Hydraulic Test Data

Nozzle	Mid-flow Speed cm/sec	Testing Elev	TR or AM	Flow Speed at Point Number, cm/sec 1	2	3	4	5	6	7	8	9	E_h
2.5cm x15cm	43	BOT	(TR)	24.9	25.9	28.5							
			(AM)	36.4	38.2	38.4							0.70
		MID	(TR)	37.6	30.7	29.7							
			(AM)	48.3	48.6	48.5							0.68
		2ST	(TR)	24.6	27.4	28.1							
				29.6	33.2	33.1							
			(AM)	44.0	44.5	45.5							
				44.7	43.5	44.5							0.66
	74	BOT-1	(TR)	48.9	56.9	56.0							
			(AM)	60.8	63.1	61.3							0.87
		BOT-2	(TR)	49.2	52.0	53.3							
			(AM)	61.5	61.9	61.6							0.84
		MID-1	(TR)	58.1	66.6	63.4							
			(AM)	77.9	77.7	78.4							0.80
		MID-2	(TR)	56.8	57.1	63.9							
			(AM)	78.0	78.5	78.9							0.76
		2ST	(TR)	62.4	58.2	64.1							
				61.1	64.5	64.3							
			(AM)	77.8	77.7	78.4							
				76.9	77.4	77.3							0.81
2.5cm x15cm, CL	43	BOT	(TR)	25.3	28.8	28.1							
			(AM)	34.9	35.3	35.0							0.78
	74	BOT	(TR)	46.9	52.8	55.7							
			(AM)	58.7	61.5	63.7							0.84
2.5cm x15cm, 2.5cmH	43	MID	(TR)	41.4	43.5	43.9							
			(AM)	45.8	46.3	46.6							0.93
		2ST	(TR)	42.5	43.8	44.6							
				40.9	40.8	39.9							
			(AM)	45.7	45.8	46.6							
				41.6	41.1	43.3							0.95

(Continued)

Table B1 (Continued)

Nozzle	Mid-flow Speed cm/sec	Testing Elev	TR or AM	Flow Speed at Point Number, cm/sec 1	2	3	4	5	6	7	8	9	E_h
	74	MID	(TR)	74.7	77.0	79.6							
			(AM)	79.5	79.7	79.9							0.97
		2ST	(TR)	75.8	79.0	75.8							
				70.9	70.4	70.0							
			(AM)	77.2	78.3	78.1							
				71.4	73.2	73.0							0.98
2.5cm x15cm, 5.1cmH (SUPER-DUCK)	22	BOT	(TR)	6.1	6.1	8.4							
			(AM)	12.1	15.1	13.8							0.50
		MID	(TR)	23.0	23.3	23.0							
			(AM)	24.0	24.4	24.1							0.96
		2ST	(TR)	13.3	13.6	12.6							
				8.5	9.4	10.7							
			(AM)	21.2	22.3	23.4							
				16.3	16.2	16.1							0.59
	43	BOT	(TR)	22.1	22.9	24.1							
			(AM)	30.0	31.8	30.5							0.75
		MID	(TR)	45.7	46.0	47.0							
			(AM)	44.7	45.5	45.5							1.02
		2ST	(TR)	45.6	46.4	47.3							
				40.8	41.3	41.2							
			(AM)	45.6	46.1	46.2							
				42.2	43.4	42.4							0.96
	59	BOT	(TR)	36.3	40.0	40.3							
			(AM)	37.9	41.6	43.1							0.95
		MID	(TR)	66.9	67.7	65.1							
			(AM)	62.3	62.7	63.0							1.06
		2ST	(TR)	50.2	53.1	48.7							
				33.5	36.5	40.3							
			(AM)	53.2	54.7	57.7							
				40.4	39.1	45.0							0.90
	74	BOT	(TR)	48.0	51.1	51.9							
			(AM)	47.1	47.8	51.9							1.03
		MID	(TR)	78.9	79.9	80.2							
			(AM)	77.1	77.1	76.5							1.04
		2ST	(TR)	79.4	79.8	80.5							
				67.8	66.0	72.6							
			(AM)	77.0	77.6	77.0							
				72.5	73.2	73.2							0.99

(Continued)

Table B1 (Continued)

Nozzle	Mid-flow Speed cm/sec	Testing Elev	TR or AM	Flow Speed at Point Number, cm/sec 1	2	3	4	5	6	7	8	9	E_h
2.5cm x15cm, 5.1H, CL	43	BOT	(TR)	30.1	32.4	33.0							
			(AM)	32.7	33.6	32.9							0.96
	74	BOT	(TR)	54.9	56.6	56.8							
			(AM)	55.0	53.5	54.3							1.03
5.1cm x15cm	43	BOT	(TR)	32.0	33.0	35.5	28.2	30.6	30.4				
			(AM)	37.9	37.2	38.5	33.5	33.3	34.8				0.86
		MID	(TR)	42.3	43.3	41.2	40.6	42.2	40.6				
			(AM)	44.2	45.2	45.9	44.9	44.9	45.6				0.92
		2ST	(TR)	40.8	43.1	41.8	40.1	42.9	41.9				
				35.7	38.1	36.2	33.7	35.1	34.3				
			(AM)	45.1	45.2	45.3	45.1	44.8	45.4				
				42.3	43.0	44.5	42.0	42.8	41.8				0.88
	74	BOT	(TR)	61.0	63.5	61.5	56.3	58.0	58.8				
			(AM)	68.0	67.4	67.6	63.3	61.3	61.4				0.92
		MID	(TR)	72.9	74.2	74.1	73.9	76.2	74.8				
			(AM)	75.9	77.2	77.6	76.2	76.8	77.0				0.97
		2ST	(TR)	75.9	79.1	76.6	76.5	79.8	76.2				
				70.7	73.3	67.4	67.6	71.2	65.5				
			(AM)	77.0	78.3	78.6	77.3	77.5	77.7				
				74.3	76.2	75.8	72.2	72.3	73.7				0.97
5.1cm x15cm, CL	43	BOT	(TR)	27.1	30.7	32.7	27.3	31.7	30.4				
			(AM)	39.4	39.0	40.0	32.8	35.5	36.1				0.78
	74	BOT	(TR)	50.9	56.9	60.6	52.4	55.1	57.1				
			(AM)	65.4	66.7	67.8	60.1	60.8	61.5				0.87
5.1cm x15cm, 2.5cmH, CL	43	BOT	(TR)	36.9	35.4	36.3	33.1	33.8	34.4				
			(AM)	40.9	40.8	39.8	36.3	37.1	36.0				0.90
	74	BOT	(TR)	63.8	64.7	63.3	59.7	61.0	59.0				
			(AM)	66.8	68.4	68.0	61.4	63.3	63.6				0.95

(Continued)

Table B1 (Continued)

Nozzle	Mid-flow Speed cm/sec	Testing Elev	TR or AM	Flow Speed at Point Number, cm/sec 1	2	3	4	5	6	7	8	9	E_h
5.1cm	43	BOT	(TR)	38.5	38.3	38.1	34.1	34.4	35.9				
x15cm,			(AM)	39.3	39.0	40.8	35.2	33.7	37.5				0.97
5.1cmH		MID	(TR)	42.8	43.6	44.1	42.6	43.4	43.5				
			(AM)	45.8	45.8	46.4	45.6	46.1	45.6				0.94
	74	BOT	(TR)	61.2	57.1	59.8	56.3	52.8	53.2				
			(AM)	64.7	68.2	67.4	60.2	62.2	60.8				0.89
		MID	(TR)	67.7	73.8	73.9	66.4	73.5	73.8				
			(AM)	76.8	77.1	78.9	76.3	77.8	78.7				0.92
5.1cm	43	BOT	(TR)	38.0	38.8	40.8	35.1	34.3	36.1				
x15cm,			(AM)	40.0	40.4	39.2	35.9	35.8	36.9				0.97
5.1cmH,													
CL	74	BOT	(TR)	68.5	69.2	72.6	63.8	63.1	61.9				
			(AM)	67.9	66.7	68.5	62.6	62.9	62.1				1.02
5.1cm	22	BOT	(TR)	16.3	17.7	15.9	15.2						
x5.1cm,			(AM)	18.8	17.8	18.1	17.5						0.90
5.1cm H		MID	(TR)	17.4	19.0	18.4	17.9						
(CUBE)			(AM)	22.9	24.6	23.2	23.4						0.77
		2ST	(TR)	16.7	16.6	17.8	16.7						
				15.5	16.4	15.3	15.1						
			(AM)	22.3	23.3	22.1	22.6						
				15.7	19.2	15.6	15.4						0.83
	43	BOT	(TR)	32.2	31.3	29.9	30.0						
			(AM)	34.6	37.3	33.2	33.9						0.89
		MID	(TR)	42.1	43.4	41.4	42.0						
			(AM)	44.9	43.1	43.5	43.0						0.97
		2ST	(TR)	43.9	44.0	43.1	44.4						
				34.8	34.7	31.1	29.4						
			(AM)	44.3	44.6	44.3	43.8						
				37.0	36.6	33.1	33.1						0.96
	59	BOT	(TR)	47.6	51.3	43.2	46.1						
			(AM)	45.4	51.5	41.1	44.1						1.03
		MID	(TR)	56.8	59.6	57.8	57.4						
			(AM)	59.0	60.2	60.0	59.1						0.97
		2ST	(TR)	59.0	56.5	57.5	58.0						
				47.4	46.5	43.9	45.8						
			(AM)	59.1	59.8	59.1	58.8						
				48.6	48.8	42.0	46.2						0.98

(Continued)

Table B1 (Continued)

Nozzle	Mid-flow Speed cm/sec	Testing Elev	TR or AM	Flow Speed at Point Number, cm/sec 1	2	3	4	5	6	7	8	9	E_h
	74	BOT	(TR)	59.2	59.2	56.3	56.7						
			(AM)	60.7	60.6	54.7	55.1						1.00
		MID	(TR)	71.0	73.4	74.7	71.6						
			(AM)	72.8	74.8	72.1	72.1						1.00
		2ST	(TR)	74.8	75.8	73.9	73.4						
				60.8	60.3	58.8	55.7						
			(AM)	73.5	74.1	73.3	74.2						
				59.7	61.9	56.5	53.0						1.01
9cm	22	BOT	(TR)	10.9	12.7	11.6	12.1	13.3	13.9	9.5	9.9	8.6	
x15cm			(AM)	19.4	21.0	21.6	19.7	18.8	19.4	15.4	16.4	15.5	0.61
(DUCK85)		MID	(TR)	18.9	20.7	18.8	19.0	21.0	18.9	19.0	19.9	18.0	
0.105mm			(AM)	24.2	24.2	24.3	23.9	24.3	24.6	24.1	23.6	24.2	0.80
(Cloth		2ST	(TR)	17.2	21.2	18.0	17.8	19.4	17.9	15.8	17.9	16.2	
V)				11.6	14.9	13.2	13.6	14.1	13.3	9.6	9.8	11.4	
			(AM)	23.6	23.4	24.6	23.1	23.7	23.9	22.9	23.5	20.6	
				20.6	19.8	21.0	17.2	19.7	18.3	15.9	16.6	16.6	0.73
	43	BOT-1	(TR)	39.9	41.1	39.6	38.3	39.4	38.2	25.9	26.1	24.6	
			(AM)	42.2	43.0	43.3	37.7	38.3	41.2	29.2	27.7	30.1	0.93
		BOT-2	(TR)	38.8	40.8	39.4	36.5	39.3	37.8	32.2	34.1	32.1	
			(AM)	43.8	44.2	44.2	39.9	42.0	41.4	32.6	36.7	37.1	0.91
		MID-1	(TR)	43.9	45.8	44.2	45.4	46.4	45.0	44.2	45.3	43.9	
			(AM)	44.9	44.5	45.1	45.1	44.6	44.6	45.1	44.2	45.2	1.00
		MID-2	(TR)	42.5	44.5	41.4	43.9	45.6	43.3	43.0	44.6	42.2	
			(AM)	44.9	43.4	45.5	44.8	43.4	45.6	44.7	43.8	46.2	0.97
		2ST-1	(TR)	43.7	45.3	42.6	45.3	46.2	43.2	44.5	45.1	41.7	
				38.1	39.5	37.7	37.7	36.9	35.9	24.1	24.6	22.2	
			(AM)	45.2	46.2	46.4	45.4	46.6	46.6	45.2	46.0	46.6	
				43.4	42.6	44.7	38.4	39.6	41.3	29.4	27.9	32.0	0.92
		2ST-2	(TR)	44.5	45.1	45.3	45.6	46.3	46.9	44.2	45.1	45.4	
				38.8	39.6	39.4	38.1	38.7	39.3	33.0	33.4	31.6	
			(AM)	47.0	46.5	45.8	47.1	46.8	46.8	46.8	46.1	46.4	
				45.1	46.1	44.7	41.4	41.0	39.4	34.5	36.8	36.7	0.94
	59	BOT	(TR)	45.8	51.0	44.8	44.3	44.8	45.3	33.8	36.7	36.3	
			(AM)	46.6	51.3	54.2	45.4	46.3	49.1	36.3	39.5	43.3	0.93
		MID	(TR)	59.4	61.9	61.4	60.9	63.4	61.9	60.0	59.8	57.2	
			(AM)	62.8	63.6	63.9	63.8	63.8	64.3	63.8	63.7	64.3	0.95
		2ST	(TR)	51.5	55.3	49.1	53.1	57.7	55.2	51.9	52.8	49.0	
				43.7	46.9	49.0	43.1	48.3	47.1	33.6	36.3	39.6	
			(AM)	58.4	59.9	62.4	57.8	58.5	61.5	56.0	59,2	59.4	
				48.6	53.1	51.6	45.3	48.1	50.0	39.2	36.9	45.1	0.91

(Continued)

Table B1 (Continued)

Nozzle	Mid-flow Speed cm/sec	Testing Elev	TR or AM	Flow Speed at Point Number, cm/sec 1	2	3	4	5	6	7	8	9	E_h
	74	BOT	(TR)	66.6	68.8	67.6	64.0	67.7	67.0	61.3	59.6	59.6	
			(AM)	70.1	72.6	71.2	66.4	66.2	67.9	58.5	61.8	61.7	0.97
		MID	(TR)	70.3	71.1	67.8	69.7	72.2	65.0	67.0	71.7	62.0	
			(AM)	74.4	75.1	74.9	74.7	74.9	75.4	73.6	74.2	75.4	0.91
		2ST	(TR)	64.5	72.5	71.8	65.5	73.3	72.4	62.4	73.5	72.3	
				63.9	67.8	67.7	62.5	68.4	68.3	56.5	61.1	58.8	
			(AM)	75.0	75.8	76.3	74.9	75.7	76.7	74.5	75.8	76.2	
				70.7	72.2	72.9	66.4	66.6	68.1	57.9	59.1	60.6	0.94
9cm x15cm, SL	43	BOT	(TR)	31.8	32.6	31.8	32.0	31.8	31.3	25.5	29.2	27.8	
			(AM)	43.3	43.2	42.4	39.7	40.1	41.2	33.2	33.2	35.8	0.78
	74	BOT	(TR)	62.6	59.8	61.6	62.9	64.2	61.3	54.8	58.0	53.9	
			(AM)	72.9	73.0	73.1	69.5	69.7	69.3	61.2	59.6	61.6	0.88
9cm x15cm, CL	43	BOT-1	(TR)	36.0	34.3	29.8	33.5	35.4	32.2	22.6	25.0	25.4	
			(AM)	42.5	42.7	43.0	39.0	38.7	40.1	31.0	28.4	30.5	0.81
		BOT-2	(TR)	38.1	35.7	33.0	36.6	36.3	34.8	31.8	35.6	32.9	
				43.2	43.5	43.8	39.4	40.0	41.3	35.6	35.8	37.2	0.87
	74	BOT	(TR)	72.5	68.8	64.2	67.0	66.3	64.8	59.4	63.5	63.1	
			(AM)	72.6	73.0	73.5	67.1	68.3	69.0	57.4	59.1	58.9	0.99
9cm x15cm, 0.149mm (Cloth T)	43	MID-1	(TR)	34.1	36.7	35.7	34.8	37.9	37.0	33.0	36.6	34.2	
			(AM)	45.9	45.6	46.1	46.4	46.5	46.0	45.9	46.5	46.8	0.77
		MID-2	(TR)	34.4	36.6	35.6	34.9	38.3	36.9	33.6	37.1	35.6	
			(AM)	44.0	45.1	45.4	44.0	45.3	45.3	44.3	44.9	45.0	0.80
	74	MID	(TR)	70.7	73.5	70.3	70.0	73.8	71.2	65.5	70.9	67.8	
			(AM)	76.6	77.0	77.4	76.2	77.4	77.6	75.8	76.9	77.2	0.91
9cm x15cm, 0.074mm (Cloth X)	43	MID-1	(TR)	40.0	43.5	42.9	40.7	43.6	41.3	37.4	41.4	38.8	
			(AM)	44.6	45.5	47.1	44.8	44.7	47.0	45.5	45.0	46.9	0.89
		MID-2	(TR)	42.5	43.3	43.0	42.3	44.0	43.1	38.8	40.8	40.1	
			(AM)	45.4	45.3	46.2	44.5	45.2	45.9	44.8	45.1	45.3	0.92
	74	MID	(TR)	74.4	77.0	76.5	76.4	78.5	78.3	75.6	78.1	76.3	
			(AM)	77.0	77.1	77.4	76.3	76.9	77.4	75.2	77.0	77.1	1.00

(Continued)

Table B1 (Continued)

Nozzle	Mid-flow Speed cm/sec	Testing Elev	TR or AM	Flow Speed at Point Number, cm/sec 1	2	3	4	5	6	7	8	9	E_h
9cm x15cm, Open	43	MID	(TR)	42.1	44.8	42.7	43.3	46.0	43.8	43.2	44.5	42.6	
			(AM)	44.6	45.5	47.1	44.8	44.7	47.0	45.5	45.0	46.9	0.95
	74	MID	(TR)	74.4	77.0	76.5	76.4	78.5	78.3	75.6	78.1	76.3	
			(AM)	77.0	77.1	77.4	76.3	76.9	77.4	75.2	77.0	77.1	1.00
9cm x15cm, 36cm length	43	2ST	(TR)	42.0	44.0	40.7	43.7	45.0	41.9	42.9	44.0	41.0	
				37.5	38.1	36.4	36.4	37.0	36.0	31.2	33.0	30.8	
			(AM)	45.4	45.4	45.7	45.7	45.7	45.2	44.9	44.8	45.4	
				42.2	41.7	43.3	38.5	37.8	40.8	32.8	35.9	36.1	0.92
	74	2ST	(TR)	73.7	74.2	73.3	74.9	75.8	74.9	72.7	69.2	69.2	
				63.2	67.0	66.4	64.2	66.3	64.7	54.6	57.6	55.5	
			(AM)	78.2	78.4	78.2	77.8	78.5	79.4	78.3	78.3	78.5	
				71.3	70.0	72.3	67.6	65.9	69.4	59.7	59.9	58.1	0.93
9cm x15cm, Door	43	MID	(TR)	46.4	46.1	46.6	47.7	47.2	45.9	45.7	44.5	43.6	
			(AM)	46.3	46.7	47.0	46.4	46.8	46.8	46.3	46.6	46.4	0.98
	74	MID	(TR)	73.2	72.2	73.5	75.1	75.5	76.5	75.4	76.3	76.2	
			(AM)	78.3	79.0	79.5	78.2	79.1	79.4	78.2	78.9	78.7	0.95
9cm x15cm, Door, CL	43	BOT	(TR)	39.5	40.1	38.0	37.8	38.8	37.8	33.3	33.7	32.6	
			(AM)	39.6	41.4	40.2	37.7	37.0	38.4	32.5	33.8	34.4	0.99
	74	BOT	(TR)	69.1	70.3	67.1	70.3	70.0	69.7	63.4	62.1	61.6	
			(AM)	74.5	74.1	74.3	69.8	70.4	70.0	61.3	62.6	64.9	0.97
9cm x15cm, Door, SL	43	BOT	(TR)	42.3	39.9	38.6	39.1	37.4	38.3	34.8	34.1	33.5	
			(AM)	39.6	41.4	40.2	37.7	37.0	38.4	32.5	33.8	34.0	1.01
	74	BOT	(TR)	76.4	73.7	77.5	70.3	70.9	72.3	58.7	58.1	59.0	
			(AM)	72.6	70.9	74.5	66.5	67.1	68.3	58.5	60.7	60.4	1.03
9cm x15cm, with person	43	2ST	(TR)	44.6	44.8	42.3	44.7	44.8	43.4	42.7	42.8	42.3	
				35.9	38.3	37.1	35.4	36.5	38.5	30.9	33.0	31.8	
			(AM)	43.8	43.8	45.3	44.0	43.9	44.7	44.1	44.1	44.8	
				40.8	40.7	42.9	39.1	38.4	39.7	35.0	34.8	34.8	0.95

(Continued)

Table B1 (Continued)

Nozzle	Mid-flow Speed cm/sec	Testing Elev	TR or AM	Flow Speed at Point Number, cm/sec 1	2	3	4	5	6	7	8	9	E_h
	74	2ST	(TR)	82.4	82.8	79.0	82.9	83.1	78.4	77.9	73.7	71.2	
				70.6	74.1	73.0	70.6	70.6	70.6	60.4	61.3	58.9	
			(AM)	78.2	75.6	79.3	77.1	76.6	78.3	78.0	75.4	79.0	
				71.3	70.0	72.3	68.1	65.8	68.7	59.0	57.6	60.8	1.02
9cm	43	MID	(TR)	40.0	42.0	42.6	39.6	42.4	42.8	39.7	41.5	41.7	
x15cm,			(AM)	43.4	43.2	43.9	43.2	43.6	43.8	43.4	42.9	43.8	0.95
10 deg													
ang	74	MID	(TR)	76.5	76.5	77.0	77.2	77.5	75.8	73.0	72.3	70.4	
				78.5	77.0	79.3	78.1	77.3	79.6	77.7	77.6	79.5	0.96
9cm	43	MID	(TR)	34.6	38.8	40.6	36.2	39.4	42.1	36.2	39.2	41.5	
x15cm,			(AM)	43.4	43.2	43.9	43.2	43.6	43.8	43.4	42.9	43.8	0.89
30 deg													
ang	74	MID	(TR)	70.7	78.0	77.2	69.4	77.6	77.8	64.6	71.5	73.9	
			(AM)	78.5	77.0	79.3	78.1	77.3	79.6	77.7	77.6	79.5	0.93
9cm	43	MID	(TR)	40.7	42.7	42.8	40.4	41.3	42.2	39.0	40.4	40.3	
x15cm,			(AM)	43.5	44.4	45.0	43.9	44.3	44.6	43.9	44.6	44.5	0.93
5.1cm H													
	74	MID	(TR)	70.9	74.2	75.4	70.4	73.1	74.2	67.7	70.3	71.0	
			(AM)	77.1	77.5	77.6	77.7	77.6	78.0	77.0	77.1	77.5	0.93
9cm	43	BOT-1	(TR)	35.4	37.3	38.8	35.4	35.6	35.9	28.9	31.9	30.4	
x15cm,			(AM)	40.5	41.9	41.7	39.3	39.9	39.4	35.5	35.5	36.4	0.88
5.1cm H,		BOT-2	(TR)	38.5	39.8	40.8	36.4	38.1	37.8	32.9	32.3	33.6	
SL			(AM)	42.3	43.9	42.8	39.7	40.9	40.2	34.7	35.9	34.6	0.93
	74	BOT	(TR)	67.0	69.0	70.6	65.5	68.1	69.3	56.8	56.8	60.0	
			(AM)	72.2	74.1	73.8	69.9	69.7	70.0	60.8	60.4	61.7	0.95
9cm	43	BOT	(TR)	38.8	40.1	39.9	36.7	38.3	39.6	32.4	34.2	33.8	
x15cm,			(AM)	43.8	44.1	44.8	41.3	40.2	42.7	38.7	38.0	38.4	0.89
5.1cm H,													
5.1 cm	74	BOT	(TR)	67.2	69.8	69.2	66.1	67.9	66.4	61.1	60.4	60.1	
LIP			(AM)	73.8	74.2	74.3	70.6	71.5	70.4	65.3	65.6	66.1	0.93

(Continued)

Table B1 (Continued)

Nozzle	Mid-flow Speed cm/sec	Testing Elev	TR or AM	Flow Speed at Point Number, cm/sec 1	2	3	4	5	6	7	8	9	E_h
9cm x15cm, H, CL	43	BOT-1	(TR)	40.3	40.5	40.5	36.8	37.5	36.3	31.1	30.4	32.3	
			(AM)	41.6	43.5	46.9	38.9	39.8	40.1	34.2	34.4	34.6	0.92
		BOT-2	(TR)	39.6	39.1	41.4	36.8	36.6	39.2	30.1	29.9	30.6	
			(AM)	42.5	41.9	42.3	38.5	40.2	39.1	33.8	34.2	34.1	0.93
	74	BOT-1	(TR)	71.1	73.8	75.9	65.2	70.5	70.9	60.1	62.2	62.7	
			(AM)	74.6	78.1	78.1	71.7	72.5	74.8	62.1	64.2	63.9	0.96
		BOT-2	(TR)	73.3	73.1	73.3	68.7	67.7	68.1	60.3	60.0	59.5	
			(AM)	7.26	74.6	75.1	70.8	70.3	71.3	58.3	62.0	61.9	0.98
7.6cm x7.6cm	43	BOT	(TR)	34.1	34.2	34.4	34.1						
			(AM)	44.1	44.2	43.8	44.1						0.78
	74	BOT	(TR)	69.1	69.1	73.2	72.7						
			(AM)	78.0	77.2	77.2	78.2						0.91
7.6cm x7.6cm, H, CL	43	BOT	(TR)	35.5	37.3	31.7	32.1						
			(AM)	41.8	38.3	35.9	36.9						0.89
	74	BOT-1	(TR)	70.0	71.9	58.8	61.2						
			(AM)	73.2	73.6	67.6	67.3						0.93
		BOT-2	(TR)	70.9	71.1	61.2	61.3						
			(AM)	72.2	72.5	66.4	64.7						0.96
		MID	(TR)	80.4	79.7	79.9	78.2						
			(AM)	78.5	78.0	78.4	78.3						1.02
7.6cm x7.6cm H-S	22	BOT	(TR)	27.9	28.1	22.9	24.6						
			(AM)	21.2	21.6	17.5	18.1						1.32
		MID	(TR)	27.7	27.7	27.0	26.7						
			(AM)	22.2	22.3	22.1	22.1						1.23
	43	BOT	(TR)	51.6	52.0	46.8	48.1						
			(AM)	40.2	40.3	36.2	36.2						1.30
		MID	(TR)	51.9	53.5	52.5	53.2						
			(AM)	42.7	42.4	42.6	42.3						1.24
	59	BOT	(TR)	73.6	78.4	67.8	66.3						
			(AM)	52.1	53.0	43.7	44.0						1.48
		MID	(TR)	75.5	78.7	75.1	71.8						
			(AM)	62.5	62.9	62.3	62.6						1.20

(Continued)

Table B1 (Concluded)

Nozzle	Mid-flow Speed cm/sec	Testing Elev	TR or AM	Flow Speed at Point Number, cm/sec 1	2	3	4	5	6	7	8	9	E_h
	74	BOT-1	(TR)	98.9	100.2	93.2	96.4						
			(AM)	69.3	72.2	63.3	64.8						1.44
		BOT-2	(TR)	95.7	99.6	91.7	92.0						
			(AM)	73.2	73.6	67.6	67.3						1.35
		MID	(TR)	99.5	98.8	99.6	98.3						
			(AM)	78.3	79.0	78.1	78.2						1.26
20cm x24.4cm	22	BOT	(TR)	23.8	21.8	23.4	24.8	23.9	24.1	23.3	22.6	23.7	
			(AM)	22.2	22.5	22.7	20.6	19.9	20.6	18.7	19.5	19.0	1.14
	43	BOT	(TR)	44.2	42.5	43.2	46.2	44.7	45.3	44.8	43.9	44.3	
			(AM)	42.7	44.1	43.8	42.0	40.1	41.0	35.4	36.7	35.6	1.10
	74	BOT	(TR)	80.8	78.7	81.9	84.0	81.6	84.5	78.7	78.9	78.7	
			(AM)	74.0	74.0	75.4	67.4	69.4	68.1	61.0	58.9	61.0	1.19
24.4cm x20cm	43	BOT	(TR)	40.9	41.0	41.0	43.3	44.7	44.8	43.3	44.5	44.5	
			(AM)	44.5	44.5	38.1	42.8	40.8	41.7	38.5	38.4	38.8	1.05
	74	BOT	(TR)	77.5	76.6	80.1	81.8	80.8	83.8	81.9	81.3	82.6	
			(AM)	73.5	75.3	75.7	71.1	70.5	71.3	65.6	63.1	65.0	1.15

APPENDIX C: NOZZLE PHOTOGRAPHS

1. Streamer trap nozzle configurations investigated in the hydraulic and sand-trapping tests described in the main text are illustrated in Figures C1 through C8. Nozzle height and width varied between 2.5 x 15 cm and 25 x 20 cm. Nozzle hoods, when present, ranged in length from 2.5 to 5.1 cm. Other components such as streamer mesh size and a plexiglass door designed to shut during flow reversals were also evaluated.

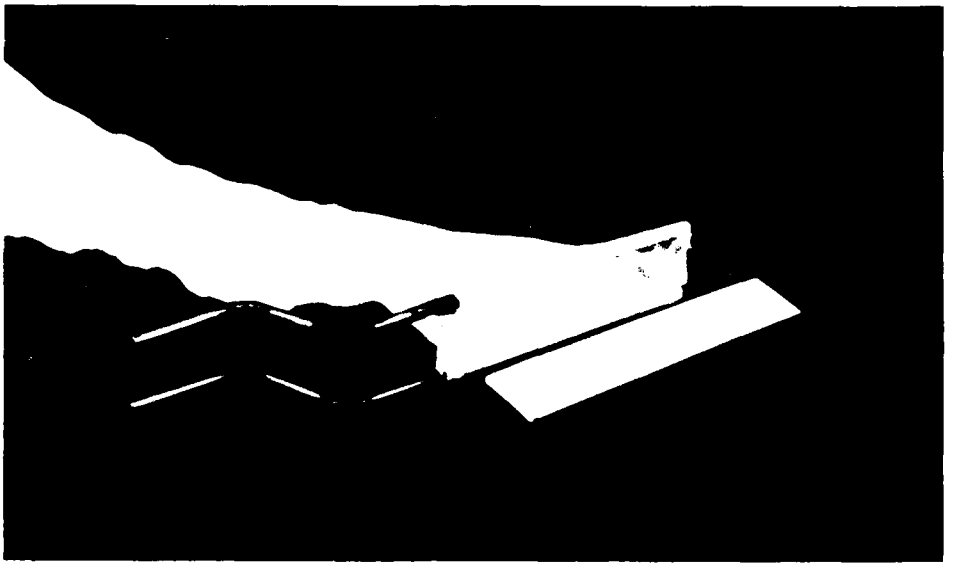

(a) Nozzle

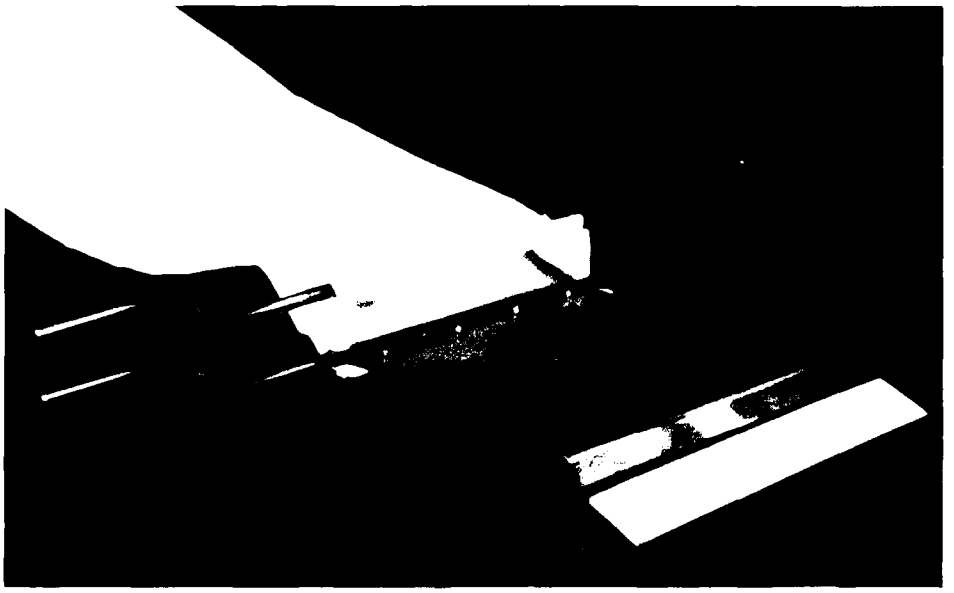

(b) Nozzle with curved lip

Figure C1. Photographs of 2.5-cm x 15-cm nozzle

(Sheet 1 of 3)

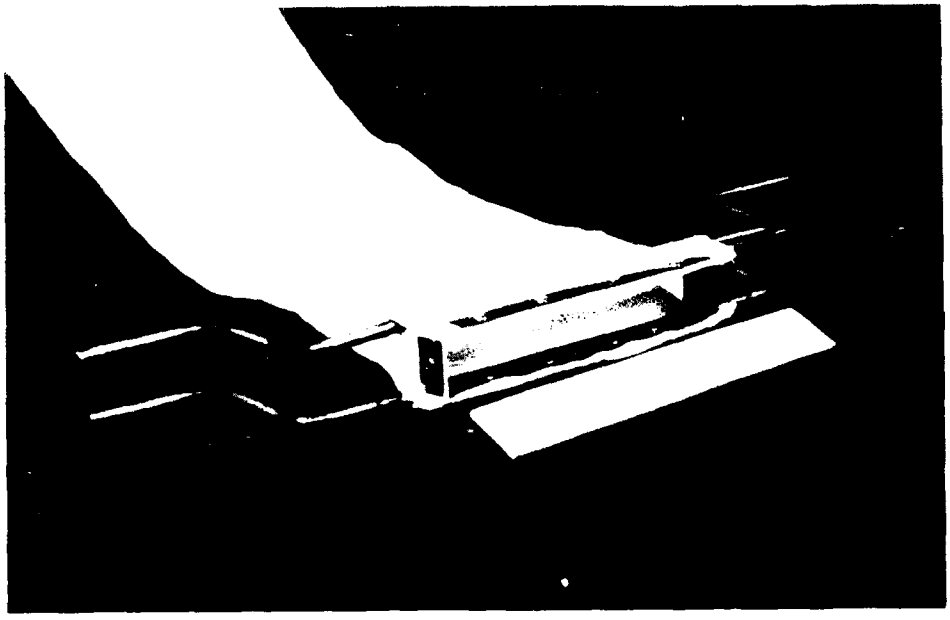

(c) Nozzle with 2.5-cm hood

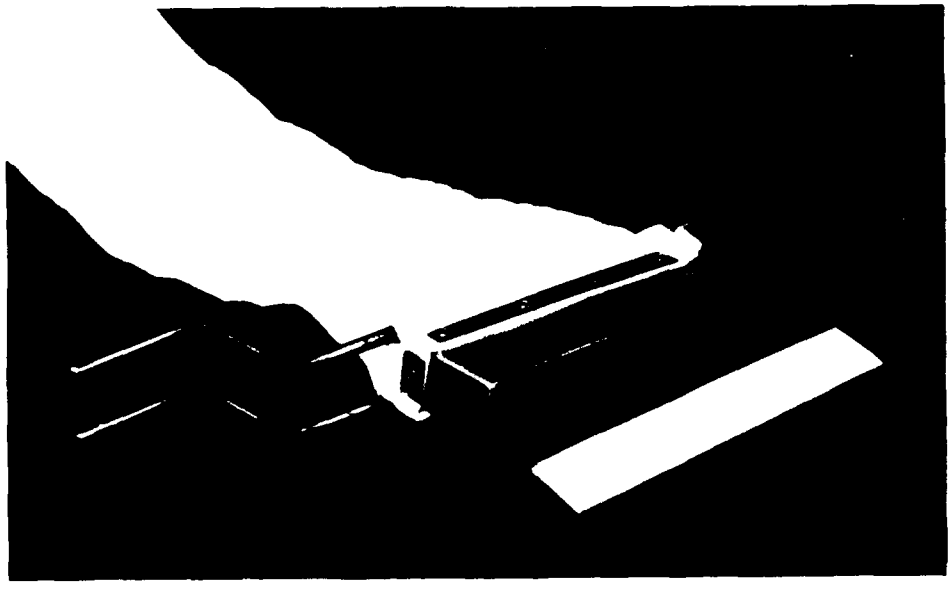

(d) Nozzle with 5.1-cm hood

Figure C1. (Continued)

(Sheet 2 of 3)

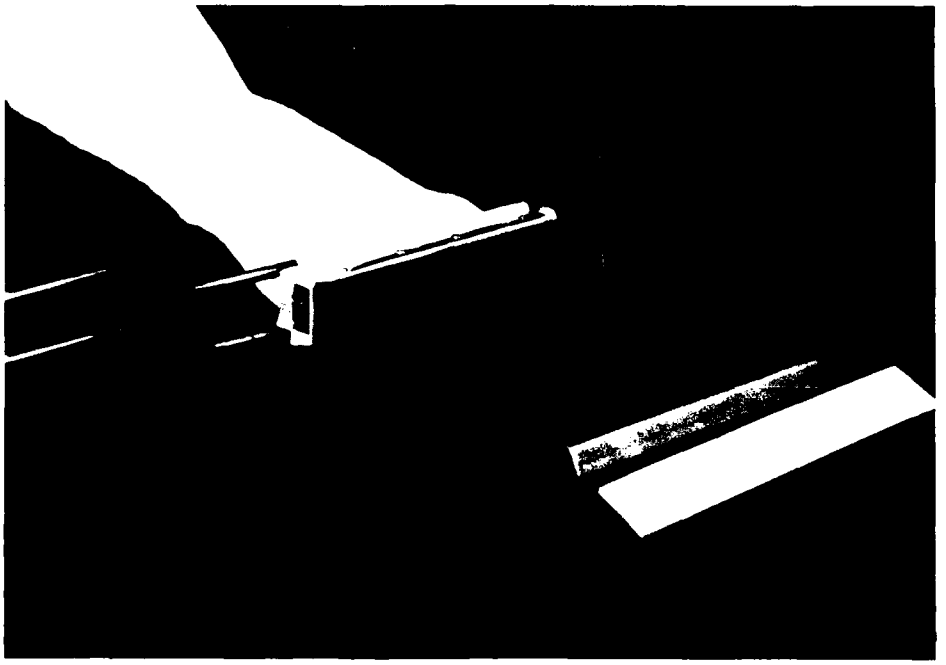

(e) Nozzle with 5,1-cm hood and curved lip

Figure C1. (Concluded)

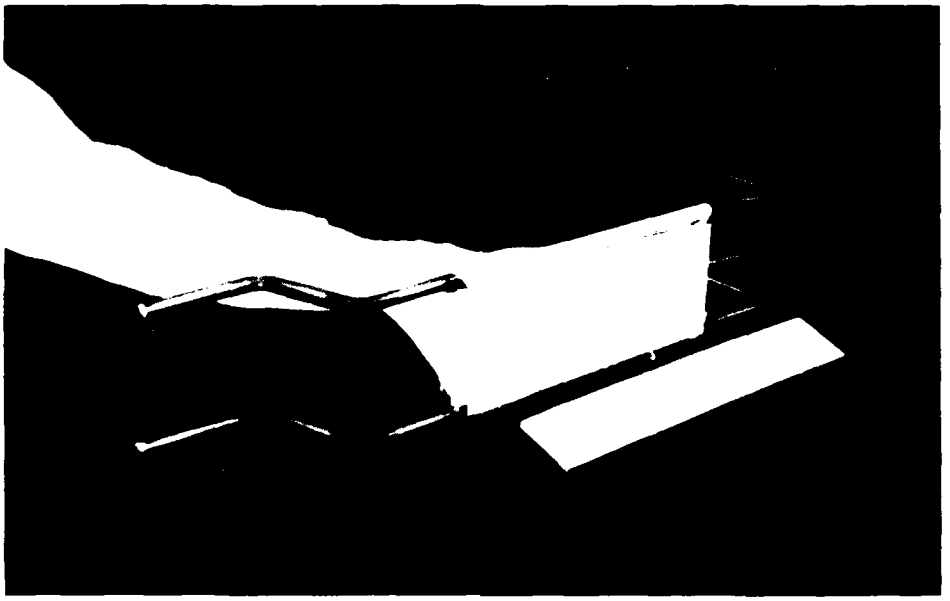

(a) Nozzle

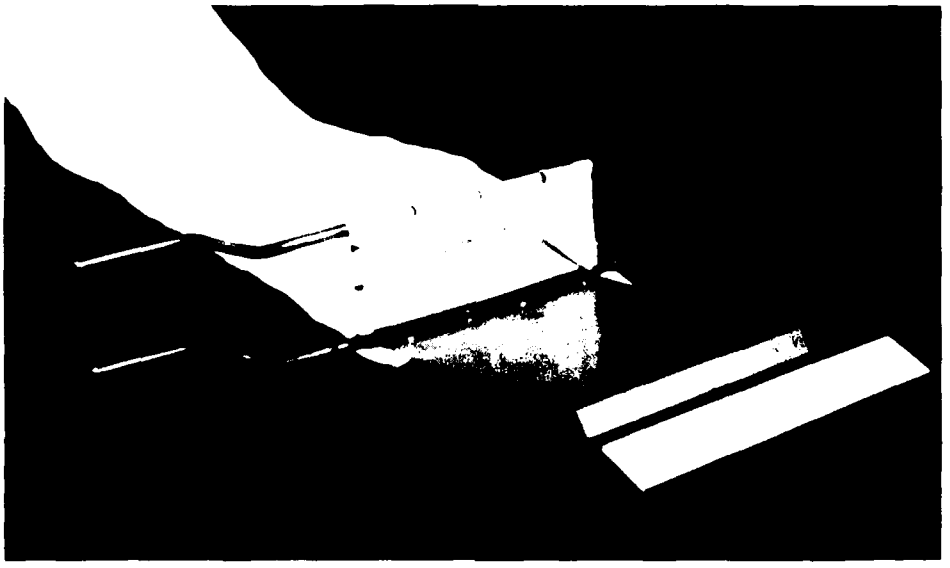

(b) Nozzle with curved lip

Figure C2. Photographs of 5.1- x 15-cm nozzle

(Sheet 1 of 3)

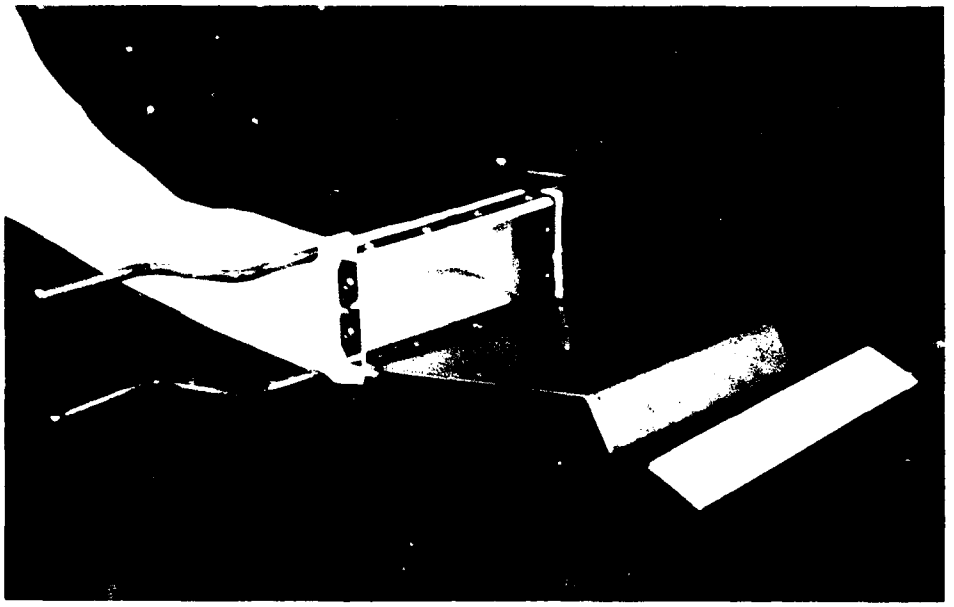

(c) Nozzle with 2.5-cm hood and curved lip

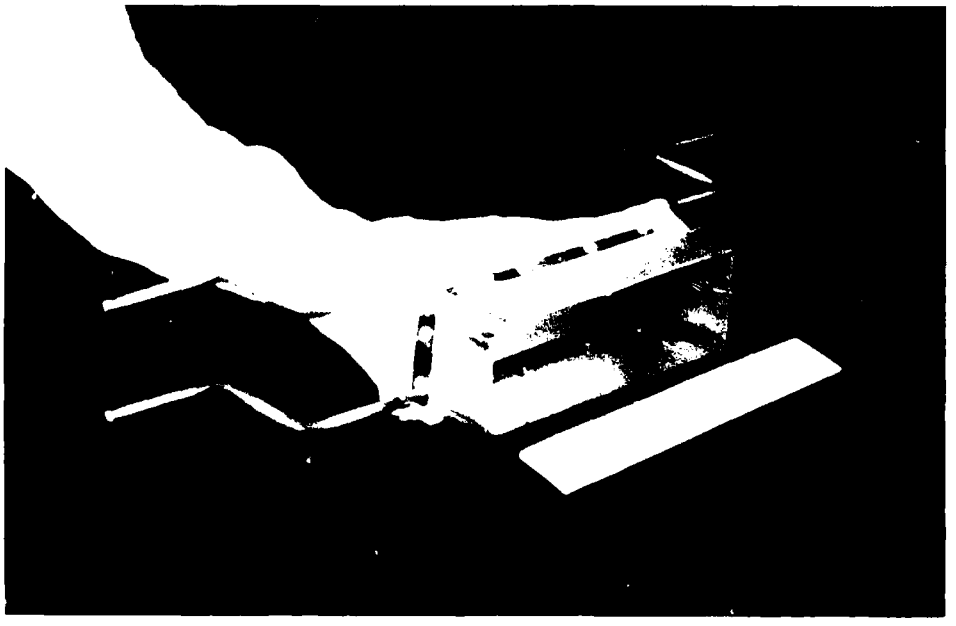

(d) Nozzle with 5.1-cm hood

Figure C2. (Continued)

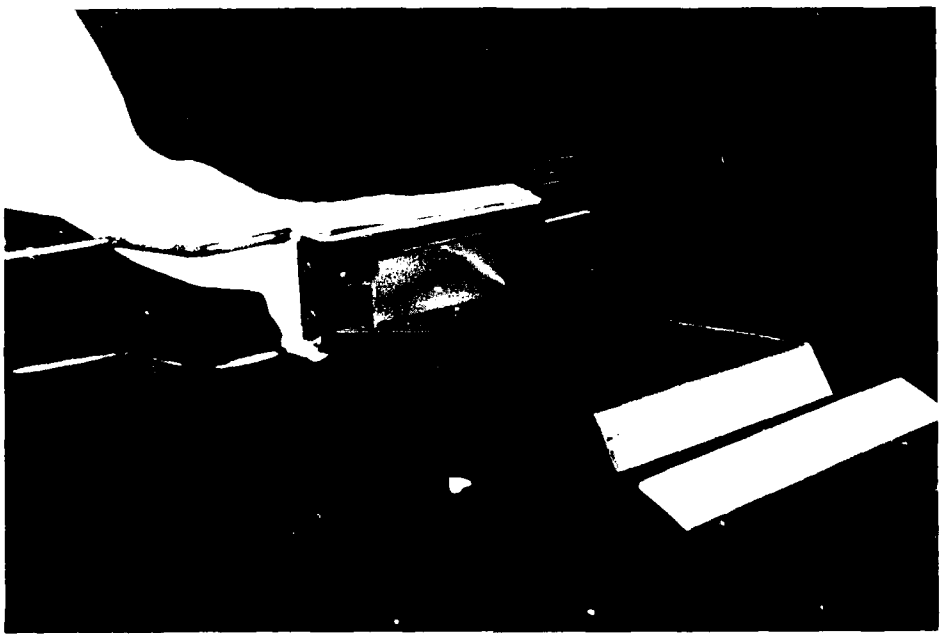

(e) Nozzle with 5.1-cm hood and curved lip

Figure C2. (Concluded)

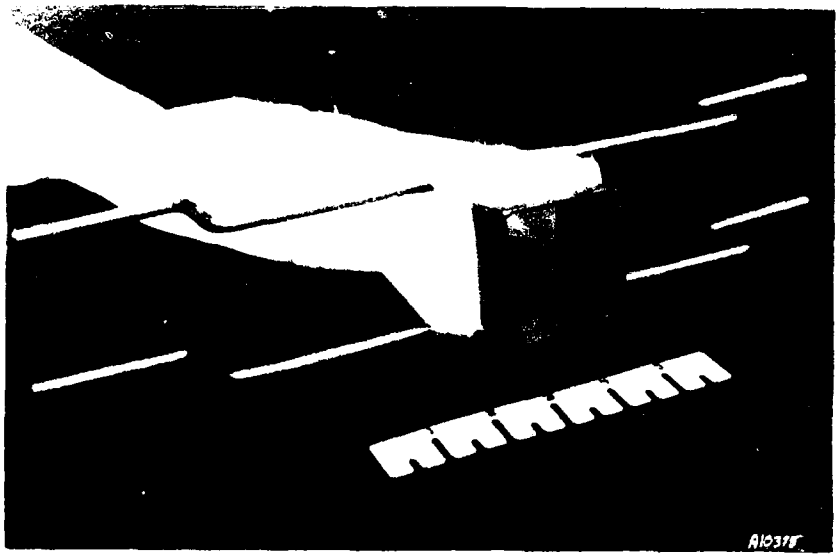

Figure C3. Photograph of 5.1- x 5.1-cm nozzle with 5.1-cm hood

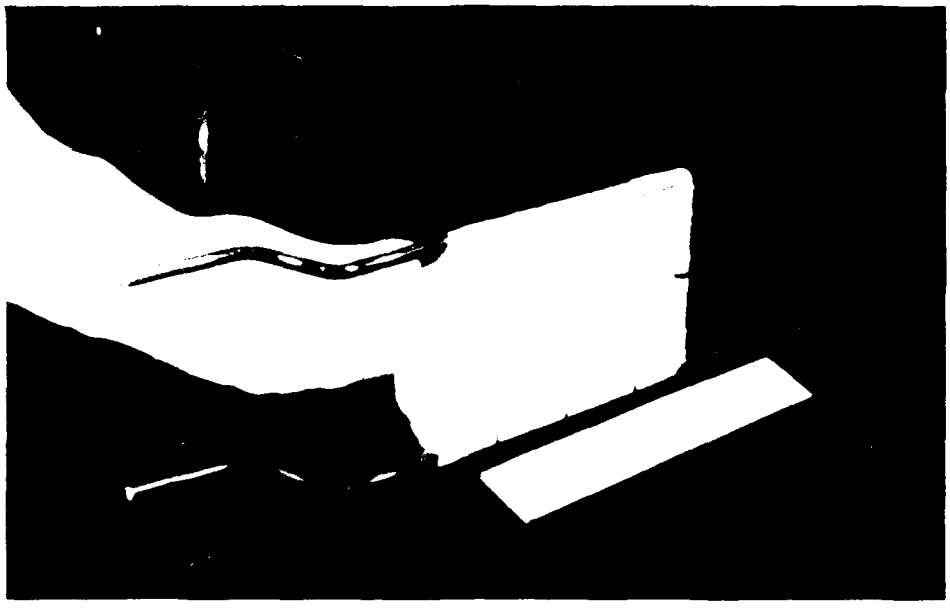

(a) Nozzle

(b) Nozzle with straight lip

Figure C4. Photographs of 9- x 15-cm nozzle

(Sheet 1 of 5)

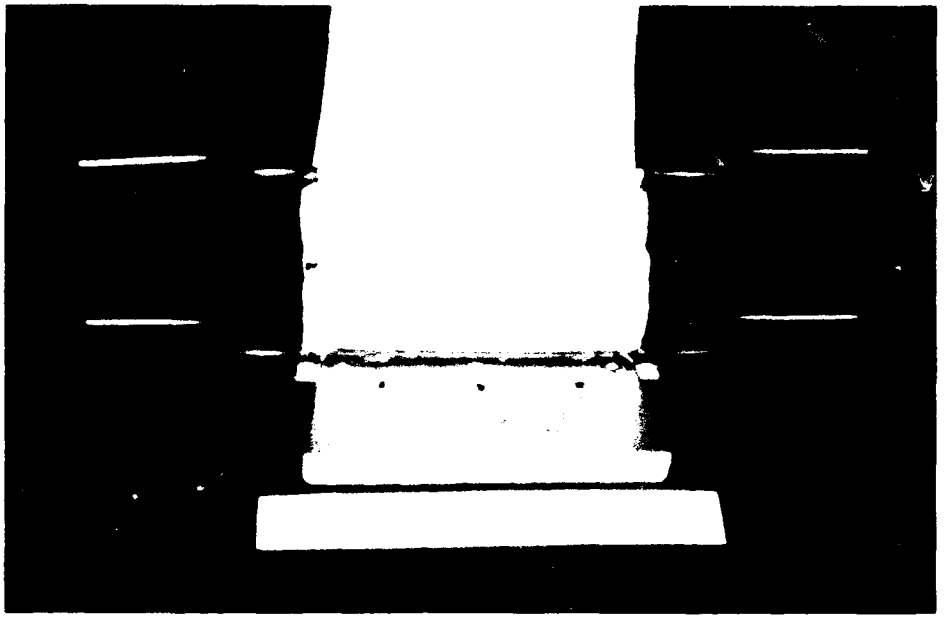

(c) Nozzle with curved lip

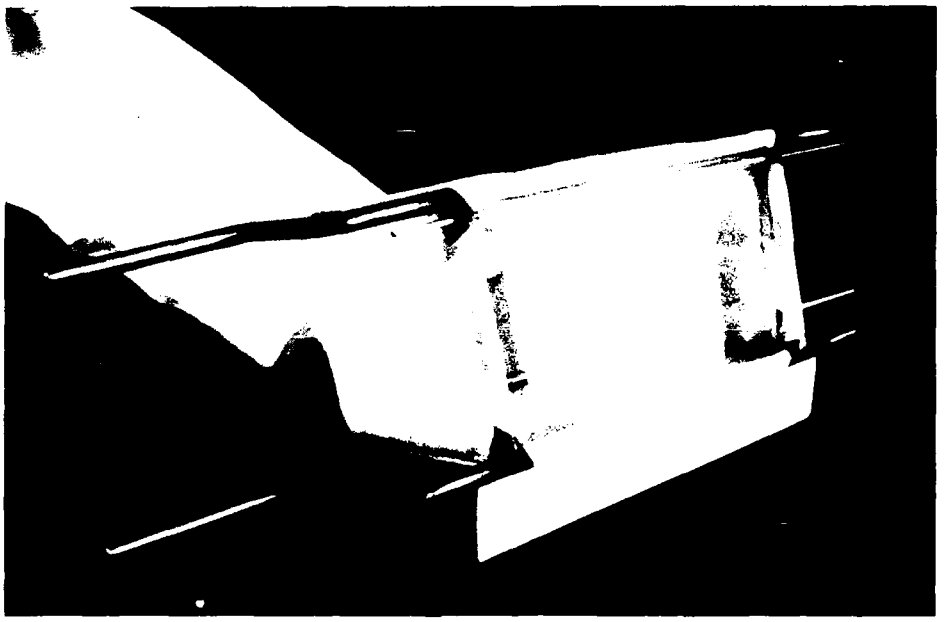

(d) Nozzle with door

Figure C4. (Continued)

(Sheet 2 of 5)

(e) Nozzle with door and curved lip

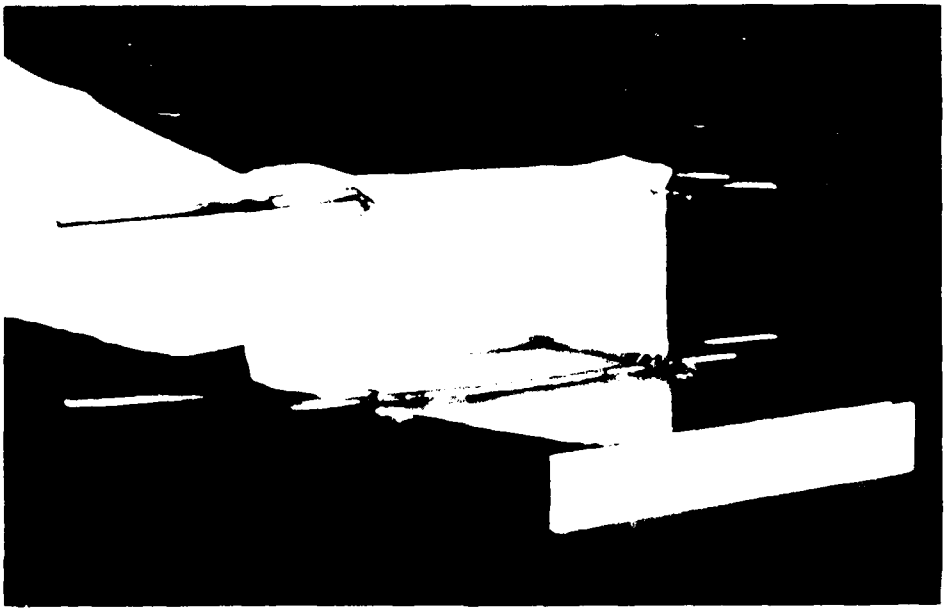

(f) Nozzle with door and straight lip

Figure C4. (Continued)

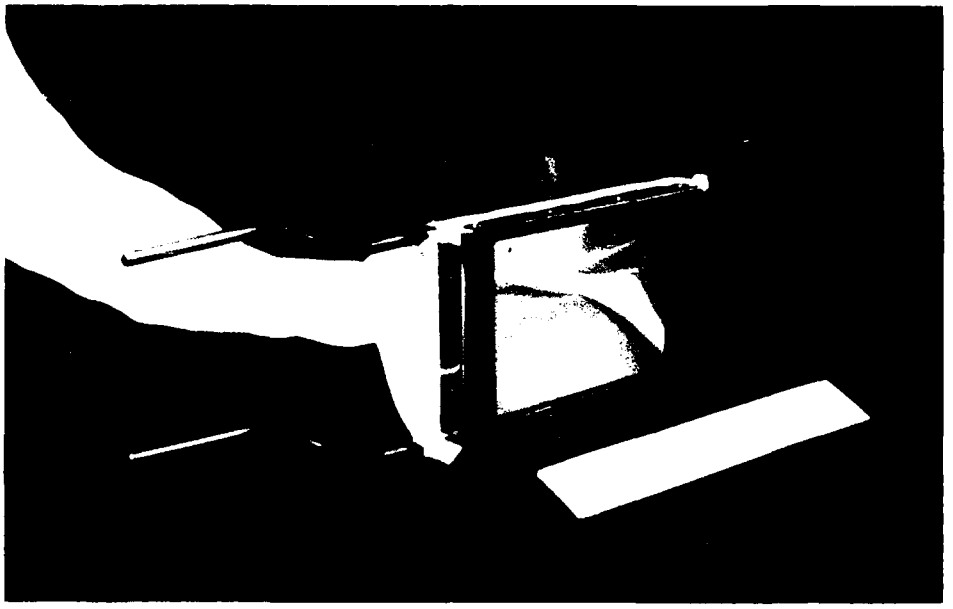

(g) Nozzle with 5.1-cm hood

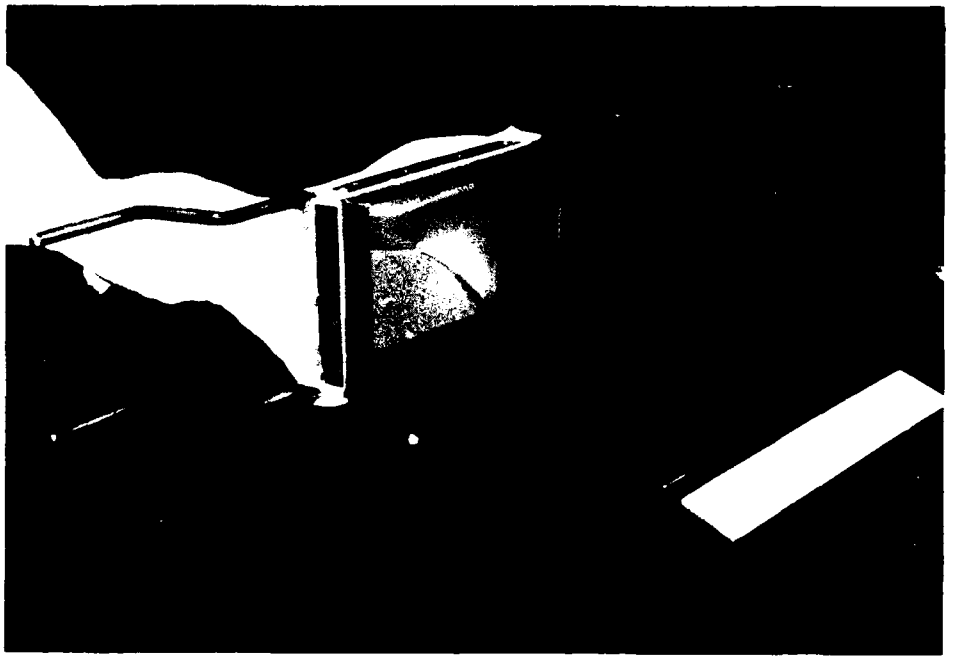

(h) Nozzle with 5.1-cm hood and straight lip

Figure C4. (Continued)

(Sheet 4 of 5)

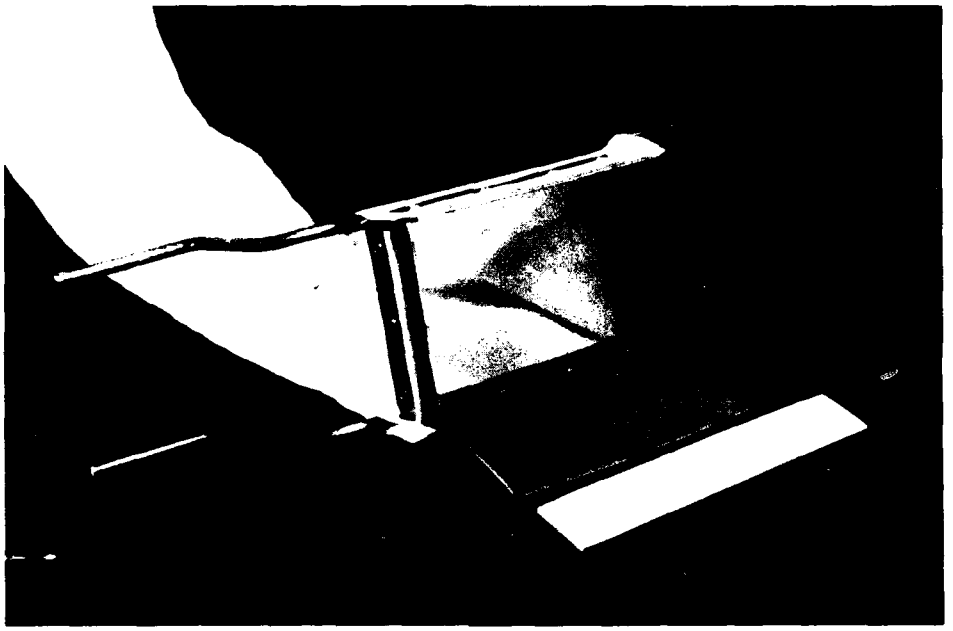

(i) Nozzle with 5.1-cm hood and 5.1-cm lip

(j) Nozzle with long hood and curved lip

Figure C4. (Concluded)

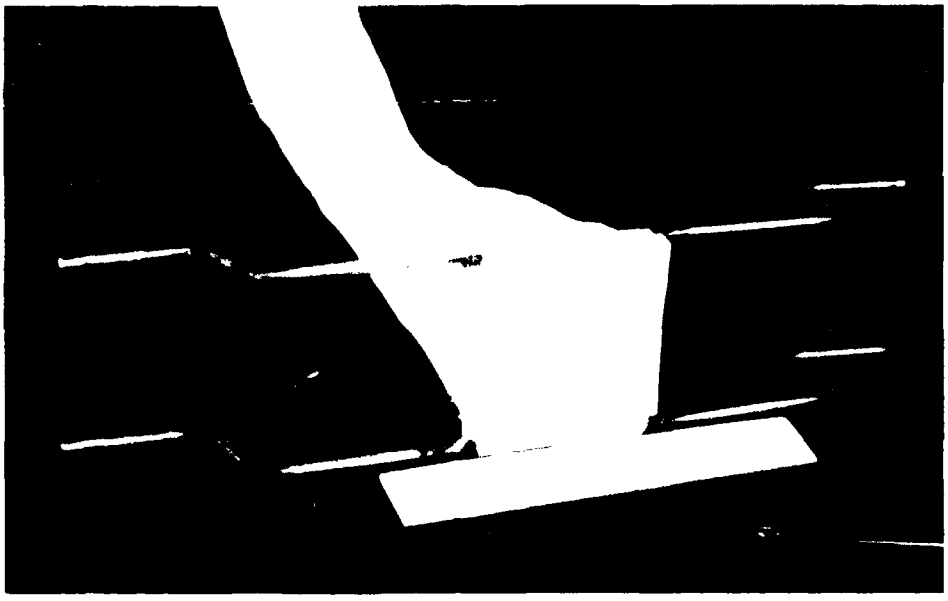

(a) Nozzle

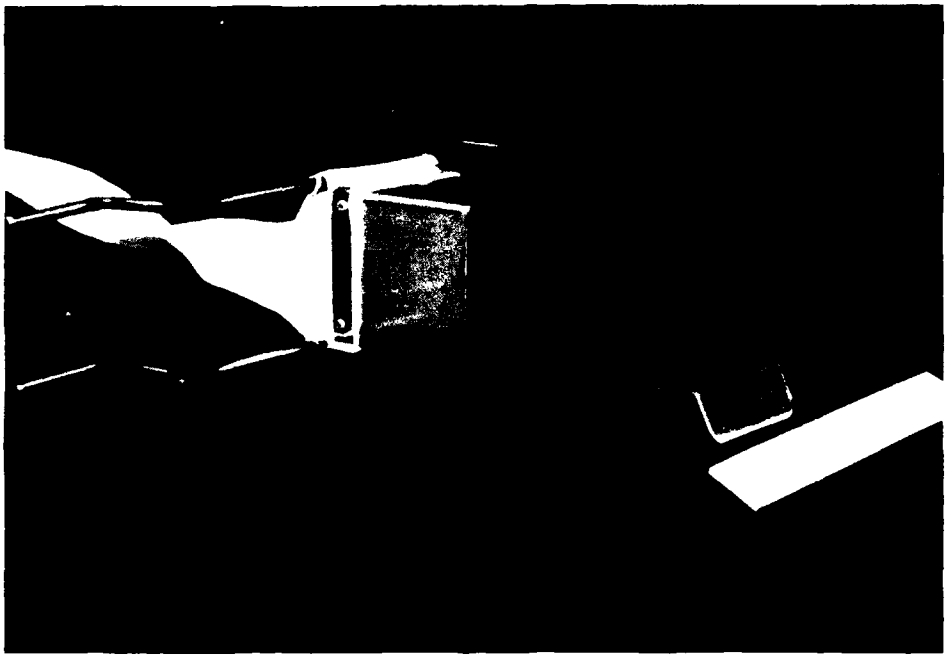

(b) Nozzle with hood and curved lip

Figure C5. Photographs of 7.6- x 7.6-cm nozzle

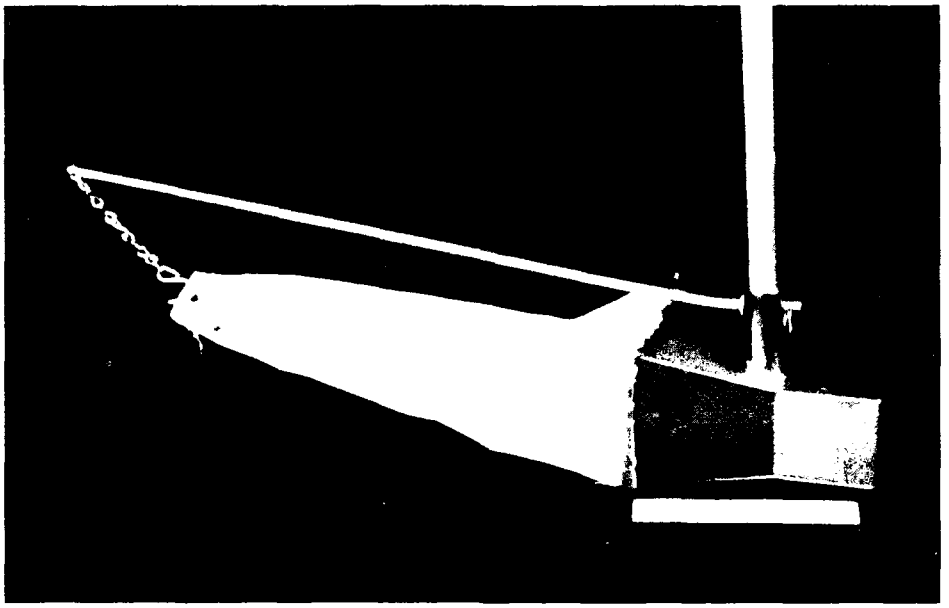

Figure C6. Photograph of 7.6- x 7.6-cm H-S sampler

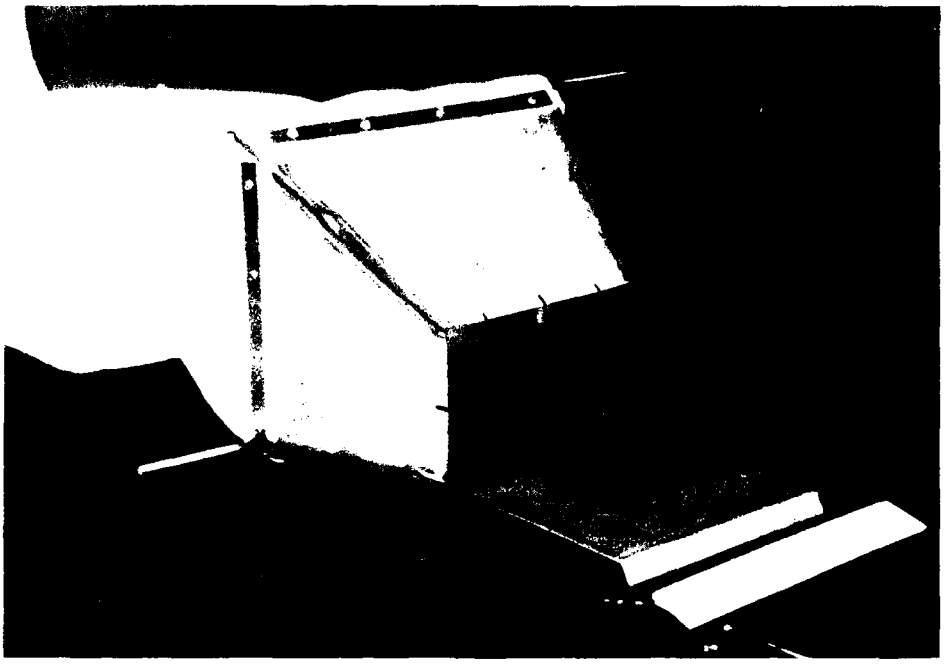

Figure C7. Photograph of 20- x 24.4-cm pressure differential nozzle

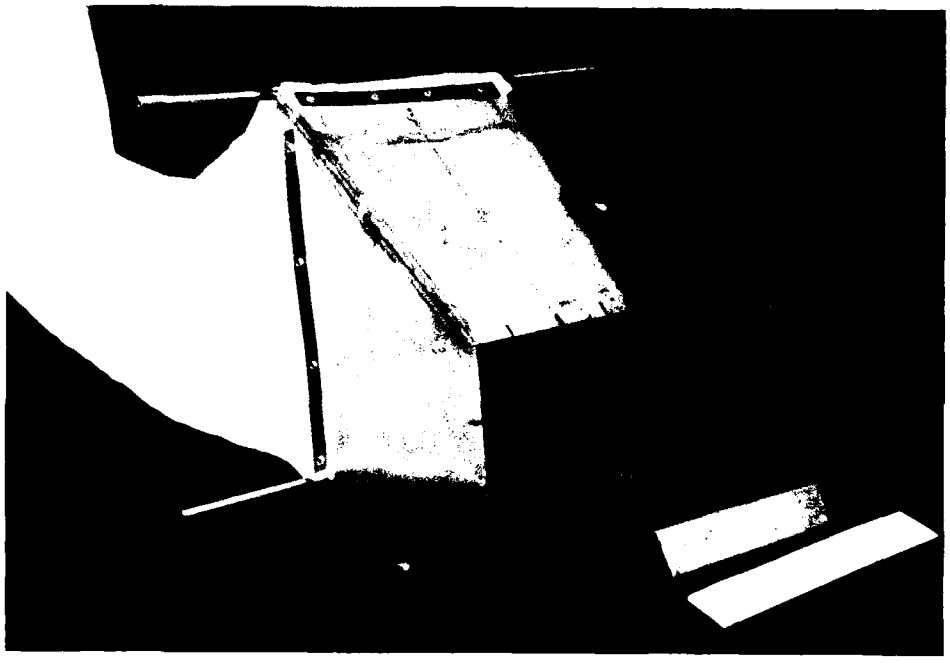

Figure C8. Photograph of 24.4- x 20-cm pressure differential nozzle

APPENDIX D: SAND-TRAPPING EFFICIENCY TEST DATA

1. Data presented in Tables D1 through D6 were collected during the sand-trapping efficiency tests. The data are organized by nozzle or type of basin test (2.5-min or 7.5-min), and each test is uniquely designated by its run number and date. Tables presenting data collected during the nozzle tests (Tables D1 through D4) are organized with the testing midflow V_{mid} and near-bed V_{bot} flow speed, the weight of material collected in the near-bed streamer S1, in the next higher elevation streamer S2, and so on. The distances between streamers 1 and 2 ($\Delta a1$) and between streamers 2 and 3 ($\Delta a2$) are given in the last two columns of the tables. The notation 'tr' indicates that only a trace of sand was collected for that particular entry.

2. Tables presenting the basin data (Tables D5 and D6) are organized with the width of the basin w, the midflow and bottom flow speeds, and quantities collected in Basin 1 (upflow) B1, Basin 2 (middle) B2, and Basin 3 (downflow) B3. The total weight collected in all basins is presented in the last column.

Table D1

SUPERDUCK Nozzle Sand-Trapping Experiment Data

Run No.	Date	V_{mid} cm/sec	V_{bot} cm/sec	S1 g	S2 g	S3 g	Δa1 cm	Δa2 cm
4	4-2-88	59.4	46.2	609.7	8.3	0	3.94	3.94
6	4-2-88	62.4	46.0	747.4	13.4	tr	3.94	3.94
9	4-2-88	63.3	49.8	699.0	6.5	tr	3.94	3.94
3	4-4-88	57.5	41.5	132.8	13.2	tr	3.94	3.94
4	4-4-88	63.3	49.5	1007.0	5.5	0.6	2.29	3.81
4	4-5-88	63.9	50.8	361.1	15.3	2.3	2.29	3.81
5	4-5-88	65.6	53.3	930.4	28.9	2.8	1.91	3.81
6	4-5-88	69.3	56.4	1131.4	21.2	2.4	1.91	3.81
7	4-5-88	71.7	56.3	1277.0	16.4	1.8	1.91	3.81
8	4-5-88	56.1	42.9	287.1	5.1	1.6	1.91	3.81
3	4-6-88	55.6	43.0	228.5	7.8	1.9	1.91	3.81
4	4-6-88	43.8	33.9	12.2	1.9	1.2	1.91	3.81
5	4-6-88	59.0	46.2	186.7	12.1	1.9	1.91	3.81
6	4-6-88	59.5	46.1	220.7	17.1	2.7	1.91	3.81
7	4-6-88	64.8	52.3	878.4	23.9	3.1	1.91	3.81
8	4-6-88	60.7	47.4	355.8	16.8	4.6	1.91	3.81
1	4-7-88	59.6	47.6	375.2	9.5	2.0	1.91	3.81
2	4-7-88	62.6	50.4	572.7	19.6	5.8	1.91	3.81
3	4-7-88	62.2	49.9	632.4	13.3	7.6	1.91	3.81
4	4-7-88	66.4	52.5	988.7	17.4	4.1	1.91	3.81
5	4-7-88	68.7	54.3	1322.4	17.2	8.3	1.91	3.81
6	4-7-88	69.1	54.5	1270.4	22.3	3.7	1.91	3.81
7	4-7-88	68.0	53.4	1229.7	13.2	2.8	1.91	3.81
8	4-7-88	50.0	38.5	136.1	9.9	3.4	1.91	3.81
3	4-8-88	53.2	40.8	103.5	6.2	0.8	1.91	3.81
4	4-8-88	58.2	45.4	266.4	9.6	9.5	1.91	3.81

Table D2

CUBE Nozzle Sand-Trapping Experiment Data

Run No.	Date	V_{mid} cm/sec	V_{bot} cm/sec	S1 g	S2 g	S3 g	Δa1 cm	Δa2 cm
2	4-10-88	49.4	38.7	88.7	1.9	2.3	3.18	2.16
3	4-10-88	63.2	49.5	595.7	1.3	0.8	3.18	2.16
4	4-10-88	56.6	43.5	299.2	tr	tr	3.18	2.16
1	4-11-88	56.7	44.0	419.7	3.6	1.7	3.18	2.16
2	4-11-88	59.4	46.3	486.4	0.8	0.5	3.18	2.16
3	4-11-88	42.7	33.0	35.4	0.9	tr	3.18	2.16
5	4-11-88	62.7	48.7	527.4	1.6	0.7	3.18	2.16
6	4-11-88	63.2	49.2	711.4	0.7	0.9	3.18	2.16
4	4-16-88	65.4	51.2	987.7	0.9	0.9	3.18	2.16
5	4-16-88	54.1	41.3	203.0	0.2	tr	3.18	2.16
6	4-16-88	51.6	38.9	83.2	2.5	0.9	3.18	2.16
7	4-16-88	66.1	51.6	697.0	11.0	0.5	3.18	2.16

Table D3

DUCK85 Sand-Trapping Experiment Data

Run No.	Date	V_{mid} cm/sec	V_{bot} cm/sec	S1 g	S2 g	S3 g	Δa1 cm	Δa2 cm
5	4-8-88	57.8	45.2	61.4	0.5	---	0	---
6	4-8-88	70.8	57.0	1028.7	1.8	---	0	---
1	4-9-88	63.7	50.1	232.1	16.5	---	0	---
8	4-16-88	64.3	51.6	355.7	2.6	---	0	---
9	4-16-88	61.1	49.1	151.1	2.4	---	0	---
10	4-16-88	69.4	55.3	1266.4	4.0	---	0	---

Table D4

H-S Sand-Trapping Experiment Data

Run No.	Date	V_{mid} cm/sec	V_{bot} cm/sec	S1 g	S2 g	S3 g	Δa1 cm	Δa2 cm
7	4-9-88	59.2	45.4	3595.8	---	---	---	---
8	4-9-88	52.1	39.9	4091.4	---	---	---	---

Table D5

2.5-Min Basin Sand-Trapping Experiment Data

Run No.	Date	w cm	V_{mid} cm/sec	V_{bot} cm/sec	B1 g	B2 g	B3 g	Total g
1	4-2-88	67.31	60.7	--	885.7	24.0	2.7	912.4
7	4-2-88	67.31	65.6	--	2530.0	75.0	5.8	2610.8
1	4-3-88	67.31	63.7	--	2420.0	87.2	36.8	2544.0
6	4-4-88	67.31	70.6	--	4172.0	111.5	49.6	4333.1
1	4-5-88	67.31	73.5	--	5299.0	120.6	48.9	5468.5
1	4-6-88	67.31	55.8	--	1063.7	21.7	9.4	1094.8
9	4-7-88	67.31	53.3	--	282.7	8.2	2.4	293.3
1	4-8-88	67.31	45.7	--	149.5	1.5	2.7	153.7
2	4-9-88	67.31	56.2	--	482.9	8.1	3.2	494.2
4	4-9-88	67.31	58.4	--	1179.4	11.3	2.3	1193.0
1	4-12-88	24.8	68.7	--	1636.7	----->	20.1	1656.8
1	4-13-88	24.8	60.0	--	431.8	----->	4.4	436.2
1	4-15-88	24.8	66.5	--	1016.4	----->	3.4	1019.8

Table D6

7.5-Min Basin Sand-Trapping Experiment Data

Run No.	Date	w cm	V_{mid} cm/sec	V_{bot} cm/sec	B1 g	B2 g	B3 g	Total g
2	4-2-88	67.31	60.7	47.9	4948.3	67.3	30.6	5046.2
5	4-2-88	67.31	62.8	49.3	6872.1	156.4	19.3	7047.8
8	4-2-88	67.31	64.6	51.8	9758.4	81.4	63.1	9902.9
2	4-3-88	67.31	66.9	52.6	10181.1	144.0	125.4	10450.5
7	4-4-88	67.31	69.8	56.0	13101.7	148.7	39.6	13290.0
2	4-5-88	67.31	72.4	56.7	17313.2	329.6	175.1	17817.9
2	4-6-88	67.31	56.0	43.6	4405.7	66.3	27.3	4499.3
10	4-7-88	67.31	51.9	40.1	1149.7	11.5	4.9	1166.1
2	4-8-88	67.31	46.0	35.7	854.0	10.1	5.3	869.4
3	4-9-88	67.31	56.6	45.2	3787.2	11.3	12.5	381'
5	4-9-88	67.31	58.9	47.0	4057.8	20.2	5.6	4083.6
6	4-9-88	67.31	58.5	45.8	3615.8	31.2	9.3	3656.3
5	4-10-88	24.8	58.0	45.4	1395.4	17.0	9.4	1421.8
2	4-12-88	24.8	69.2	53.3	5354.4	----->	48.9	5403.3
2	4-13-88	24.8	59.8	45.5	1847.4	----->	9.8	1857.2
2	4-15-88	24.8	66.1	52.1	4222.0	----->	14.3	4236.3
1	4-16-88	24.8	57.9	46.0	1401.7	----->	13.0	1414.7
2	4-16-88	24.8	61.9	46.4	1766.7	----->	4.6	1771.3
3	4-16-88	24.8	62.1	47.8	1943.7	----->	7.3	1951.0

APPENDIX E: NOTATION

a	Empirically determined coefficient
A	Empirical coefficient
A_{CU}	Area beneath Cube predictive equation
A_{D85}	Area beneath DUCK85 predictive equation
A_{lCU}	Area below lower confidence limit for Cube predictive equation
A_{lTR}	Area below lower confidence limit for trap-predictive equation
A_{SD}	Area beneath SUPERDUCK predictive equation
A_{TR}	Area beneath a trap-predictive equation
A_{uCU}	Area below upper confidence limit for Cube predictive equation
A_{uTR}	Area below upper confidence limit for trap-predictive equation
b	Empirically determined constant
c	Constant in logarithmic law taken equal to zero
C	Empirical coefficient in wet weight to dry weight conversion; also concentration of sediment
D	Characteristic depth for use in Reynolds number calculation
D	Grain diameter
DW	Dry weight of sand
d_s	Mean diameter of sand
E_h	Hydraulic efficiency
E_s	Sand-trapping efficiency
F	Sand flux
f	Friction factor
f_m	Measured flux ($g/cm^2/sec$)
f_p	Predicted flux ($g/cm^2/sec$)
F(k)	Flux of sand at streamer k (weight per unit area and unit time, $g/cm^2/sec$)
F(k+1)	Flux of sand at streamer k+1 (weight per unit area and unit time, $g/cm^2/sec$)
F_1	Basin sand flux, flow speed less than 58 cm/sec ($g/cm^2/sec$)
F_2	Basin sand flux, flow speed greater or equal to 58 cm/sec ($g/cm^2/sec$)
FE(k)	Estimated flux between streamers k and k+1 (weight per unit area and unit time, $g/cm^2/sec$)
g	Acceleration of gravity

g_b	Weight of bed load collected
H_b	Breaking wave height
i	Transport rate density (weight per unit width of surf zone per unit time)
k	Von Karman constant, taken to be 0.4
m	Empirical constant
n	Empirical constant
N	Total number of streamers in trap
N	Number of data points
Q_s	Volumetric bed-load transport
q	Water discharge
q_b	Bed-load transport rate
q_o	Ambient sand transport rate (weight per unit width per unit time)
q_{ss}	Suspended sediment transport rate
q_t	Trap-predicted transport rate (weight per unit width per unit time)
r^2	Squared correlation coefficient
R	Discharge parameter
Re	Reynolds number
S	Energy grade line
S(k)	Weight of sand collected in streamer k (g)
S_{xx}	Variable defined in terms of N and x
S_y	Standard error of estimate
$t_{\alpha/2}$	t-statistic
u_m	Maximum horizontal orbital speed
u(z)	Flow speed at elevation z
U_*	Shear flow speed (cm/sec)
U_{*c}	Critical shear speed (cm/sec)
V	Characteristic velocity for use in Reynolds number calculation
V_{bot}	Bottom flow speed (cm/sec)
V_{mid}	Midflow speed (cm/sec)
V_o	Average flow speed without trap (cm/sec)
$V_{o,k}$	Flow speed without trap (cm/sec)
V_t	Average flow speed directly in front of trap nozzle (cm/sec)

V_{tjk}	Flow speed directly in front of trap nozzle (cm/sec)
V_*	Threshold midflow or bottom flow speed for sand movement (cm/sec)
WW	Wet weight of sand
w_s	Weight of sediment collected
x	Independent variable
$\bar{x}$	Average x
y	Dependent variable
z	Elevation from bed (cm)
z_o	Representative bed roughness (cm)
Z	Distance from seabed to mid-streamer (cm)
$\Delta a(k)$	Distance between nozzles k and k+1 (cm)
$\Delta a1$	Distance between streamers 1 and 2 (cm)
$\Delta a2$	Distance between streamers 2 and 3 (cm)
Δh	Height of nozzle (cm)
Δt	Sampling interval (min, sec)
Δw	Width of nozzle (cm)
Δy_j	Representative horizontal distance (cm)
Δz_k	Representative vertical distance (cm)
ϵ	Maximum error corresponding to E_s
Ψ	Shields number
ν	Kinematic viscosity of water (cm^2/sec)
ρ	Density of water (kg/m^3)
ρ_s	Density of sand (kg/m^3)
τ_c	Critical shear stress at the bed
τ_o	Shear stress at the bed